Robin Lyngseth Bakken

Reliable Power Cable Screen Connections

Evaluation of test procedures for power cable screen connections

Master's thesis in Energibruk og energiplanlegging
Supervisor: Frank Mauseth & Hans Lavoll Halvorson
June 2019

Master's thesis

NTNU
Norwegian University of Science and Technology
Faculty of Information Technology and Electrical Engineering
Department of Electric Power Engineering

NTNU
Norwegian University of
Science and Technology

Robin Lyngseth Bakken

Reliable Power Cable Screen Connections

Evaluation of test procedures for power cable screen connections

Master's thesis in Energibruk og energiplanlegging
Supervisor: Frank Mauseth & Hans Lavoll Halvorson
June 2019

Norwegian University of Science and Technology
Faculty of Information Technology and Electrical Engineering
Department of Electric Power Engineering

Preface

This master thesis has been carried out at the Department of Electrical Power Engineering at the Norwegian University of Science and Technology (NTNU) during the spring of 2019. The work is conducted in co-operation with SINTEF Energy Research and counts for 30 credits of my master's degree.

I would like to thank my supervisor Frank Mauseth and co-supervisor Hans Lavoll Halvorson for their support, guidance and help throughout this semester. Further, I would like to thank Magne Runde from SINTEF Energy for help and discussion on theoretical matters of the project.

Finally, I would like to thank Svein Erling Norum at the Department of Electrical Power Engineering, Horst H. Förster, Arild Følstad and Morten Koksæther at SINTEF Energy Research for help with practical matters and the experimental setup.

Trondheim, June 2019.

Robin Lyngseth Bakken

Abstract

In recent years, several comprehensive and expensive faults have occurred in the Norwegian power grid due to local hotspots in power cables. The main reason for this is poor contact within the ground screen connections at joints and terminations. There is generally little experience exchange and there are no international nor Norwegian standards that require testing for such connections.

Based on this, REN AS initiated a project that deals with reliable ground screen connections in 2016. The project is in cooperation with SINTEF Energy Research, Norwegian utilities and cable manufacturers, and will run until the end of 2019. The intention of the project is to develop a better understanding of the fault mechanisms and further use this information to introduce a standardized test for screen connections.

As a part of the work to introduce a standardized test for screen connections, this master thesis addresses laboratory challenges, both practical and theoretical. The main objectives of this project are to establish a reliable and effective test procedure and laboratory setup that can be used to evaluate power cable screen connections.

A laboratory setup was made to evaluate two test procedures that uses different load types and methodology for testing screen connections. Two identical test setups were made with 6 test objects that consisted of the common screen connection type “constant force springs”. The first test procedure was a heat cycle test which initiated cyclic strains in the test objects by continuously heating and cooling down the test objects. The second test procedure was a constant current test which had a simpler approach with constant loads throughout the entire test period.

Results show that test objects from both test procedures experienced a significant increase in contact resistance with an average increase of 507 % for the heat cycle test and 190 % for the constant current test.

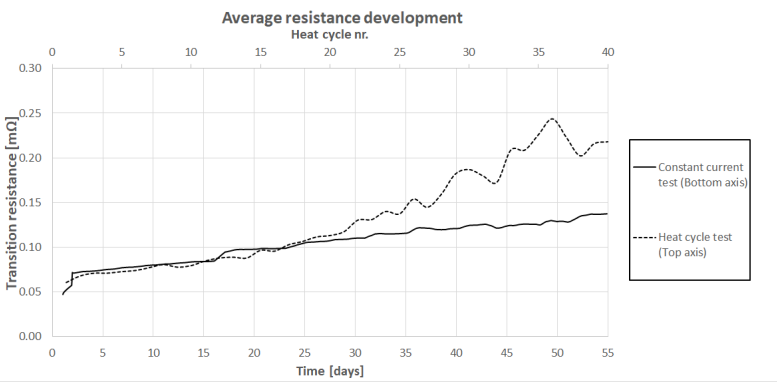

Figure 4.9. Average test object resistance development at 85-90 °C.

Figure 4.9 compares the average test object resistances for the heat cycle test and the constant current test at stabilized test object temperatures of 85-90 °C. The results show that the test objects from the heat cycle test gradually worsened and gained variating contact resistances compared to the test objects from the constant current test. Both test procedures experienced an increase in contact resistance, but the heat cycle test seemed to have had a bigger impact on the ampacity of the screen connections over time.

The experiments performed in this master thesis proved that both test procedures give a certain value for testing screen connections, but the results showed that the cyclic strains from the heat cycle test is a necessary factor to fully evaluate the properties of power cable screen connections.

Sammendrag

I de senere år har det oppstått flere omfattende og kostbare feil i det norske kraftnettet på grunn av lokal varmgang i kraftkabler. Hovedårsaken til dette er dårlig kontakt i skjermtilkoblinger ved skjøter og endeavslutninger. Det er generelt lite utveksling av erfaring og det er ingen internasjonal eller norsk standard som setter krav til slike tilkoblinger.

Basert på dette satte REN AS i gang et prosjekt som handler om pålitelige skjermtilkoblinger i 2016. Prosjektet er i samarbeid med SINTEF Energi, norske kraftselskap og kabelprodusenter, og vil vare til slutten av 2019. Formålet med prosjektet er å utvikle en bedre forståelse av feilmekanismene og videre bruke denne informasjonen til å introdusere en standardisert test for skjermtilkoblinger.

Som en del av arbeidet med å innføre en standardisert test for skjermtilkoblinger har denne masteroppgaven omhandlet laboratorieutfordringer, både praktisk og teoretisk. Hovedmålet med dette prosjektet var å etablere en pålitelig og effektiv testprosedyre og et laboratorieoppsett som kan brukes til å evaluere skjermtilkoblinger i kraftkabler.

Et laboratorieoppsett ble satt sammen for å evaluere to testprosedyrer som bruker forskjellige belastningstyper og metodikk for testing av skjermtilkoblinger. To identiske testoppsett ble satt sammen med 6 testobjekt som besto av «fjærklemmer» som er en vanlig skjermtilkobling i det norske kraftnettet. Den første testprosedyren var en varmesyklustest som skaper syklisk belastning i testobjektene ved å kontinuerlig varme opp og kjøle ned testobjektene. Den andre testprosedyren var en konstant strøm test som hadde en enklere tilnærming med en konstant belastning gjennom hele testperioden.

Resultatene viser at testobjekter fra begge testprosedyrene opplevde en betydelig økning i kontaktmostand med en gjennomsnittlig økning på 507 % for varmesyklustesten og 190 % for konstant strøm testen.

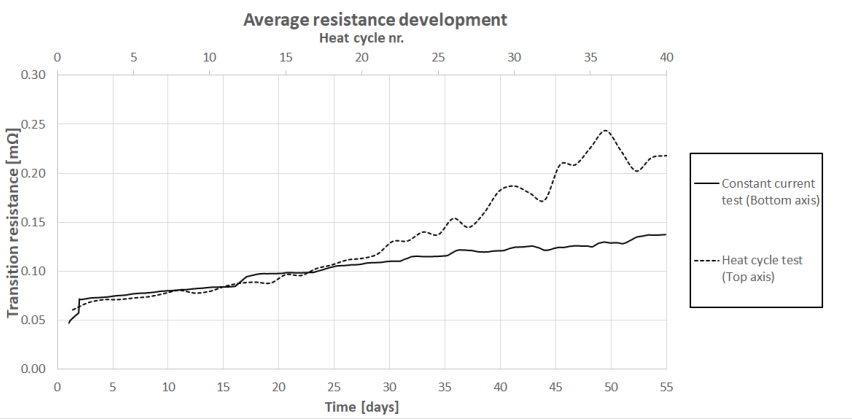

Figure 4.9. Gjennomsnittlig utvikling av kontaktmostand i testobjekt ved 85-90 °C.

Figur 4.9 sammenligner utviklingen av gjennomsnittlig kontaktmotstand i testobjektene ved 85-90 °C. Resultatene viser at testobjektene fra varmesyklustesten gradvis utviklet en kontaktmotstand som var høyere og mere varierende sammenlignet med testobjektene fra konstant strøm testen. Begge testprosedyrene opplevde en økning i kontaktmotstand, men varmesyklustesten ser ut til å ha en større innvirkning på strømføringsevnen til skjermtilkoblingene over tid.

Eksperimentene utført i denne masteroppgaven viste at begge testprosedyrene gir en viss verdi for testing av skjermtilkoblinger, men resultatene viser at de sykliske belastningene som varmesyklustesten introduserer er nødvendig for å fullt ut vurdere egenskapene til en skjermtilkobling.

Table of contents

List of symbols

Symbols	Explanation	Unit
A	Area	[mm^2]
A_a	Apparent contact area	[mm^2]
A_b	Load bearing area	[mm^2]
A_c	Conducting metal-to-metal area	[mm^2]
AC	Alternating current	
B	Magnetic flux density	[T]
DC	Direct current	
E	Young's modulus of elasticity	[N/m^2]
F	Lorentz force	
$F_{Thermal}$	Force due to thermal expansion	[N]
H	Material hardness	[N/mm^2]
I_{DC}	Applied direct current	[A]
I_{Screen}	Induced screen current	[A]
J	Current density	[A/mm^2]
L_0	Material reference length	[m]
M	Mechanical load	[N]
P	Electrical power	[W]
Pr	Pressure	[N/m^2]
R	Electrical resistance	[Ω]
R_C	Constriction resistance	[Ω]
R_{TO}	Test object transition resistance	[Ω]
T	Temperature	[°C]
T_0	Reference temperature	[°C]
TSLF	Type of cable configuration	
T.O	Test object	
$U_{Measured}$	Measured voltage	[V]
U_{Screen}	Induced voltage in cable screen	[V]
X	Electrical reactance	[Ω]
XLPE	Cross-linked polyethylene	
α	Temperature coefficient of resistivity	[1/K]
β	Coefficient of thermal expansion	[1/K]
ρ	Electrical resistivity	[Ωm]
ρ_0	Electrical resistivity at 0 °C	[Ωm]
ΔL	Extension of a material length	[m]
ΔT	Change in temperature	[°C]

1.Introduction

1.1 Motivation

The fundamental objective behind this project is to ensure that reliable power cable screen connections are installed to joints and terminations in the electrical distribution grid. In recent years, several comprehensive and expensive faults have occurred in the Norwegian power grid due to local hotspots in power cables. The main reason for this is unexpected high screen currents and poor contact within the cable screen connections at joints and terminations. In the Norwegian distribution grid, it is common to ground the cable screen at each end of the cable length. As a result, a ground screen current will flow due to a voltage induced in the cable screen, caused by the current in the cable conductor and surrounding current carrying objects.

There is generally little experience exchange and there are no international nor Norwegian standards that require testing for such connections.

Based on this, REN AS initiated a project that deals with reliable ground screen connections in 2016. The project is in cooperation with SINTEF Energy Research, Norwegian utilities, cable accessory and cable manufacturers, and will run until the end of 2019. The intention of the project is to develop a better understanding of fault mechanisms and properties of screen connections and further use this information to introduce a standardized test for screen connections. The project is partly funded by the Norwegian Research Council.

1.2 Previous work

Fault mechanisms of incorrectly installed force springs

SINTEF has previously performed dissections and analyzed faults on screen connections [1]. Some of the dissections indicated that cable faults had occurred because of incorrectly installed force springs. Laboratory experiments have been conducted to evaluate the fault mechanisms and properties of constant force springs which is commonly used for screen connections in power cables [2, 3]. A test setup was made to investigate the properties of an incorrect installation of the force spring method. Currents was applied to twelve test objects which consisted of different types of force springs throughout several heat cycles, while temperature and transition resistance were measured.

All test objects experienced high temperatures when applying relatively low currents to the cable screen and dissection of the force springs indicated excessive overheating on multiple test objects. Overall results show that an incorrectly installed force spring can cause substantial damage and contribute to cable failure at moderate screen currents. A picture showing deformations in the XLPE insulation and a hotspot from one of the screen connections is shown in Figure 1.1.

Figure 1.1. Deformations in XLPE insulation and hotspot caused by an incorrectly installed force spring. [3]

Reliable voltage measuring points

The laboratory experiments performed in the summer project "Fault mechanisms of incorrectly installed force springs" experienced loosened voltage measuring points when measuring transition resistance over the test objects [3]. As a part of the summer project the transition resistance over different types of screen connections were calculated while applying a known current in the screen and measuring the voltage drop over the screen connections.

To be able to measure the voltage drop across the screen connections, voltage potential points (equalizers) had to be installed on each side of the test objects. The current carrying parts of the cable screen consist of stranded copper wires, making it challenging to find a fitting equalizer. The equalizer had to make sure that the cable screen parts at each measuring point were at the same voltage potential throughout the heat cycles. An illustration of voltage measuring points for a cable screen is shown in Figure 1.2.

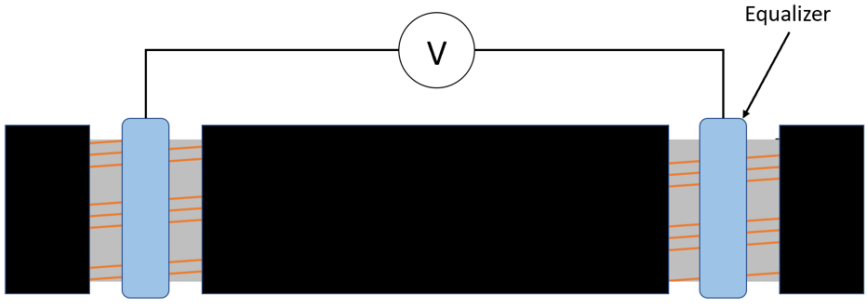

Figure 1.2. Illustration of cable screen voltage measuring points. [4]

After conducting a few heat cycles, heating and cooling of the cable XLPE insulation had caused the equalizers to loosen. The equalizers were not able to fluctuate with the XLPE insulation when the insulation had expanded and shrunk again. This had caused the insulation to deform and effectively loosen the equalizers. [3]

As a part of the work to introduce a standardized test for screen connections as well as forming the base of this master's thesis, a specialization project [4] was conducted to address laboratory challenges associated with the standardized test. The main objective of the specialization project was to find a reliable and suited solution for voltage measurements in cable screen connections.

A test setup was made to investigate the impact of alternating currents (AC) as opposed to direct current (DC) when measuring transition resistance in cable screens. Four test objects with different voltage

measuring points were tested and evaluated through heat cycles to determine if the equalizers could provide reliable resistance measurements. The following solutions were tested:

- Test object 1: Metal Clamp Rings
- Test object 2: Self-vulcanizing tape
- Test object 3: Force springs v1
- Test object 4: Force springs v2

Results showed that measuring transition resistance while applying DC current in the cable screen and AC current in the conductor gives reliable and stable results. Resistance measurements when applying AC current in both the conductor and the cable screen showed inconsistent and variating values which were clearly influenced by the conductor current magnitude and the test setup configuration. [4]

Based on the heat cycle results, all test objects provided reliable transition resistance measurements. Despite a high contact resistance, test object 2 with self-vulcanizing tape seemed to be a promising solution. The simple installation made these equalizers suitable for several test objects along a cable sample. [4]

1.3 Scope

The work conducted in this master thesis continues the work to substantiate a standardized test for screen connections. Similar to the specialization project, this thesis addresses laboratory challenges, both practical and theoretical. The main objectives of this project are to establish a reliable and effective test procedure and laboratory setup that can be used to evaluate power cable screen connections.

The work that was performed in the summer project and the specialization project [3, 4] contributed to finding a reliable and effective laboratory setup for heat cycling power cable screen connections. However, the projects did not evaluate whether heat cycling is a necessary test procedure for screen connections. The heat cycle procedure is inspired by the standard IEC-61238-1 "Compression and mechanical connectors for power cables for rated voltages up to 30 kV (Um = 36 kV)" [5], which provides a recommendation for heat cycle testing of power cable connectors.

The test procedure requires manual interaction and continuous monitoring of the laboratory setup throughout numerous heat cycles. It is uncertain whether the heat cycle procedure is necessary to completely evaluate the screen connections. Thus, this master thesis focuses on finding an effective test procedure as well as a reliable laboratory setup for testing screen connections. With this in mind, the following topics have been addressed:

- Finding an effective procedure for testing power cable screen connections. Two different test procedures will be evaluated. Compare and substantiate choice of load types and methodology when testing screen connections. The following test procedures were evaluated:
    - Heat cycle test
    - Constant current test

- Implementing reliable transition resistance measurements and temperature monitoring in the laboratory setup.

1.4 Power cable design

For better perception of the laboratory setup and screen connection installment, this chapter gives a brief explanation of power cable layout and design requirements.

TSLF cable

Several different types of XLPE cable constructions were developed in Europe and Norway throughout the 80's and 90's. The development of the 12/24 kV power cable in Norway has gone from paper insulated mass cable before 1980 to axially and radially waterproof XLPE cables with diffusion barriers in the form of aluminum laminate today.[1] To distinguish between different types of cable design and structures a four-letter code system has been developed:

- 1st letter: Type of insulation
- 2nd letter: Sheathing
- 3rd letter: Armoring, screen
- 4th letter: Exterior sheathing, corrosion protection

The cable used in this project is a 24 kV single aluminum core XLPE cable with a TSLF cable configuration that follows the four-letter code system. A short description of the TSLF configuration is explained in Table 1.1.

Table 1.1 TSLF power cable -configuration explanation. [6]

Code	1	2	3	4
TSLF	XLPE Insulation	Filler/taping and concentric conductor	Aluminum Laminate	Semi-conductive Polyethylene

Power cables with a TSLF cable configuration are the most commonly used power cables in onshore power grids today. The TSLF cable is also installed with an outer semiconductive layer that allows for electrical testing of the sheath and detection of damages. The XLPE insulation have a rated maximum temperature of 90 °C and emergency rating up to 140 °C. [1] An illustration of a TSLF Cu power cable and the different layers can be seen in Figure 1.3.

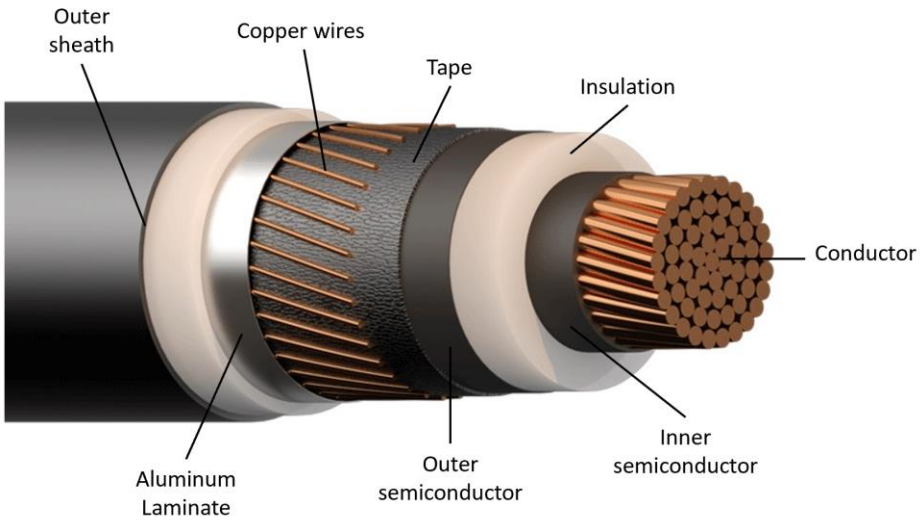

Figure 1.3. Illustrative sketch of the different layers in a TSLF cable.[7]

Cable screen

The cable screen is usually made of stranded copper wires which are twisted around the outer semiconductor. Its purpose is to define the electrical field over the insulation and serve as a conductor for capacitive currents in the cable. The screen also ensures as a safe return path for possible short circuit currents. The aluminum laminate is mainly applied to prevent radial water ingress in the cable that might cause water treeing in the XLPE insulation in addition to be a mechanical barrier.

The cross-section of the cable screen is based on several factors like short circuit current, residual current, circuit breaker trip-time and the length of cable sections. The electrical standard, CENELEC HD620, states that "provided there is electrical contact between the wire screen and the metallic tape its conductance may be regarded as part of the metallic screen". [8] Hence, the aluminum laminate may effectively become a part of the cable screen. This lets the manufacturer determine the cross section of the screen wires relative to the laminate.

The copper screen may be specified as, e.g. 35 mm^2 for a 24 kV cable with 240 mm^2 cross section, but the laminate (typical 0.2 mm thick) may also be included giving a reduced copper screen cross section. This implies that the effective equivalent copper screen cross section can be 21 mm^2 and the equivalent laminate copper cross section can be 14 mm^2 [9]. If the standard CENELEC HD620 and its corresponding Norwegian guidelines (part K) are followed, the screen cross section and resistance shall be designed according to requirements as shown in Table 1.2 and Table 1.3 [8].

Table 1.2. Minimum screen cross-section.[8]

Conductor cross-section mm²	Metal screen – minimum cross-section mm²		
	12 kV	24 kV	36 kV
25	16	16	-
35	16	16	-
50	16	16	25
70	16	16	25
95	25	25	25
120	25	25	35
150	25	25	35
185	35	35	35
240	35	35	35
300	35	35	35
400	35	35	35
500	35	35	35
630	35	50	50

Table 1.3. Minimum screen resistance. [8]

Area of screen mm²	Resistance of screen @ 20 °C maximum Ω/km
16	1,15
25	0,727
35	0,524
50	0,387

1.5 Electromagnetic background

As mentioned earlier, several comprehensive and expensive faults have occurred in the Norwegian power grid due to high currents and faults in power cable screen connections. This chapter gives a short description of the currents that can flow in the ground screen of power cables and how the currents are affected by the cable system configuration.

1.5.1 Screen currents

In the Norwegian distribution grid, it is common to ground the cable screen at each end of the cable length. As a result, a ground screen current will flow due to the voltage induced in the cable screen by the current in the cable conductor and surrounding current carrying objects. The main reason to ground the cable screen at both ends of power cables is to avoid contact voltage and the dangers this poses for personal safety throughout the distribution grid.

In medium and high voltage cable systems, single core cables are often installed instead of three-core cables. Under common service conditions, circulating currents flows in the cable screen of the power cables. For some cable system configurations, the screen and laminate current can reach magnitudes up to **5-35 %** of the load current. The circulating currents are divided into two parts; capacitive current and induced current.

Capacitive screen current

As the single-core cable act as a cylindrical capacitance, the high-voltage side of the capacitance is the cable conductor, while the low-voltage side is the cable screen coupled with the dielectric insulation. Depending on the permittivity of the insulation, a capacitive current is produced per unit length of the cable screen. [10]

For cable screens connected to ground at one end only, the total capacitive current is given by multiplying the current by the total cable length for each phase. For cable screens connected to ground at both ends, the capacitive current can flow in two directions toward the ground. This can be added or subtracted to the induced current to give an estimate of the total screen current. [10]

Induced screen current
According to Faraday's law an alternating current will create a magnetic field which will interact with surrounding electrical circuits and create electromagnetic induction. Due to the alternating load current in the cable conductor, as well as from the current in surrounding cables, a time dependent magnetic field will induce a voltage per length across the cable screen. [10]

The induced current appears in the cable screen if the screen is connected to earth at more than one point, leading to a circuit loop for the induced current. This inductive current, I_{screen}, can be found by dividing the induced screen voltage, U_{screen}, by the screen impedance, as shown in equation 2.1. [10]

$$I_{screen} = \frac{U_{screen}}{R_s - jX_s} \ [A] \tag{2.1}$$

Where R_S and X_S is the screen resistance and reactance, respectively. A sketch of the induced screen current in a single-core cable without the contribution from surrounding cables is shown in Figure 1.4.

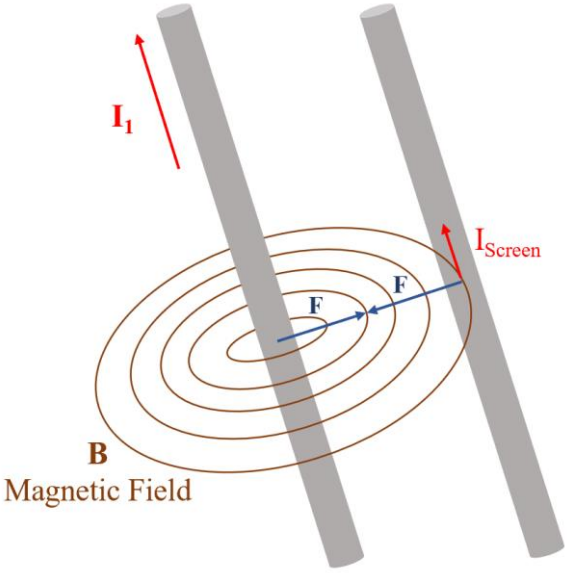

Figure 1.4. Illustration of induced screen current caused by alternating current in cable conductor. [4]

1.5.2 Laying configurations
Single core cables are usually laid in groups of three, causing the current in each cable to act mutually on each other. The calculation of the induced voltage and screen currents is complex and is affected by the load current, the physical construction of the cable, laying configurations and possible parallel current paths.

Two laying configurations are normally used for single core cable systems: Flat and trefoil cable configurations, see Figure 1.5. Flat configuration will provide additional spacing between the phases, giving better thermal conditions and raising the current carrying capability of the system. The increased spacing will however lead to an increased reactance between the cables, giving higher induced screen voltages and a higher screen current. [6]

Trefoil configuration is a more compact configuration compared to a flat configuration and have worse thermal conditions. It does however have less spacing, giving a reduction in the induced cable screen voltage. For the flat configuration the induced voltages will be largest and equal for the two outer phases, given equal spacing between the phases. For the trefoil configuration, the induced screen voltage will be equal in size for all three phases. [6]

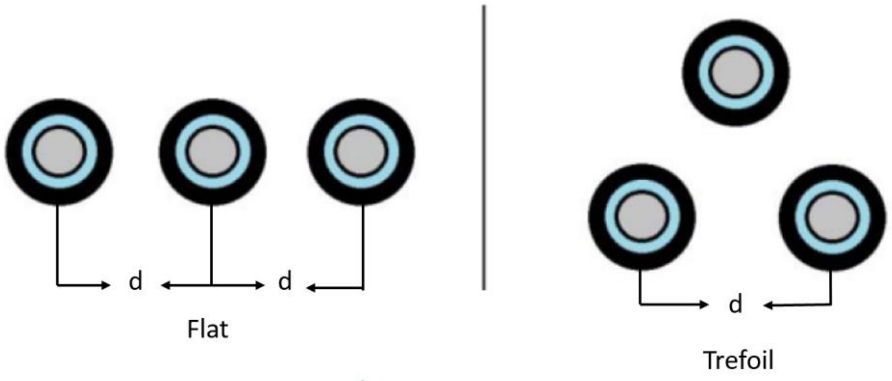

Figure 1.5. Single core laying configurations. [6]

Revolving and cross bonding

To reduce induced voltages and the losses caused by circulating currents, long cables lengths are often cross bonded and revolved. The method consists of dividing the cable length into three approximately equal sections with the cable screen connected and grounded at the ends of the circuit. In this way the induced voltage in each section is 120^{o} phase shifted. Thus, the summation of the phase shifted voltages reduces the overall induced voltage and circulating currents in the cable screen. Figure 1.6 illustrates the cross bonding and transposition of power cables. [11]

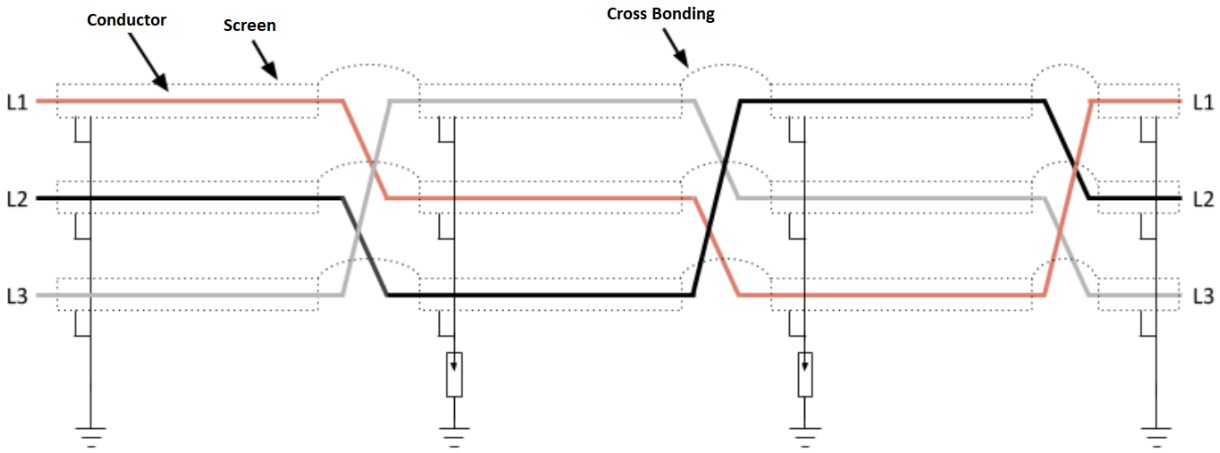

Figure 1.6. Cross bonding and revolving of power cables. [11]

The circulating current in each cable screen therefore depends on the following factors:

- Magnitude of the load current
- Laying configuration
- Cross bonding
- The spacing between each cable
- Impedance of the cable screen
- Surrounding cables and electrical circuits

In particular, large cable cross sections (> 240 mm^2) with high load currents and flat cable formation will induce high currents because of an increased inductivity. Calculations and laboratory measurements have shown that the current distribution between copper wire and aluminum laminate can be a problem. It is therefore important to ensure good electrical contact between the laminate and the screen at cable terminations and joints. If the cable is long, the distribution of the current in the Cu screen and the Al-laminate in the center of the cable will be determined by the electrical conductivity of the Cu screen and the laminate; typically about 1/3 of the screen current flow in the Al-laminate and 2/3 in the Cu screen. [3]

2. Theory & Literature

2.1 Cable jointing & Screen connections

When manufacturing power cables there are limitations to production lengths due to transportation and practical challenges. Power cables are therefore rarely manufactured in its full length to be used in the cable system which makes electrical contacts inevitable in any electrical system. If the cable system consists of long lengths, the cables are delivered in pieces which needs to be jointed at several locations along the full cable route. For medium voltage power cables (7.2-36 kV), the jointing is usually performed on-site during the installation of the cable. The jointing is performed manually by an authorized installer and the quality of the joint therefore strongly depends on the performance of the installer. [6]

The most used cable joints use heat shrinking or cold shrinking methodology. Heat shrink joints consists of several layers that are placed in a given order before being shrunk and fixed with the help of a blow torch. Cold shrink joints consist of kits with one body which contains all the individual layers in a heat shrink joint. The joint body is then shrunk in place by removing a spiral from the inside of the joint body. Both methods use the same principle where the conductor is spliced and covered with protective layers of insulation before the cable screen is jointed and placed across the conductor. Usually the screen is jointed at each side of the conductor splice with a joint screen laying across the conductor splice. A picture showing the principle of a cable joint is shown in Figure 2.1. [6]

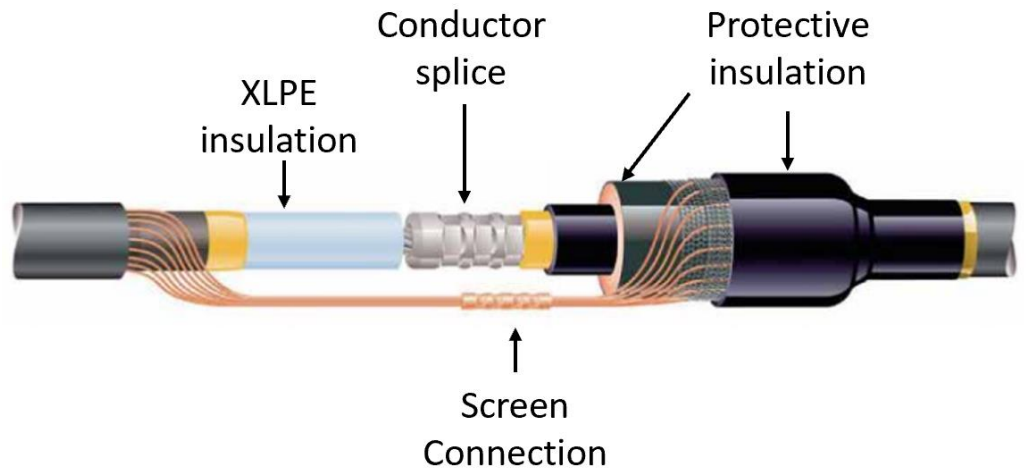

Figure 2.1. Principle sketch of a power cable joint. [12]

TSLF cables includes the aluminum laminate which makes it more complicated to perform jointing of the cable. Since the aluminum laminate may effectively become a part of the cable screen cross-section it is important that the jointing of the cable screen provides a good connection between the cable screen and the aluminum laminate. Cable and joint manufacturers use different methods for connecting the laminate and the cable screen wires at joints and terminations. The most common methods are [13]:

- **Constant force springs:**
  Thin strip of steel with constant width and thickness rolled into a spiral. Maintains a radial constant force all the way around the cable screen. This force spring is used to clamp the screen wires, aluminum laminate and the joint screen together.

- **Soldering:**
  The aluminum laminate is carefully cleansed and treated before a tinned copper lace is applied and soldered to the aluminum. The copper lace is connected to the screen wires and joint screen with the help of a contactor.

- **Contact sheets:**
  A contact sheet made out of conductive material is placed between the aluminum laminate and the screen wires. The contact sheet has spikes that pierce the aluminum laminate when being clamped to the cable. The contact sheet also comes with pre-attached copper wires which are connected to the cable screen wires and the joint screen with the help of contactors.

- **Clamp rings**
  The aluminum laminate is carefully cleansed and treated before a clamp ring is placed under the laminate. A second clamp ring is placed over the aluminum laminate and tightened to make good contact. One of the clamp rings is equipped with a copper lace that is connected to the screen wires and the joint screen with the help of contactors.

2.1.1 Constant force springs

This report focuses on constant force springs or "spring rolls", which have previously led to malfunction of power cables, see [1]. A constant force spring is designed to maintain a radially constant force all the way around the screen of a cable. The main task of the force spring is to maintain good contact between the cable screen and the joint screen at joints or terminations. It is made up of a thin strip of steel with constant width and thickness rolled into a spiral. The clamp is easily applied by rolling the clamp around the cable screen and joint screen without a need for special tools or soldering. Examples of different sizes of constant force springs are shown in Figure 2.2. [6]

Figure 2.2. Different sizes of constant force springs made out of steel. [6]

Different suppliers utilize the force springs in different ways in their joint designs. Some manufacturers use two force springs per screen connection, four per joint (two on each side of the joint). One of the force springs is mounted directly on the outer sheath. Cu wires from the cable and the joint screen are then placed together over the force spring and a new, larger, force spring is applied directly over the first clamp and the cable screens. [6]

Another type of joint design use only one force spring per screen connection (two per joint). One round of the force spring is laid directly on the outer sheath of the cable. The Cu wires and the joint screen are then placed together on the force spring so that the rest of the spring can be rolled over to apply pressure on the screen connection [6]. A detailed description of the installation method that is used in this thesis is given in Chapter 3.1. Both methods use the same principle and an illustration of a correct installation is shown in Figure 2.3.

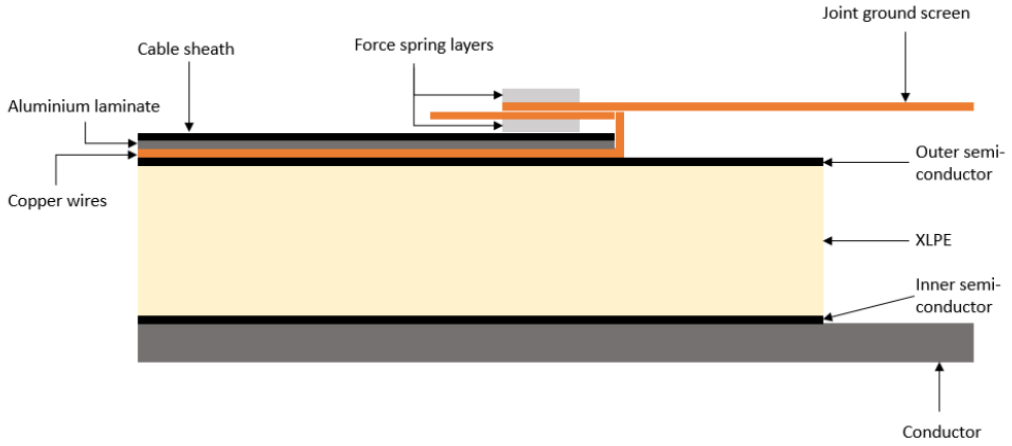

Figure 2.3. Sketch of constant force spring installation. [6]

2.2 Electrical contacts

The main purpose of electrical contacts is to pass a current between two electrodes as if they were a continuous conductor. This chapter is meant to give an overview of basic theory behind stationary electrical contacts and to give an idea of how a good contact should be made.

Irrespective of the area of application, every electrical contact must fulfill the following requirements [14]:

- **The electrical contact must be an almost perfect electrical conductor.**
  Because of Ohmic losses in the electrodes and the current carrying components, heat is generated in the contacts. The heat causes the temperature to rise, so to obtain a high rated load current a low resistance in the contact is necessary.

- **The electrical contact must be capable to carry all possible currents that may flow through the network.**
  In event of a fault in the cable network a short circuit current may pass through the contact over a short time. Consequently, currents that can pass through the contacts are either high currents for a short time or continuous load currents for long times.

2.2.1 Stresses on electrical contacts

Mechanical stress

At a short circuit event it takes at least a few power cycles to open the cable system circuit breaker and clear the short circuit current. During this period, the electrical contacts are exposed to high mechanical forces generated by the short circuit current. The electromagnetic force or Lorentz force, **F,** is given as the vector product of current density, **J**, and magnetic flux density, **B**, as seen in equation 2.2. [14]

$$F = J \times B \qquad [\mathrm{N}] \tag{2.2}$$

As the flux density is proportional to the current, the Lorentz force between two electrical conductors are proportional to the current squared.

Thermal stress

Short circuit currents lead to a short-term heating of the cable system. However, it is the continuous rated load current that is the main cause for thermal stress in electrical contacts. The energy dissipated due to the electrical resistance of contacts, joints and terminations in the cable system is the primary heat source. It is therefore crucial that the connection design minimizes contact resistance and carries heat away efficiently to avoid unacceptably high temperatures. In addition to this, heat may also be generated by eddy currents and/or hysteretic losses in the ferromagnetic materials. [14]

2.2.2 Contact resistance

Electrical contacts are designed to transmit electrical currents or signals across two separable electrodes with as few changes to the signal as possible. However, because of electrical resistance the signal will lose some of its power along the way. There are two types of resistance that the signal will come across: bulk resistance and contact resistance. [15]

Bulk resistance

Bulk resistance is the electrical resistivity of the material along the current's path. Electrical resistivity is a fundamental property of materials used for conducting electrical currents. The resistivity quantifies how strongly the material opposes the flow of electric current, and a low resistivity indicates that the material allows the flow of current. For an ideal case, the cross-section and the physical composition of a conductor are uniform across a sample and the resistance in the cable can be determined by equation 2.3.

$$R = \rho \frac{l}{A} \quad [\Omega] \tag{2.3}$$

Where R is the electrical resistance of a uniform sample of the conductor, l is the length of the sample and A is the cross-sectional area of the sample. ρ is the resistivity of the conductor material. [6]

Contact resistance

While bulk resistance is a constant value, the contact resistance is a variable resistance that occurs at the interface between two contact surfaces. Contact resistance is made up of *constriction resistance* and *film resistance* and is dependent upon the contact force between the two surfaces in contact. An ideal electrical contact would have a resistance corresponding to only the bulk resistance of the electrodes. [15] An illustration of an electrical signal through two separable conductors is shown in Figure 2.4.

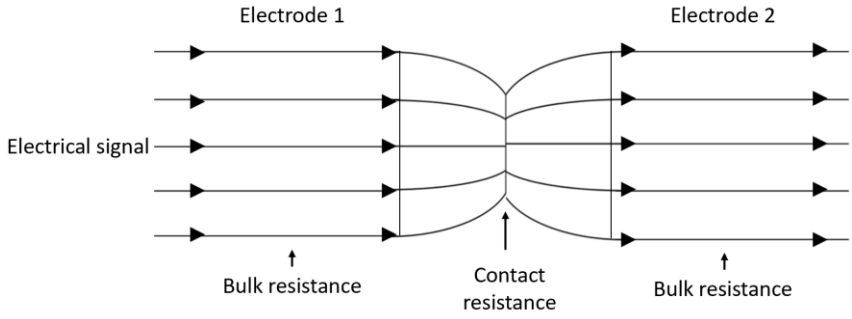

Figure 2.4. Sources of electrical resistance in an electrical contact. [16]

When looking at electrical contact between two electrodes, the area which seems to be in physical contact between two electrodes is called the *apparent contact area*, A_a. However, the electrodes have a rough surface in a microscopic point of view with small peaks and valleys. The two mating surfaces will make contact with each other only where the surface peaks meet. These contact points are called asperities or A-spots. The total sum of these A-spots is known as the *load bearing area*, A_b. The load bearing area is only a fraction of the apparent contact area and can be represented by the mechanical load and the hardness of the electrodes, as shown in equation 2.4. [15]

$$A_b = \frac{M}{H} \quad [m^2] \tag{2.4}$$

Where H is the hardness [N/m^2] and is a measure of materials ability to oppose plastic deformation. M is the mechanical load [N]. It can be seen from equation 2.4 that given a certain force the small roughness in the electrodes can be deformed gaining a bigger load bearing area. [15]

Further, the actual *conducting metal-to-metal area,* A_C can be considerably smaller than the load bearing area. Film resistance is created by thin layers of oxides and dirt that form material surfaces on the contact electrodes. The insulating film layers have higher resistivity than the electrode material and increases the contact resistance. The conductive area, A_C, can be increased by applying enough force or by applying sufficient voltage between the electrodes so that the oxide-layers gets pierced. An illustration of the different contact areas in an electric contact are shown in Figure 2.5. [15]

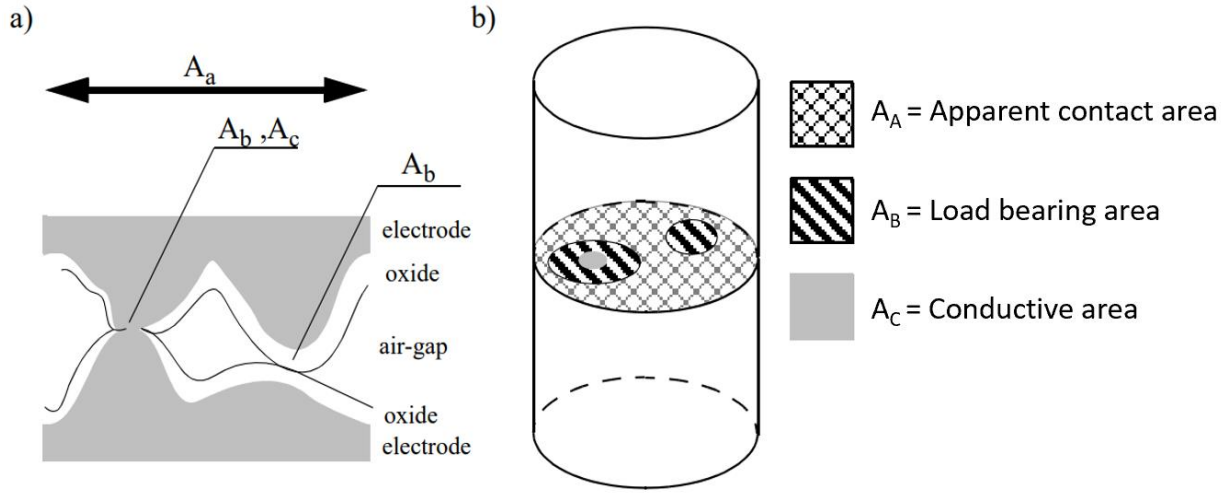

Figure 2.5. a) Cross-section of surface roughness and oxide layer. b) Transparent cylindrical electrodes in contact. [15]

The reduced contact area, A_C, caused by the microscopic roughness of the electrode surfaces constricts the lines of current which makes them deviate from a straight line. This effectively increases the resistance between the electrodes beyond the case of a fully conducting apparent contact surface. This is called *constriction resistance,* R_C, and depends on the number, the dimensions and the condition of the small asperities/A-spots between the electrodes. These small conductive bonds will cause the current to divide into several flow lines like shown in Figure 2.6. [15]

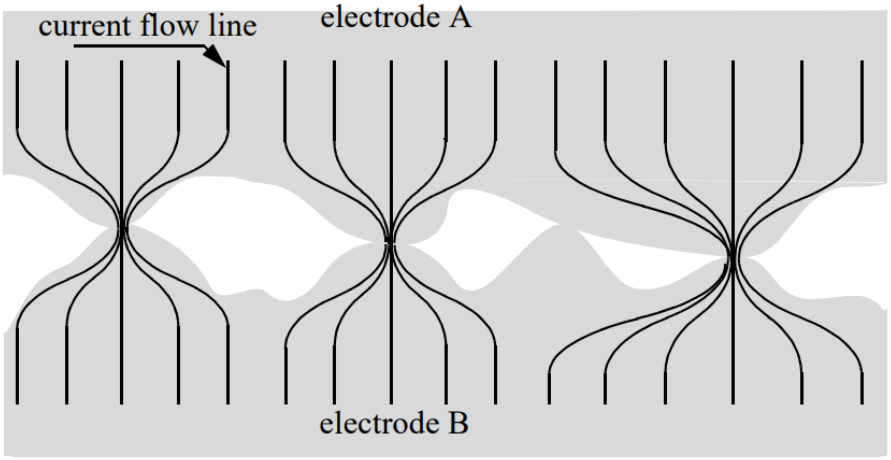

Figure 2.6. Current flow lines caused by microscopic contact points (A-spots). [15]

2.2.3 Contact resistance as a function of pressure

By increasing the pressure and mechanical force between the electrodes in an electric contact, the Hertz stress (highly localized stress created by contact) experienced by the areas in contact will increase. This introduces highest forces on the A-spots between the interfaces which again will cause the peaks in contact to yield. The mating surfaces will then move closer together, causing the A-spots to become shorter with wider peaks and expanding the contact area in an effort to counter the additional pressure. [16]

Since the asperities are wider, the current can more easily pass through any oxide layer that might still exist between the electrodes. Therefore, the film resistance and constriction resistance decrease as well. Figure 2.7 shows how the increased force allows the current to travel across the interfaces more easily. Conversely, if the contact pressure decreases, some of the asperities will lose their contact. In this situation, film resistance and constriction resistance becomes the dominant component of overall contact resistance. [16]

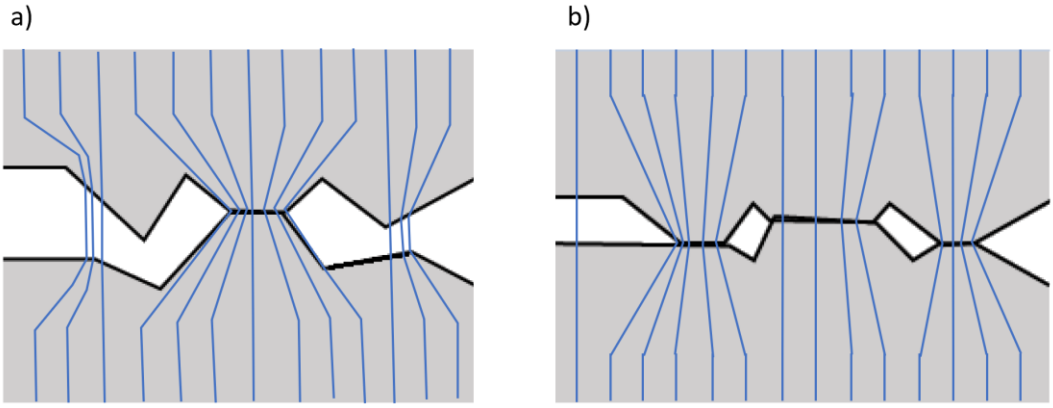

Figure 2.7. Effect of increased contact pressure on constriction resistance. a) low pressure contact b) high pressure contact [16]

Using the load bearing area, A_b, as the functional area in an electrical contact, pressure can be introduced when calculating contact resistance. By combining the general equation for electrical resistance in equation 2.3, with the equation for load bearing area in equation 2.4, contact resistance can be calculated by equation 2.5.

$$R = \frac{\rho \cdot l \cdot H}{Pr} \quad [\Omega] \tag{2.5}$$

Assuming that the hardness of the material is constant across the conductor, the resistance will be a function of pressure, Pr, in the electrical contact and equation 2.5 can be written as equation 2.6: [17]

$$R = kPr^{-x} \quad [\Omega] \tag{2.6}$$

In equation 2.6, the variable x indicates the type of deformation the contact experiences. For elastic deformation x is $\frac{1}{3}$, for plastic deformation x is $\frac{1}{2}$. k is determined mainly by the hardness and the resistivity of the electrodes. An illustration of contact resistance as a function of pressure is shown in Figure 2.8. [17]

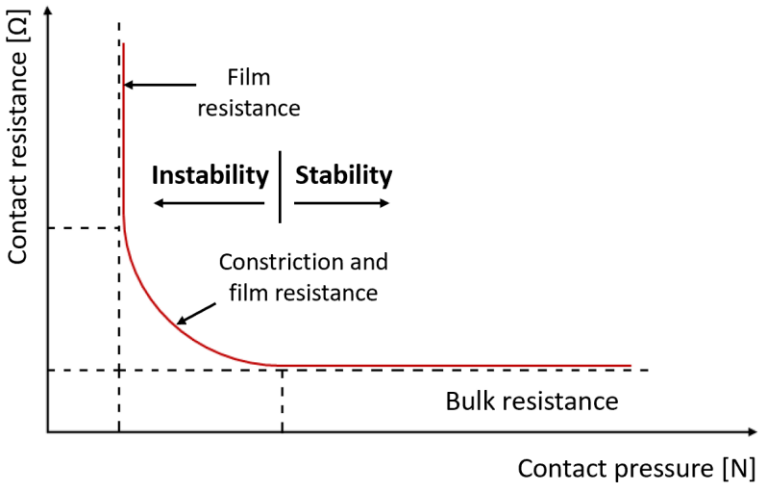

Figure 2.8. Illustration of contact resistance varying as a result of changing pressure. [16]

Figure 2.8 shows how the film resistance approaches infinity if separation between the electrodes continues to increase (i.e. normal force drops to zero). At low pressure the contact resistance is unstable since a small change in force can result in a large change in resistance. At very high pressure, most of the total electrical resistance comes from the bulk resistance. This causes the resistance to be stable since a small change in force will result in a minimal change in contact resistance.

Electrode surface treatment

Contact force is an important factor to obtain low contact resistance and stability in electrical contacts, but surface treatment of the contact surfaces has also proved to be an important factor. Figure 2.9 show results from experiments between aluminum conductors. Two 9 mm Al cylinders were placed together, and the contact resistance were measured as a function of contact force and surface treatment. [18]

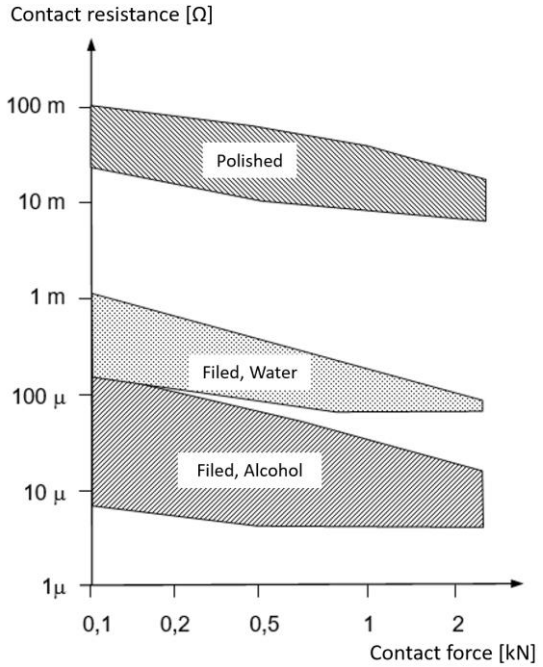

Figure 2.9. Contact resistance as a function of surface treatment and contact force between 9 mm aluminum cylinders. [18]

The shaded areas show the spread of many measurements with test objects that has the same surface treatment. Contacts with polished (smooth, slick) surface have contact resistances that is 2-4 decades higher than between filed (rough) surfaces. The difference between the water cleansed surfaces and the alcohol cleansed surfaces is because that the oxide film layer builds thicker when water molecules binds with the aluminum oxide. Thus, enforcing the oxide layer making it more resistant to mechanical stresses. [18]

In this case surface treatment proved to play a bigger part than the contact force between the electrodes. An increase in contact force from 100 N (already a considerable force) to 2500 N only gave a modest reduction in contact resistance. [18]

2.2.4 Degradation mechanisms

Knowledge about the mechanisms causing aging and degradation is of fundamental importance for the design of contacts and the testing of screen connections. An electric contact can deteriorate due to mechanical movement rupturing the A-spots, or chemical and physical reactions creating oxide layers with poor conductivity.[17]

Cyclic relative movements

If one of the electrodes move relative to the other in a direction parallel to the contact area, the initially formed A-spots lose their contact. However, at the same time new A-spots may be formed. Unidirectional movement usually favours rupture of the oxide layer which leads to a reduction of the contact resistance. [17]

NTNU has previously performed a study of the fundamental factors affecting the initial contact resistance and the degradation mechanisms for contact between aluminum and copper conductors, see [17].

Experiments showed that small relative cyclic movements between the contact electrodes can introduce a strong increase in the contact resistance. The movements can develop due to thermo-mechanical forces at temperature and load variations, or by forces/vibrations transferred from the conductors close to the contacts. Cyclic movements can, for a period of time, reduce the contact resistance. However, the small movements cause the asperities between the electrodes to wear and break. A layer of oxide or heavily oxidized metal fragments forms on the load bearing area, thus increasing the contact resistance over time. This phenomenon is called *fretting corrosion*.

Figure 2.10 shows contact resistance against number of cycles for contacts between copper electrodes. The figure shows measurements carried out for material movements of ± 4 µm and contact forces of 20 and 60 N.

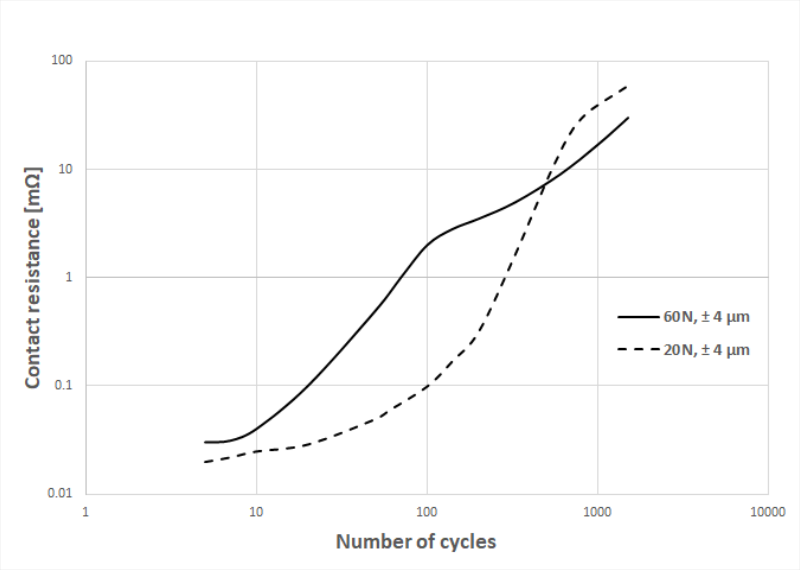

Figure 2.10. Contact resistance against number of cycles for contacts between Cu electrodes at amplitude ± 4 µm and mechanical loads 20 and 60 N. [17]

The resistance after one thousand cycles was approximately one thousand times the initial value. This indicates that the detrimental effect of cyclic movement is a higher contact resistance. Similar results were found for aluminum contacts. [17]

Chemical reactions

Various oxidation and corrosion processes that take place at the electrode interfaces causes growth of high resistivity oxide layers and impurity. A contact that experience moist or other corrosive environments is more exposed than contacts in a dry and clean environment. A factory hall with large concentrations of SO_2, H_2S, HCl, welding gases, dust and other contaminants in the air is a typical example of such a corrosive environment. [18]

Different materials

Various metallurgical processes can wear on electrical contacts that uses different metals. Diffusion can cause intermetallic phases (alloys) to form at interfaces between different metals. The conductivity of such phases is often very poor. [18]

In general, one can say that contacts between different metals should be avoided. Different electrochemical potentials may provide galvanic currents and rapid degradation. Different thermal expansion in the metals may also cause sideways displacements in the contacts. Other "incompatibility effects" may also occur. [18]

2.3 Consequences of increased temperature

2.3.1 Electrical resistivity

Material properties depends on temperature and so does the material resistivity, ρ. Material resistivity as a function of temperature can be calculated by equation 2.7.

$$\rho = \rho_0(1 + \alpha(T - T_0)) \quad [\Omega m] \tag{2.7}$$

Here, ρ_0 is the material resistivity at a temperature, T_0, of 0 °C. The temperature coefficient of resistivity, α, gives the increase in resistivity per centigrade. The equation shows how the electrical resistivity increase when the temperature increases over 0 °C. Figure 2.11 shows how the electrical resistivity for copper vary with temperature. ρ_0 and α for copper are 15.4 and 0.00451, respectively. [19]

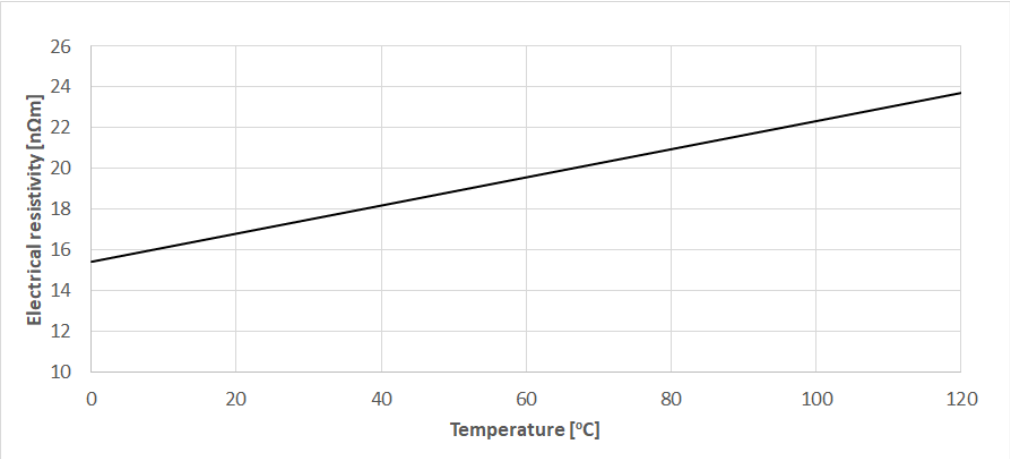

Figure 2.11. Electrical resistivity of copper as a function of temperature.

By combining equation 2.7 with the general equation for electrical resistance, equation 2.3, the overall resistance in a contact or conductor will change with temperature. Considering how the resistance in an electrical contact also depends on pressure, the electrical resistance in an electrical contact will be directly dependent on both pressure and temperature.

2.3.2 Volume expansion and contraction

Thermal expansion is defined as the general increase of a materials length, area or volume as its temperature is increased. The extension of a material length due to thermal effect can be expressed by equation 2.8. [20]

$$\Delta L = L_0 \cdot \beta \Delta T \quad [m] \tag{2.8}$$

ΔL is the length extension, L_0 is the original length, β is the coefficient of thermal expansion and the ratio of the fractional change of size in a material caused by its change in temperature, ΔT.

Different materials have different thermal behavior which have to be taken into account when designing cables and accessories for cable systems. This is an important step since it significantly affects performance and reliability of the whole cable network. The coefficients of linear thermal expansion for relevant materials are shown in Table 2.1. [21]

Table 2.1. Coefficient of thermal expansions for relevant materials in the temperature range 20-100 °C. [21]

Material	Coefficient of thermal expansion, β [m/km K]
Aluminum	0.023
Copper	0.017
Steel	0.012
XLPE	0.2-0.4

The coefficients mentioned in Table 2.1 demonstrate that a 50 K (°C) increase in temperature would increase the unconstrainted length of a copper conductor by 0.85 m/km. Using the coefficient for XLPE expansion the length would increase with 15 m/km, meaning the XLPE insulation can expand 20 times as much as copper. Material expansion as a function of temperature for copper and XLPE is shown in Figure 2.12. [21]

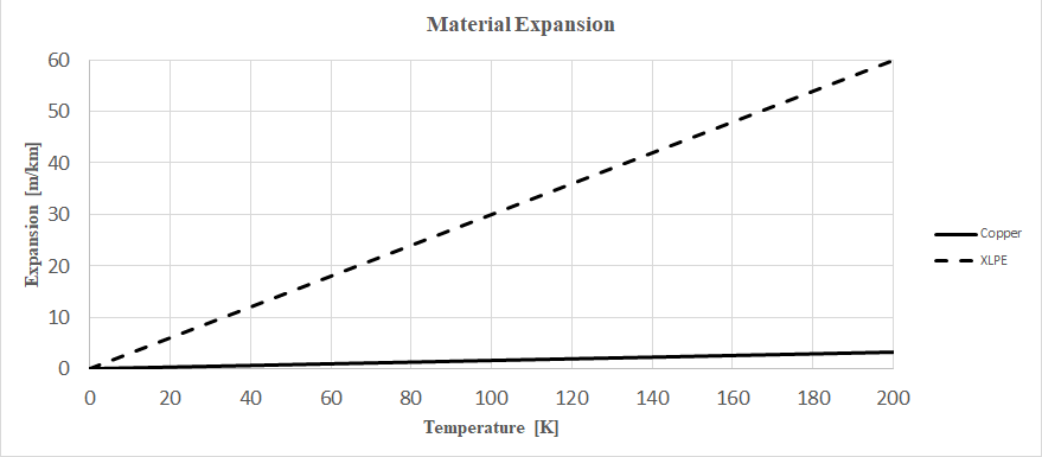

Figure 2.12. Material expansion as a function of temperature for copper and XLPE.

The variation of volume and length will have a resulting mechanical force on the cable system and the installed accessories. The force due to an extension of a cable conductor is expressed by equation 2.9. [20]

$$F_{Thermal} = \frac{E \cdot A \cdot \Delta L}{L_0} = E \cdot A \cdot \beta \cdot \Delta T \quad [\text{N}] \tag{2.9}$$

Where $F_{Thermal}$ is the theoretical force at the end of a cable sample, E is Young's modulus of the conductor material (modulus of elasticity), A is the conductor cross-section area and β is the expansion coefficient.

If a cable termination or related blocks the temperature expansion of a cable, the theoretical force is proportional to the cross-section of the conductor. In theory forces up to 30 kN could be exerted on a joint or termination of a 240 mm^2 aluminum cable. [20]

Volume expansion and radial force in force springs

Screen connections will also be affected by radial expansion of the cable insulation, meaning the volume expansion is of most interest. Volumetric expansion, ΔV, is a combination of the increase in length and area of the material caused by increased temperature and is approximately three times the linear expansion, ΔL. The ratio arises because volume is composed of three mutually orthogonal directions. As an example, the volume of a cube of steel that has side lengths, L will have a volume that equals L^3. [22]

The forces that is exerted on the force springs that is used in this project mainly consist of the radial force going outwards from the XLPE insulation, not the forces that is caused by the longitudinal extension of the cable. This is because of the short cable lengths and the coefficient of thermal expansion in the different layers of the screen connection.

Therefore, it is the expansion of cross-sectional area of the cable that is of most interest when calculating the radial force in the screen connections. It can be seen from equation 2.9 that the induced force is independent of the initial material length but varies with area. By using the surface area beneath the screen connections, the radial force exerted from the cable conductor and the XLPE insulation can be approximated by equation 2.9. Figure 2.13 shows an illustration of the radial forces caused by thermal expansion in a XLPE power cable.[22]

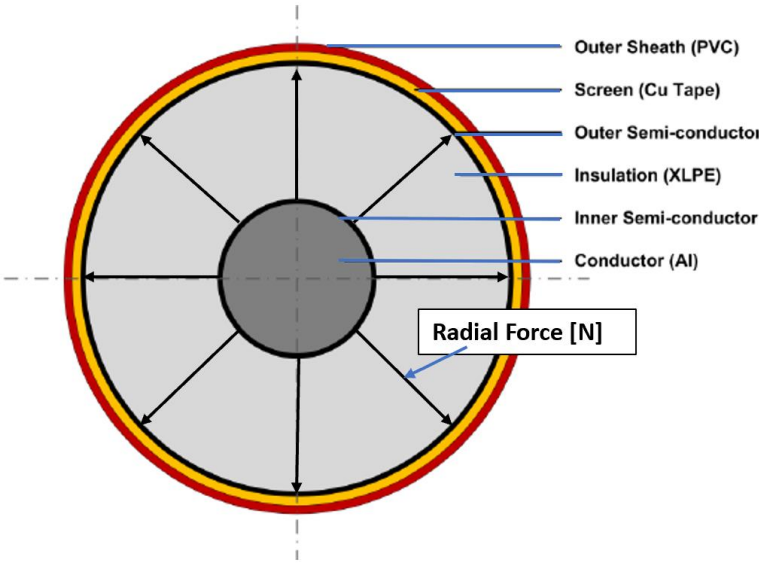

Figure 2.13. Illustration of the radial forces caused by thermal expansion in a XLPE power cable. [23]

Since the XLPE insulation can expand as much as 20 times more than copper and the steel that is used in the force spring, this phenomenon can have a large effect on the mechanical forces inside of a screen connection.

Contraction of cable insulation

When applying varying loads to a cable system the contraction of the cable materials also needs to be taken into consideration. As the volume of the conductor and insulation in a cable will expand with increased temperatures, reversibly it will also shrink when the temperatures decrease. The laboratory experiments conducted in the summer project “Fault mechanisms of incorrectly installed force springs” experienced loosened voltage measuring points, as a result of expansion and contraction of the XLPE insulation. When installing the laboratory setup a robust solution was chosen for the voltage measuring points so that the equalizers would not loosen by the expansion of the XLPE insulation. [3]

The equalizers did not loosen because of the radial forces that were exerted from the XLPE insulation. However, since the copper wires did not expand as much as the insulation (Table 2.1), the insulation was pushed on each side of the voltage point and deformed at the point of the equalizer. When the load cycles were turned off and the temperature in the system decreased the insulation started to shrink at the point of the equalizers, effectively loosening the voltage measuring points. [3]

The same phenomenon can have a significant impact on screen connections, especially screen connection types like force springs. When the temperatures are high and the thermal expansion are at its biggest, so will the forces inside of the force spring be. If the cable temperature is decreased again, so will the thermal expansion of the material inside of the screen connection. This can cause a loss of mechanical force inside of the screen connections which leads to increased contact resistance. [3]

3. Method

This chapter gives a description of the experimental work performed in this project. This includes a detailed description of test object preparations and the laboratory setup used to evaluate the test objects. Finally, the test procedures are explained and reviewed.

3.1 Test object preparation

This thesis addresses and evaluates test procedures for power cable screen connections. The purpose of the test procedures is to apply currents and stress screen connections to make sure that reliable power cable screen connections are installed to joints and terminations in the electrical distribution grid.

As mentioned in chapter 2.1, there are several methods used to joint the screen in cable joints and terminations, and one of the most common methods is constant force springs. This report focuses on constant force springs or "spring rolls", which have previously led to malfunction of power cables, see SINTEF's dissection report [1].

To be able to evaluate the effect and the impact of the different test procedures, transition resistance and temperature were measured over several force spring screen connections throughout the test cycles. The test procedures introduce load currents to the conductor and screen currents which would produce temperatures that a normal cable system could experience.

3.1.1 Test object definition

A test object is defined as *one force spring screen connection in a cable joint*. Every cable joint has one screen connection on each side of the conductor splice, meaning there is two test objects (screen connections) per cable joint in the laboratory setup. The transition resistance over the test objects were measured by placing voltage measuring points on each side of the force spring, and temperature were measured by inserting thermoelements inside the force springs as seen in Figure 3.1.

A detailed description of the transition resistance measurement and temperature monitoring is given in chapter 3.2.2 and 3.2.3.

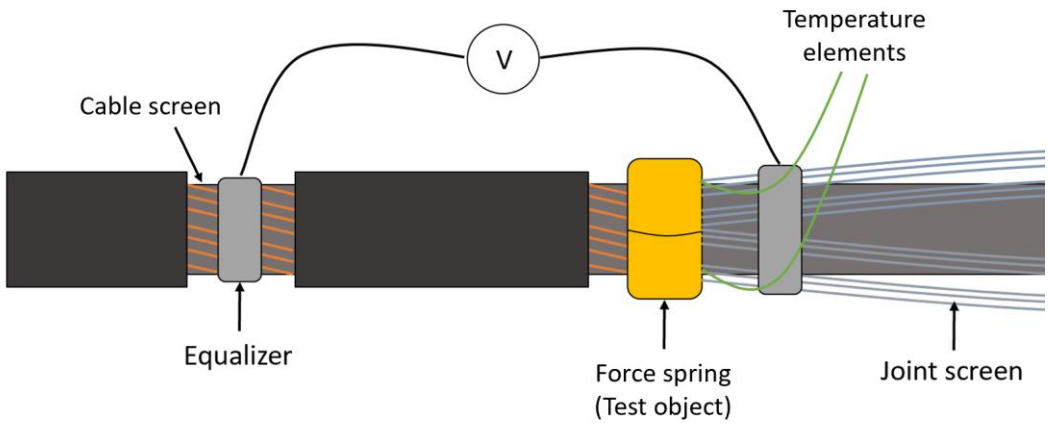

Figure 3.1. Illustration of a test object equipped with voltage and temperature measurement.

All test objects were installed in the same way with identical dimensions, materials and distances for easier comparison of measured values. A dimension sketch of a cable joint with two test objects and voltage measuring points (equalizers) for transition resistance measurement is shown in Figure 3.2.

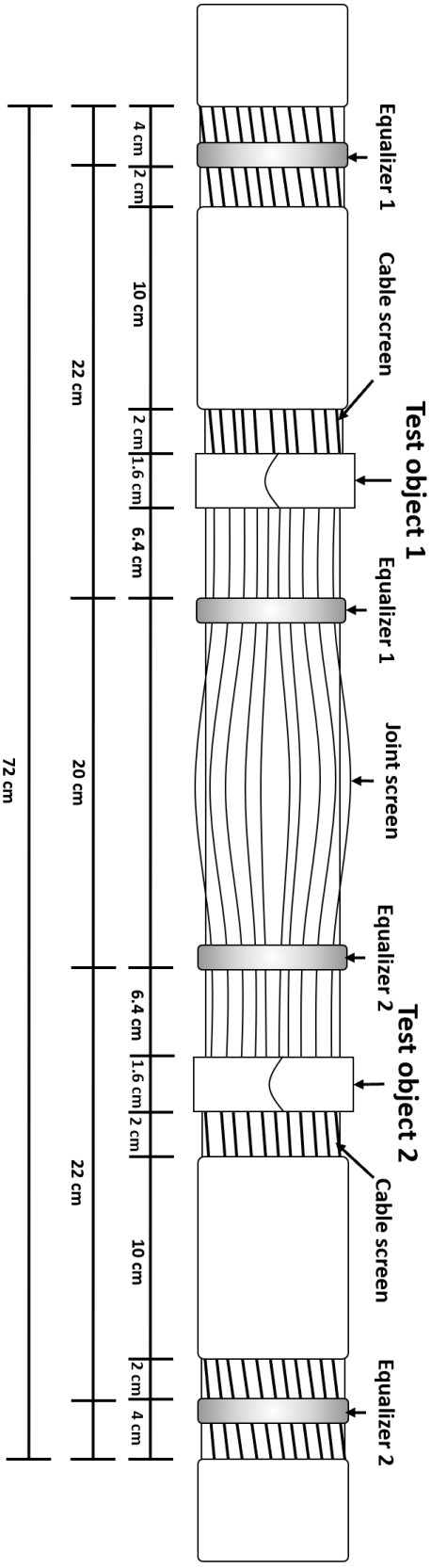

Figure 3.2. Dimensions of a cable joint with two test objects.

As seen in Figure 3.2 there is no conductor splice between the screen connections in the cable joint. Previous experiments performed in the summer project "Fault mechanisms of incorrectly installed force springs" experienced high temperatures in the conductor splices which affected the test object temperatures [3]. The influence from the conductor splices was not a desired effect because it made it harder to process test object measurements. To avoid this from happening in this project, the conductor was not spliced along the whole test setup and only the screen was cut and jointed in the "cable joints".

3.1.2 Installation of test objects

This chapter gives a detailed description on how the test objects were installed in the laboratory setup.

The test objects consist of the type of force spring where there is only one force spring per screen connection (two per joint) and follow the method explained in chapter 2.1. The dimensions of the force springs that were used are given in Table 3.1.

Table 3.1. Test object dimensions.

	Dimension
Inner diameter	24.0 mm
Outer diameter	29.0 mm
Width	16.0 mm
Thickness	0.4 mm
Length	505.0 mm
Min cable diameter	31.0 mm
Max cable diameter	50.0 mm

The joint screens used in the cable joints were braided screens with tinned copper wires and had a cross section of 35 mm^2. The joint screens belong to the same screen connection kit that the force springs were collected from.

Equipment:

- Constant force springs
- Braided joint screen, 35 mm^2
- Insulation tape
- TSLF 24 kV Al 240 mm^2/35 mm^2 power cable

Step by step installation:

1. The outer sheath and the aluminum laminate of the TSLF cable was stripped and the cable was prepared following the dimensions given in Figure 3.2.

2. The cable screen was cut at the middle of the cable joint and pulled back over the TSLF cable.

3. One round of the force spring was rolled over the outer semiconductor of the cable 2 cm from the stripped cable sheath.

4. The cable screen was bent across the force spring and cut 1 cm outside of the force spring.

5. The joint screen was applied to the cable and then placed on top of the cable screen wires and the force spring.

6. The rest of the force spring was rolled over the cable screen and the joint screen and tightened.

7. The joint screen was bent back over the force spring again before the wires were taped with insulation tape to cover sharp edges.

8. Another test object following the same procedure was placed on the opposite side of the "cable joint" making it two test objects per cable joint.

A figure illustrating the installation procedure and the cross section of a test object are shown in Figure 3.3.

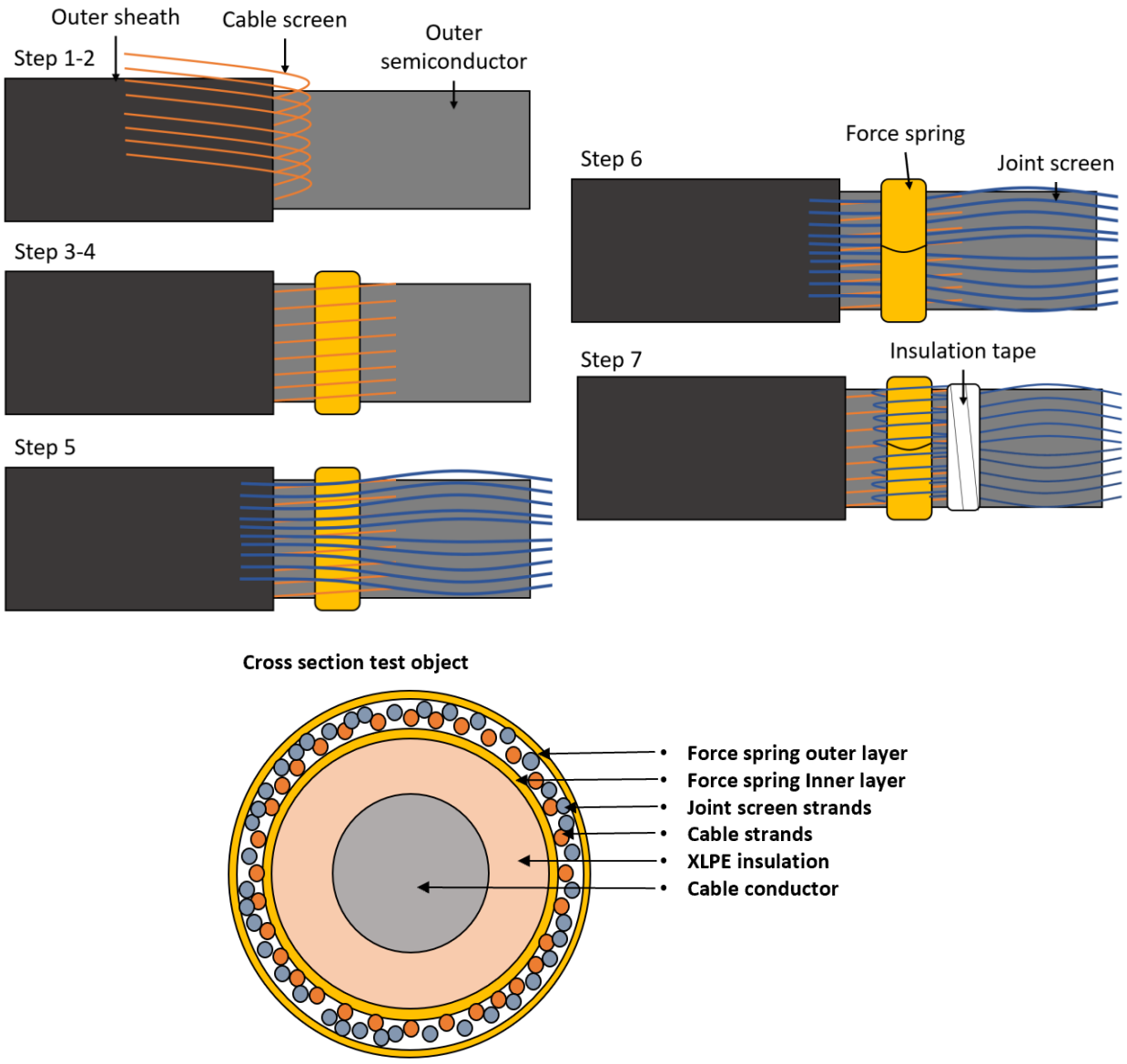

Figure 3.3. Illustrations of the installation method and cross section of a test object.

A picture of a cable joint with two installed test objects can be seen in Figure 3.4. The test objects had not been equipped with equalizers and thermoelements in this picture. Notice that the conductor has not been spliced in the cable joint, only the cable screen.

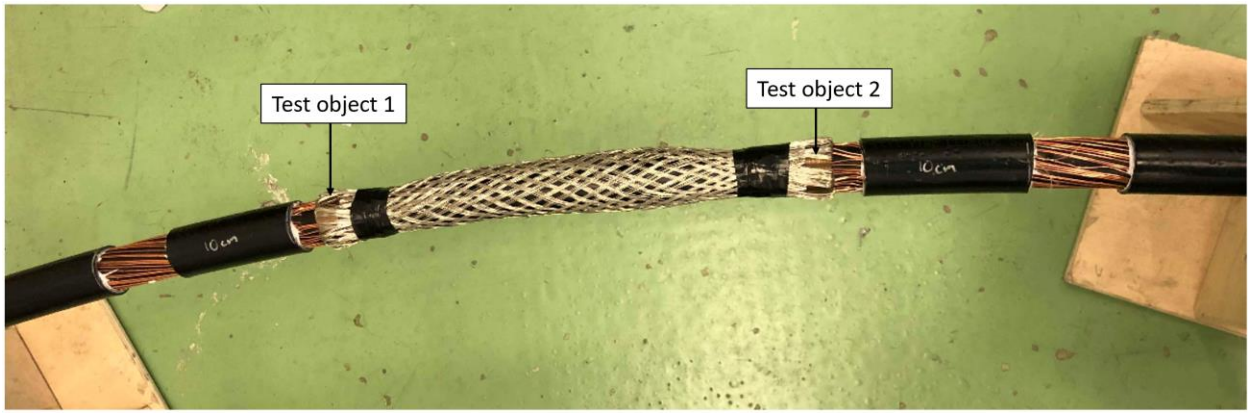

Figure 3.4. Picture of a cable joint with two test objects. Equalizers and thermoelements for transition resistance measurement and temperature monitoring had not been installed in this picture.

3.2 Experimental setup

This thesis evaluates two different test procedures for power cable screen connections, a heat cycle test and a constant current test. To be able to evaluate the test procedures independently, two individual laboratory setups were to be made. It was important that both laboratory setups were made as identical as possible with the same dimensions and properties to be able to compare results from the different test procedures. Selected pictures from the experimental setup are given in Appendix C.

Two independent but identical laboratory setups were made with three cable joints per setup. Since there are two test objects per cable joint, this gives six test objects per test setup, twelve in total. An overview of the laboratory setups and the test objects are given in Table 3.2.

Table 3.2. Overview of laboratory setup and test objects.

Laboratory setup 1 – Heat cycle test			**Laboratory setup 2 – Constant current test**		
Cable joint 1	Test object 1	1.TO-1	**Cable joint 1**	Test object 1	2.TO-1
	Test object 2	1.TO-2		Test object 2	2.TO-2
Cable joint 2	Test object 3	1.TO-3	**Cable joint 2**	Test object 3	2.TO-3
	Test object 4	1.TO-4		Test object 4	2.TO-4
Cable joint 3	Test object 5	1.TO-5	**Cable joint 3**	Test object 5	2.TO-5
	Test object 6	1.TO-6		Test object 6	2.TO-6

Incorrect force spring installation and cable screen

By looking at the correct way to apply a force spring in Figure 2.3, Chapter 2.1, the cable screen should have been rolled back on to the outer sheath of the power cable, not the outer semiconductor like the test objects in this project were. This was a mistake and is an incorrect way of installing the screen connections. However, the mistake was not considered critical to make a conclusion in this thesis. Since all of the test objects from both test procedures were installed in the same way it was still possible to compare and evaluate results from different the test procedures. The incorrect installations also made it possible to see if this would have any particular impact on the ampacity of the force spring screen connection compared to a correct installation.

It can also be noticed that the aluminum laminate in the power cable was cut and removed from where the cable sheath was stripped. As mentioned in Chapter 1.4, the aluminum laminate is a part of the cable screen and by removing it, the cross section of the cable screen gets reduced in these areas of the cable. This was done to simplify test object installation and resistance measurements over the test objects. The ampacity of the test objects and cable screen was still considered high enough for the current magnitudes used in this project.

3.2.1 Current sources and cable layout

The cable used for testing was a 24 kV 240 mm^2 / 35 mm^2 aluminum TSLF cable with the dimensions given in Table 3.3. It was reasonable to use this TSLF cable design with aluminum laminate and copper screen wires as it is a typical design used in the Norwegian distribution grid and will be used in the standardized tests for cable screen connections. Also, because of restrictions with laboratory equipment a 240 mm^2 conductor gave suitable dimensions.

Table 3.3. 24 kV TSLF 240/35 Al cable dimensions.

	Dimension
Insulation level	24.0 kV
Outer sheath diameter	38.5 mm
Outer semi-conductor diameter	29.6 mm
XLPE insulation thickness	4.9 mm
Conductor cross-section	240.0 mm^2
Copper screen cross section	21.0 mm^2
Aluminum laminate cross section	14 mm^2 (Removed from parts of the cable)

Two separate currents were applied to the cable conductor and the cable screen to be able to control the currents independently. AC voltage sources, ring transformers and DC sources were used to simulate the conductor load current and the induced current in the screen. Mainly, the conductor current was applied merely to produce the heat that a normal cable system would experience. The screen current was used to stress the test objects with different load models from the two test procedures.

Previous experiments have shown that measuring transition resistance while applying DC current in the cable screen and AC current in the conductor gives reliable results, see Chapter 1.2. Hence, to obtain reliable transition resistance measurements, DC current was applied to the cable screen and AC current was applied to the conductor throughout all test cycles.

An illustration of the laboratory setup for the first test procedure with corresponding test objects can be seen in Figure 3.5. An identical setup was made for the second test procedure.

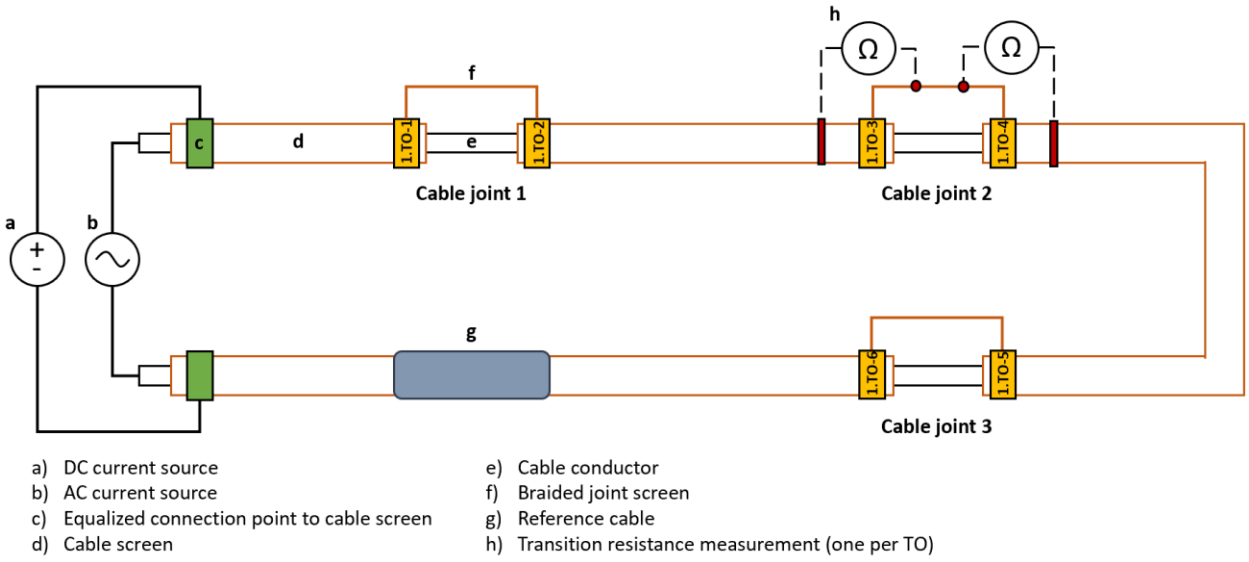

Figure 3.5. Illustration of laboratory setup 1 with corresponding test objects.

From Figure 3.5 it can be noticed that there was installed a reference cable in the laboratory setups. The reference cable was a part of the cable that was not modified or influenced by any of the test objects. By measuring temperatures in the reference cable, it made it easier to compare test object temperatures to unsullied cable.

Since two laboratory setups were made, two DC sources and two AC sources were needed. The AC sources have a current range between approximately 0-700 A while the DC sources are limited to 0-100 A. A complete list of laboratory equipment is shown in Appendix B.

3.2.2 Resistance measurement

Four-point resistance measurement

To evaluate the development of the test objects and the impact of the load models, transition resistance over each test object were measured using four-point resistance measurement. Four-point measurement calculates the transition resistance by applying a known current in the cable screen and measuring the voltage drop over the test object. The principle of transition resistance measurement over a test object and a cable screen with stranded copper wires is shown in Figure 3.6.

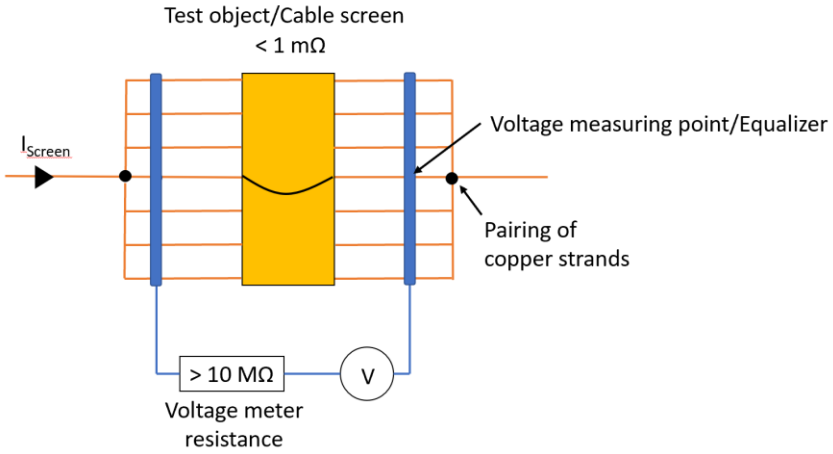

Figure 3.6. Illustration of four-point resistance measurement used in the test setups.

The known current was applied to the cable screen with the help of the DC source that was connected to the laboratory setup and the voltage drop over each test object was measured using a voltage meter and a logging equipment with preset time-samples. As indicated in Figure 3.6, the voltage meter that measure the voltage drop across the cable screen has a very high resistance compared to the screen and this prevents the current from going through the equalizers. Because of this, the transition resistance over the test objects could be easily calculated by using ohm's law in equation 3.1.

$$R_{total} = \frac{U_{Measured}}{I_{DC}} \quad [\Omega] \tag{3.1}$$

In equation 3.1, R_{total} is the transition resistance over the test object, including both contact resistance in the force spring and transition resistance in the cable and joint screen from both sides of the force spring. $U_{Measured}$ is the measured voltage drop between the installed voltage measuring points (equalizers) and I_{DC} is the known current that was applied to the cable screen.

Correction of resistance measurements

The main purpose of the test procedures was to stress the screen connections and to evaluate the development in contact resistance and temperature in the screen connections. Because of practical reasons the voltage measuring points could not be connected directly besides the force springs. This caused the measured voltages to include a small voltage drop from the cable screen wires and joint screen on each side of the force spring. As a result, the measured resistances had to be corrected with values from the cable and joint screen. The length of the two parts to be subtracted was defined as *the cable screen or joint screen from the voltage measuring point to where it entered the constant force spring*.

A figure showing the definitions of force spring contact area is shown in Figure 3.7. The area to the left of point A indicates the length from the cable screen wires. The area to the right of point B indicates the length from the joint screen. Subtracting these two from the total length between the equalizers gives the actual test object (force spring) width, referred to as L.

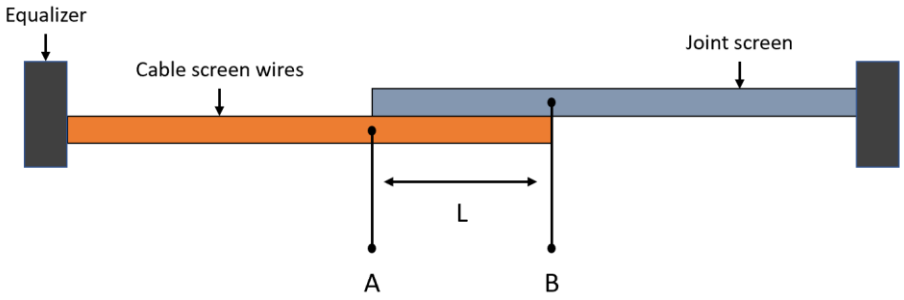

Figure 3.7. Definition of force spring contact area.

Dimensions from Figure 3.2 show that the length of the cable screen wires from the equalizer to the force spring is 14 cm and the length of the joint screen from the equalizer to the force spring is 6.4 cm. The master's thesis "Reliable power cable screen connections", ref [6], used the same type of joint screen and cable type as this project and has measured the resistance values per unit length of the cable screen and the joint screen.

By multiplying the resistance per unit length with the length of the cable screen wires and the joint screen, the correction values could be calculated. The per unit resistances, cable and joint screen correction lengths and calculated resistance correction values are given in Table 3.4.

Table 3.4. Resistance correction values.

	Correction values
Copper resistance	0,85 [Ω/km] [1]
Joint screen resistance	0,57 [Ω/km][1]
Length A	140 [mm]
Length B	64[mm]
R_A, Correction Cable screen	0,119 [mΩ]
R_B, Correction Joint screen	0,036 [mΩ]

1. Values obtained from [6].

The actual resistance in the test objects was then obtained by subtracting the correction values when calculating transition resistance in equation 3.2.

$$R_{TO} = \frac{U_{measured}}{I_{DC}} - R_A - R_B \qquad [\Omega] \tag{3.2}$$

Here, R_A and R_B are the cable screen and joint screen resistances, respectively. R_{TO} is the transition resistance in the test object, mainly consisting of contact resistance between the cable screen and joint screen inside of the force spring.

Voltage measuring points

The current carrying parts of the power cable screen consist of stranded copper wires, making it challenging to find a fitting equalizer for measuring the voltage drop over the test object. The test procedures also introduced currents that would generate heat, causing expansion of the cable insulation. Thus, a solution that was able to maintain contact with the stranded copper wires while fluctuating with the heat expansion of the cable insulation was needed.

As mentioned in Chapter 1.2, a specialization project was conducted to find a reliable and suited solution for these types of voltage measurements in the cable screen. Based on the results from the specialization project a solution with self-vulcanizing tape seemed to be a promising solution [4]. It was therefore decided to use these types of equalizers in this master thesis.

The solution uses a very simple approach with the help of braided copper laces and self-vulcanizing tape. Self-vulcanizing tape is a silicone-rubber tape which when stretched and wrapped around cables, electrical joints, hoses and pipes unites itself into a strong, seamless and electrically insulating layer. It can be made as a heat-resistant tape with properties that are able to withstand temperatures that are generated in a normal cable system.

When stretched and wrapped tightly around a cable the tape exerts a radial force that is evenly divided around the cable. By twisting a braided copper lace around the cable screen and then applying the vulcanizing tape, the evenly divided force would make sure the screen wires are at the same voltage potential. Because of a high mobility, braided copper laces were preferred over tinned copper wires, considering the heat expansion that would occur in the cable insulation.

Further comes a detailed description on how the equalizers were installed in the laboratory setup.

Equipment:

- Heat resistant self-vulcanizing tape
- Insulation tape
- Braided copper laces
- Cable lugs

Step by step installation:

1. Before applying the copper laces, the outer sheath and the aluminum laminate of the TSLF cable were stripped at the point where the equalizers were to be installed, following the dimensions given in Figure 3.2.

2. A 30 cm long braided copper lace was twisted around the cable screen two times. The remaining part of the copper lace was twirled around itself, creating a single conductor.

3. Self-vulcanizing tape was stretched and wrapped tightly over the copper lace four times.

4. Insulation tape was applied on top of the self-vulcanizing tape and around the twirled copper lace for better bonding and mechanical protection.

5. Cable lugs were connected to the copper laces to be able to connect voltage measurement equipment.

6. The same procedure was carried out for the joint screen equalizer on the other side of the test object.

Pictures from the installment of the equalizers can be seen in Figure 3.8. Equalizers were installed on each side of all the twelve test objects.

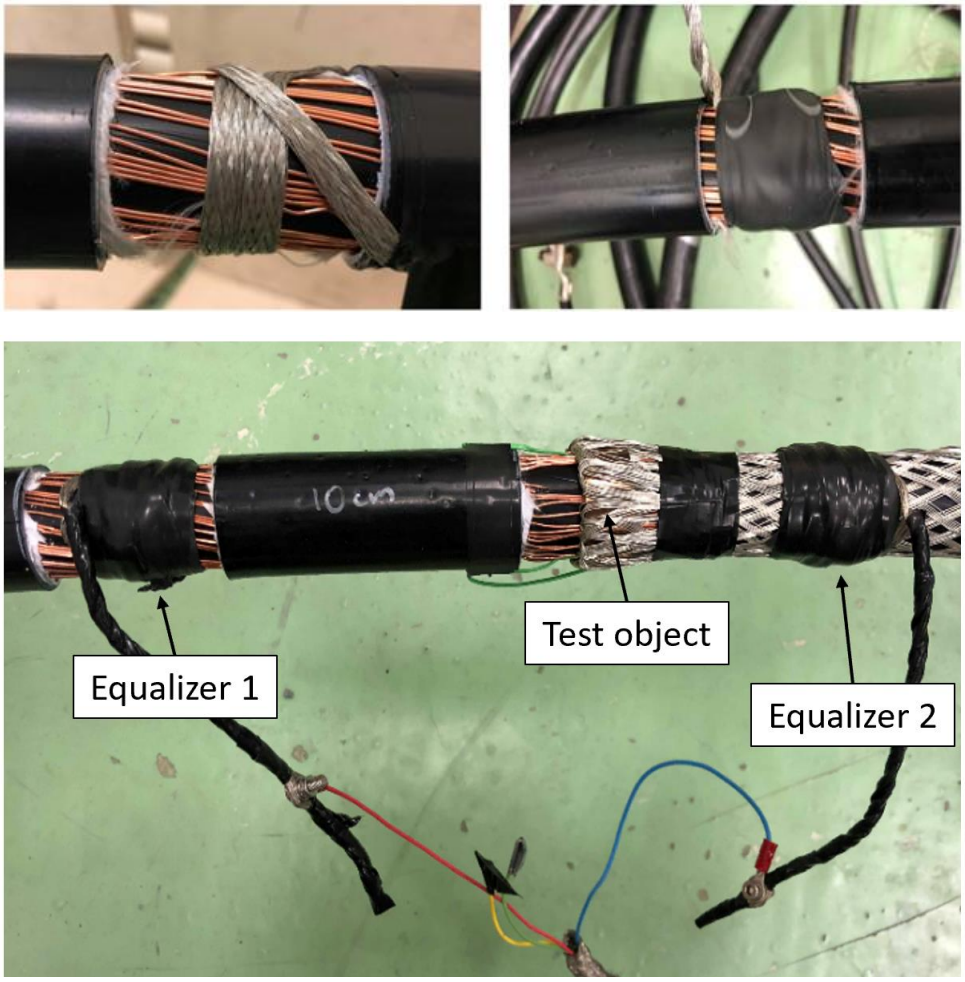

Figure 3.8. Pictures from the installment of voltage measuring points.

3.2.3 Temperature monitoring

Test object temperatures

To monitor the temperatures of the test objects, thermocouples were placed inside each force spring. Temperatures were monitored with the help of K-Type thermocouples which has a temperature range of -270 °C to +1260 °C. [24]

Experiments conducted in the project "Fault mechanisms of incorrectly installed force springs" experienced hotspots in the force springs. These hotspots generated temperature differences up to 60 °C inside the force springs [3]. To detect possible hotspots in this project, the ideal solution would be to monitor the temperature around the whole circumference of the force spring connections.

Due to limiting laboratory equipment a solution with two thermocouples inside each test object was chosen. Installing two thermocouples per test object would contribute to detect hotspots and also act as a fail safety if one of the thermocouples experienced a fault.

Two thermocouples were placed inside the force springs in between the cable screen strands, one on each side of the screen connection. Since the cross section of the thermocouples were smaller than the cross section of the copper strands this solution would not affect the properties of the screen connection. An illustration of the placement of the thermocouples are shown in Figure 3.9.

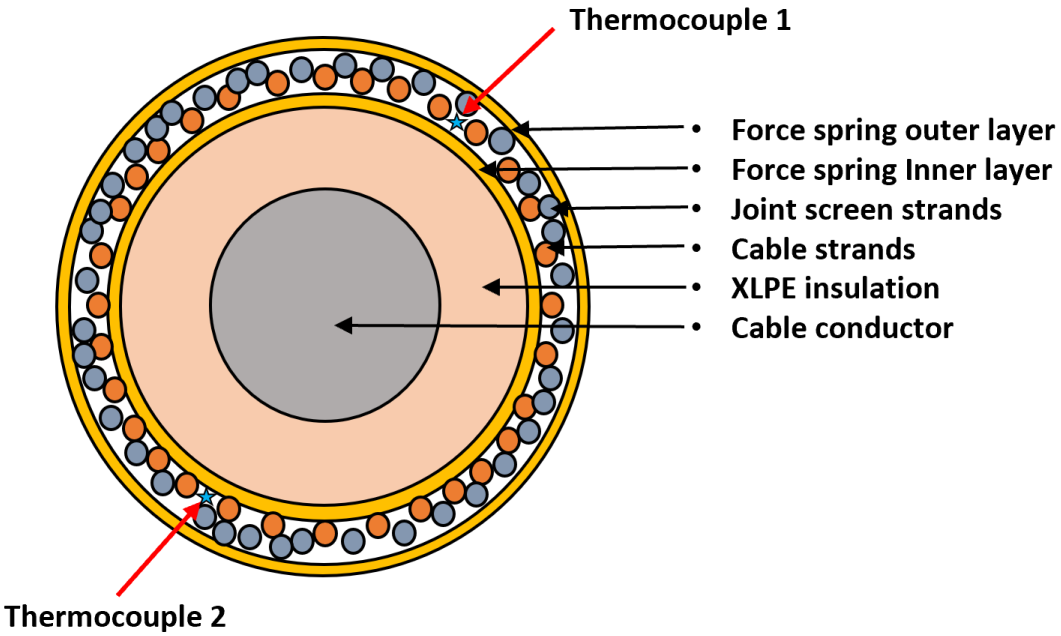

Figure 3.9. Placement of thermocouples inside a test object.

Reference cable temperatures

In addition to monitoring the temperatures of the test objects, reference temperatures of the conductor, cable screen and cable sheath were measured at a point where the cable was not influenced by any of the test objects. One thermocouple was placed at the surface of the conductor, one beneath the outer sheath at the cable screen and a final thermocouple was placed at the surface of the outer sheath. These reference temperatures made it possible to compare test object temperatures to unsullied cable parts.

The thermocouples used for reference measurements were inserted by drilling a hole down through the cable insulation. Since the experiments would not introduce any voltages that could create flashovers between the conductor and the screen, this method was considered a safe method. An illustration of the placement of the thermocouples for reference measurement is shown in Figure 3.10.

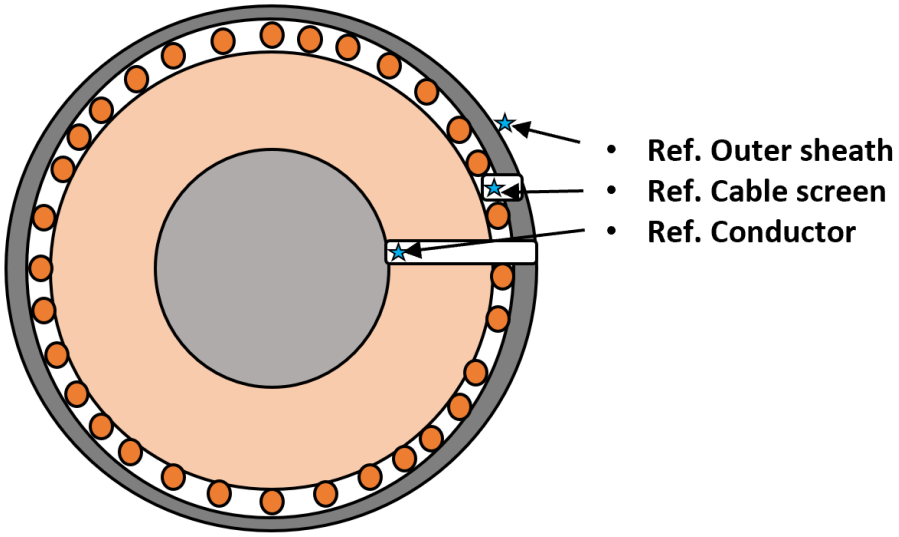

Figure 3.10. Placement of thermocouples at the reference cables.

Thermocouples were also placed at the cable lugs where the conductor was connected to the AC sources that were installed in the test setups. To monitor the temperature of the ambient air, a thermocouple was placed between a bolt and a nut and laid inside the test rig. A list of all thermocouples can be seen in Appendix A.

Thermal insulation

To obtain stable temperatures and reduce the influence of ambient air and surroundings, the test objects and the reference cables were thermally insulated. This would also give a more realistic scenario that resemble a situation where the cable and screen connections were placed in the ground.

After all test objects, thermocouples and voltage measurements were installed, each test object was covered with 13 mm thick Armaflex rubber pipe insulation which has a flexible material. On top of the Armaflex a 20 mm self-sealing fiberglass pre-slit pipe cover was applied. Pictures of the insulated test setup is shown in Figure 3.11.

a) Test object isolated with 13 mm black Armaflex pipe insulation

b) The Armaflex pipe insulation was covered with self-sealing fiberglass pre-slit pipe cover.

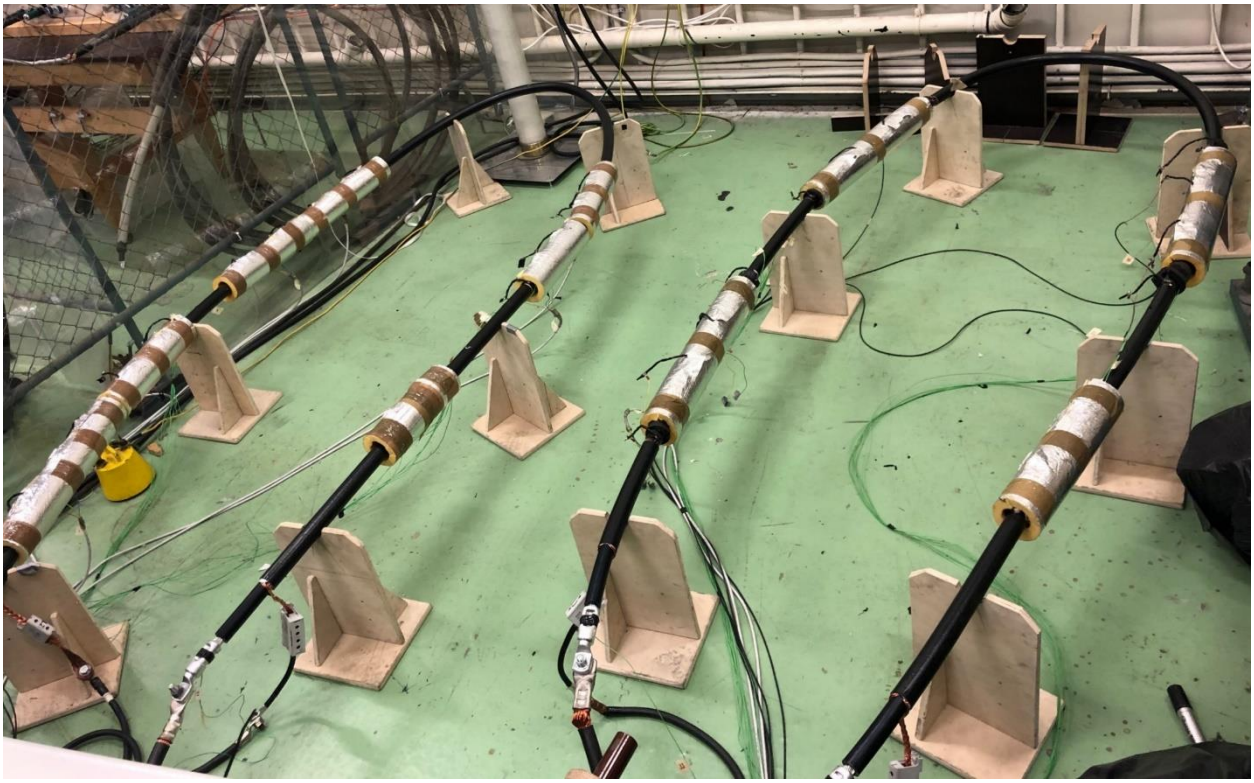

Figure 3.11. Pictures of the thermal insulation of both test setups

3.2.5 Logging equipment and external circuits

Logging equipment

To record data and view real-time measurements from transition resistance measurements and temperature monitoring, both laboratory setups were equipped with separate data acquisition tools. A data logger switch unit with built-in signal processing of thermocouples and AC/DC voltages were connected to each test setup and used to measure temperatures, voltages and currents throughout the test procedures. The channel list for both data loggers is given in Appendix A. A list of laboratory equipment is shown in Appendix B.

The currents that were applied to the conductors and cable screens were monitored with the help of AC or DC ampere meters. The DC currents in the cable screens were measured with Fluke i1010 current clamp adapters, while the AC load currents were measured with Fluke i1000s current clamp adapters. The current clamps for each laboratory setup were connected to the associated data logger.

Safety circuit

As the test procedures introduced currents that generated high temperatures in the power cable and test objects, safety was an important factor. Both test procedures involved test cycles that last over a long period of time which means that visual supervision of the laboratory setup could not be performed throughout the test periods.

In addition to recording measurements, the data logger switch unit has high and low alarm limits on each channel. To allow safe use of the laboratory setup, a safety circuit was installed for both test setups to de-energize the system in the event of an over temperature, over current or smoke development.

To prevent the insulation XLPE in the power cables to deteriorate, a high limit of 100 °C was set on all channels that measured temperatures. As XLPE-insulated cables have a rated maximum conductor temperature of 90 °C this limit was reasonable.

In addition to the temperature limit, a smoke detector and a door switch was installed to the laboratory setup. In the event of smoke or someone entering the test cell while the test setup was energized, the safety circuit would de-energize the system. The circuit diagram and the schematics of the safety circuit is shown in Figure 3.12.

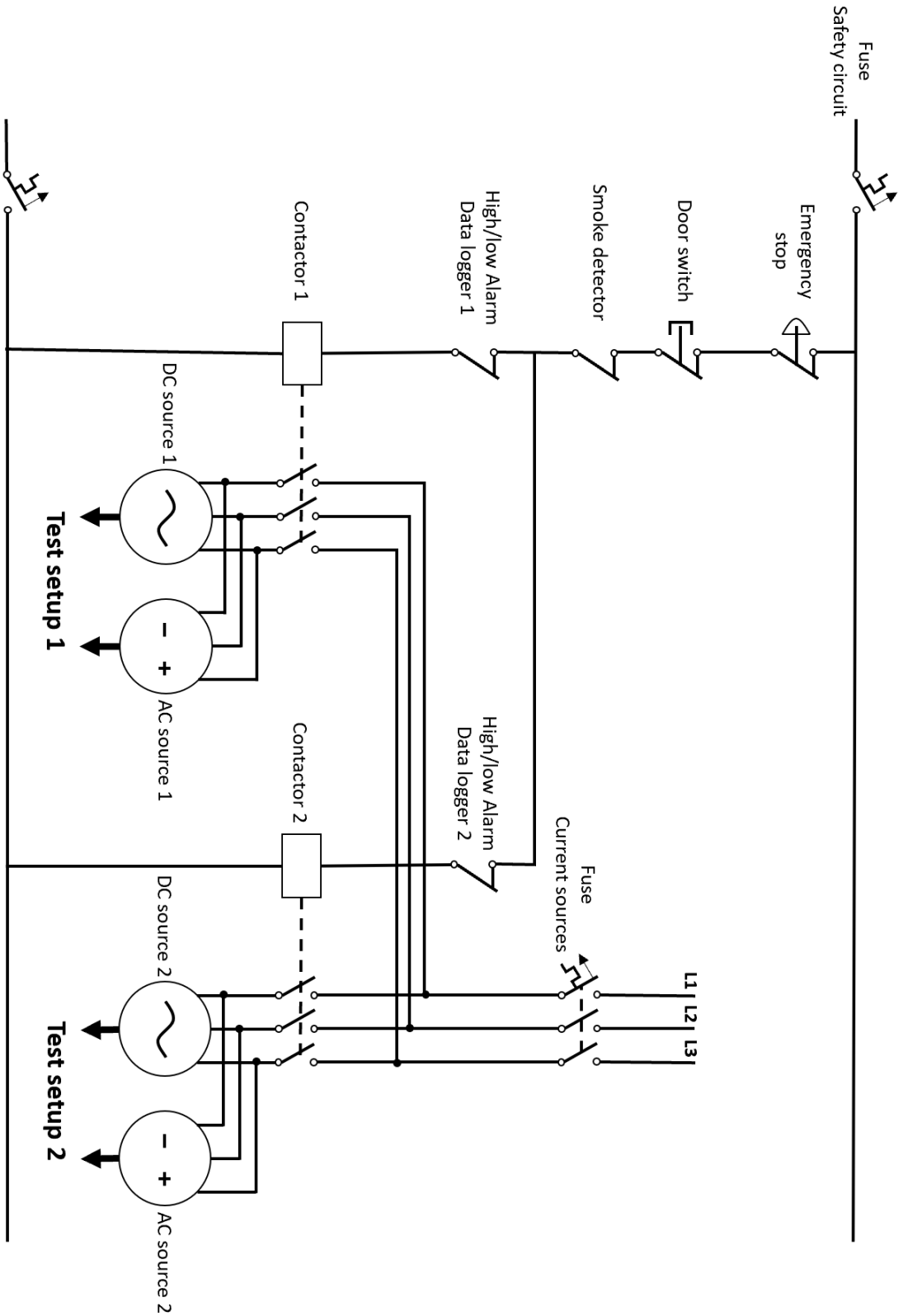

Figure 3.12. Safety circuit diagram for the laboratory setups.

As seen in Figure 3.12, the test procedures could run separately. If the high alarm in one of the laboratory setups was triggered, the other setup was not de-energized and could keep on testing. However, all current sources were de-energized if the door switch or smoke detector were triggered.

3.3 Test procedures

The main objectives of this master thesis were to establish a reliable and effective test procedure and laboratory setup that can be used to test power cable screen connections. With this in mind, this project evaluated whether heat cycling was a necessary test procedure for testing screen connections. This chapter gives a description of the two test procedures that were evaluated.

3.3.1 Test procedure 1 - Heat cycle test

The heat cycle test procedure was performed on laboratory setup 1. The procedure is a heat cycle test which is inspired by the standard IEC-61238-1 "Compression and mechanical connectors for power cables for rated voltages up to 30 kV (Um = 36 kV)" and the CIRED WG 2017-01 draft report for ground screen power cable screen connections [5, 25]. The standard and report provide a recommendation for heat cycle testing of power cables.

The procedure initiates cyclic relative movements and strains inside the force springs by continuously heating and cooling down the test objects with load currents. As mentioned in chapter 2.2.4, previous experiments have shown that small cyclic movements between the contact electrodes can introduce a strong increase in the contact resistance over time.

The objective of the heat cycles was to obtain stable temperatures in the cable around 90 °C, which is the maximal design temperature of XLPE insulation. The definition of a stable temperature was set to *the moment when the measured temperature does not vary with more than 4* °C *during a 15-minute period*. The test object with the highest temperature was used to determine when temperature stability was reached. After the temperature stability was reached the current sources were turned off and when the temperature had decreased below 35 °C, a new heat cycle could be initiated. An example of a heat cycle procedure with qualitative values are shown in Figure 3.13

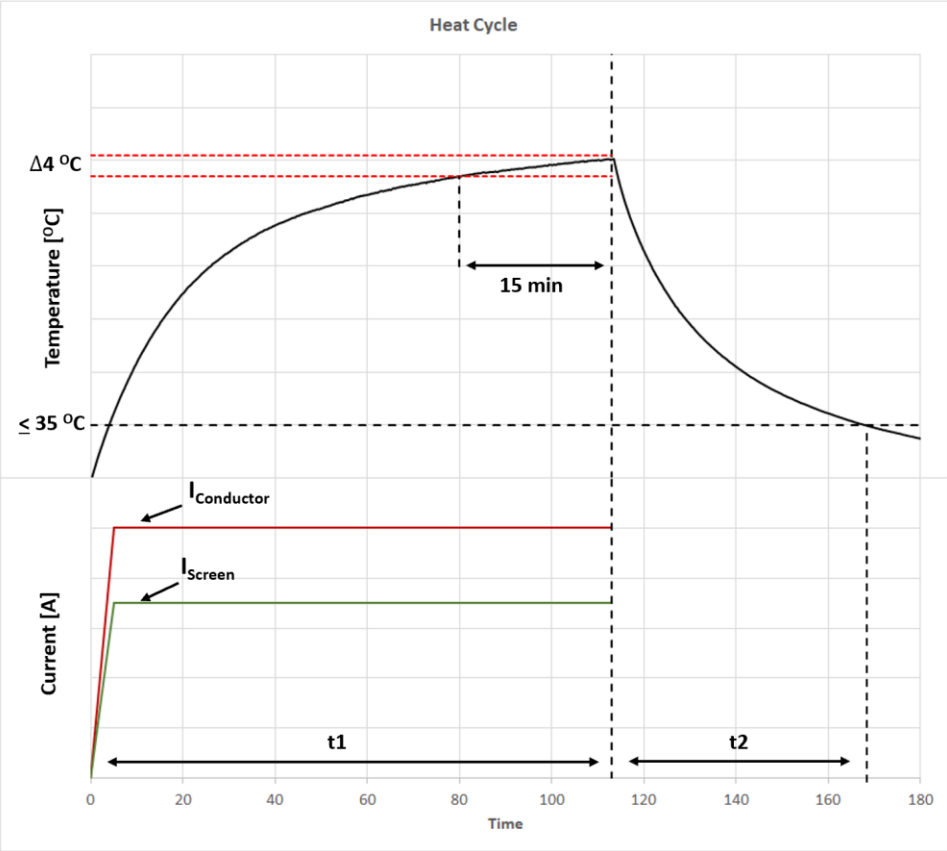

Figure 3.13. Qualitative sketch of a heat cycle from the heat cycle procedure.

As seen in Figure 3.13, the applied currents are turned on and kept constant throughout the time period t1. When temperature stability is reached, the current sources are turned off and the system cools down. The total time of the heat cycle consist of the time t1+t2.

Initial testing

Before going into the heat cycles, initial test cycles had to be conducted to find appropriate current levels in the conductor and cable screen. The conductor and screen current were increased in steps to achieve a current level that would establish a stable test object temperature level around 90 °C. According to manufacturer loading tables, a 24 kV 240 mm^2 TSLF cable should be able to operate at a load current of 455A given certain conditions [26]. As mentioned in Chapter 1.5, currents in the order of 5-35 % of the load current can be induced in the cable screen.

Based on this, the conductor current was set to 450 A and increased in steps of 50 A until the heat cycle reached a stable temperature at approximately 90 °C. The screen current was set to 70 A. The initial test cycles followed the same procedure as a heat cycle to see at what level the temperature stabilized. An overview of the initial tests is given in Table 3.5.

Table 3.5. Overview of initial heat cycle tests.

NR	Conductor current	Screen current	Stabilized test object temperatures
1	450 A	70 A	75-80 °C
2	500 A	70 A	85-90 °C

A current level of 500 A in the conductor and 70 A in the screen gave stable test object temperatures of 85-90 °C which was considered high enough to start performing the heat cycles. The total time of a heat cycle was approximately 4.5 hours. It should be mentioned that the initial test cycles also contribute as a part of heat cycle test procedure since these tests also generate volume expansion inside the test objects.

Heat cycles

After obtaining the current levels that generated the desired temperatures, the heat cycles could be initiated. An ideal screen connection should be able to maintain a reliable connection trough a cable system lifetime without it affecting the contact resistance of the connection. Due to the duration of each heat cycle and the fact that the laboratory setup was not automated, only one heat cycle was performed each weekday. The total number of heat cycles was therefore set to **40**.

The test object temperature and transition resistance were measured throughout every heat cycle. The heat cycles were started either from ambient temperatures at 20-25 °C or just below 35 °C depending on if it was the first heat cycle of the test day or one of the following throughout the day. After the last heat cycle was completed the test objects were dissected, and a visual inspection was conducted to compare and evaluate the properties of the different screen connections.

3.3.2 Test procedure 2 - Constant current test

The constant current test procedure was performed on laboratory setup 2. To determine whether the heat cycle procedure is necessary for testing screen connections it had to be compared to a simpler test procedure. Thus, the second test procedure has a simple approach with constant load and screen currents throughout the entire test period.

While the test objects in the heat cycle test procedure was cycled between ambient temperatures and 90 °C several times, the test object temperatures in the constant current test were kept constant throughout a long test period as seen in Figure 3.14.

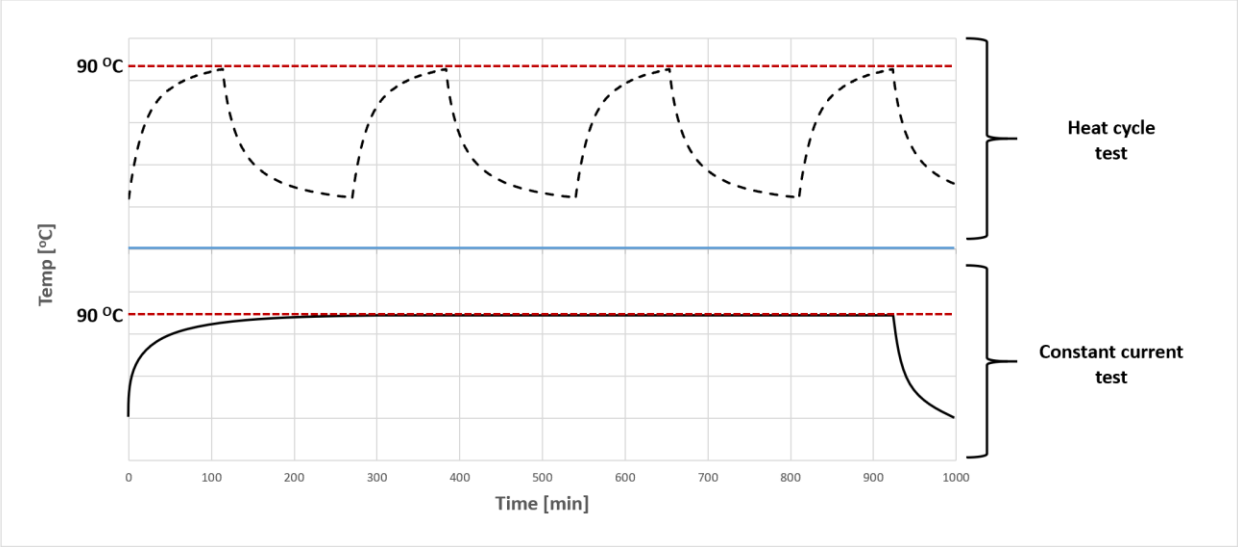

Figure 3.14. Qualitative comparison of temperature development in the heat cycle test procedure versus the constant current procedure.

The objective of the constant current test was to obtain stable temperatures in the test objects around 90 °C, which is the maximal design temperature of XLPE insulation. As opposed to the heat cycles, the definition of a stable temperature was set to *the moment when the measured temperature does not vary with more than ± 2* °C *during a period of 120 minutes.* The test object with the highest temperature was used to determine when temperature stability was reached. After the desired temperature stability was reached the current magnitudes were kept constant throughout the entire test procedure. The test procedure can be compared to one long heat cycle.

Current magnitudes

As this test procedure required that the test object temperatures stabilized at 90 °C over a longer period of time than the heat cycles, the conductor load current and the screen current had to be decreased compared to the heat cycle test procedure.

To determine the appropriate current levels, the constant current test was started at 450 A in the conductor and 50 A in the screen. Further, the screen current was increased with steps of 5 A until a stable test object temperature of approximately 90 °C was reached. An overview of the current magnitudes and the stabilized test object temperatures are shown in Table 3.6.

Table 3.6. Overview of current magnitudes in the constant current test.

Step NR	Conductor current	Screen current	Stabilized test object temperatures
1 (2 days)	450 A	50 A	75-85 °C
2 (53 days)	450 A	55 A	80-90 °C

A current level of 450 A in the conductor and 55 A in the screen gave stable test object temperatures of 80-90 °C which was considered high enough to start performing the test procedure. As seen in Table 3.6, the currents were kept constant and applied to the cable system for **55 days and nights i.e. 1320 hours.**

The test object temperature and transition resistance were measured throughout the entire test procedure. After the test procedure was completed the test objects were dissected, and a visual inspection was conducted to compare and evaluate the properties of the different screen connections.

3.3.3 Short circuit test

As an additional measure to compare test objects from the different test procedures a short circuit test was performed. The intention of the short circuit test was to reproduce the thermal effects that high currents could cause to the screen connections.

The short circuit test was conducted after both test procedures were finalized to see if the different test objects would respond differently to high currents. **Test object 5** (T.O-5) and **Test object 6** (T.O-6) from both test procedures were separated from the test setups and connected to a high current transformer. The high current transformer was equipped with a tap changer to be able to adjust the test currents to a suitable level.

The maximum permissible short circuit current for a power cable is usually determined partly by the maximum design temperature of the conductor and partly by the time from a short circuit begins until the protective switchgear breaks the current. In cases of large currents, one should also pay attention to the forces between the conductors.

According to cable manufacturers the maximum tolerable temperature in Cu screens for XLPE power cables is approximately 300 °C at short circuit currents, as long as it does not last over 5 seconds. This corresponds to a short circuit current density of 200 A/mm^2 for 1 second.

From the cable specifications given in Table 3.3 the Cu screen had a cross section of 21 mm^2. Since the aluminum laminate was removed from parts of the cable, the cross section of the Cu screen was used to determine the short circuit current level. This gives a highest permissible short circuit current in the copper screen of approximately 4200 A for 1 second. [27, 28]

Based on these values and available current levels from the tap-transformer it was decided to run the test objects through 3 short circuit tests at a current level of 2500 A, where the time of the short circuit test would be increased from 1-3 seconds. The short circuit was applied to the cable screen only and the test object resistances were measured before starting the first test and between each test. An overview of the short circuit test is given in Table 3.7 and pictures of the test setup is given in Appendix C.

The test setup was not pre-heated, meaning the short circuit test was performed on test objects with ambient temperatures.

Table 3.7. Overview of the short circuit test.

Test Nr.	Current level [A]	Time [Seconds]	Heat cycle test objects	Constant current test object
Pretest	-	-	T.O-5 & T.O-6	T.O-5 & T.O-6
1	2500	1	T.O-5 & T.O-6	T.O-5 & T.O-6
2	2500	2	T.O-5 & T.O-6	T.O-5 & T.O-6
3	2500	3	T.O-5 & T.O-6	T.O-5 & T.O-6

4. Results & discussion

This chapter both presents and discuss selected results from the heat cycle test and the constant current test. The first part evaluates the heat cycle test and constant current test separately. With the results gathered from the test procedures and the dissection of the test objects, the second part compares and discusses properties of the different test procedures.

4.1 Heat cycle test

A total of 40 heat cycles were performed on the cable system. Contact resistance in the test objects and temperatures were measured every 2 minutes throughout the heat cycles. After finalizing the test procedure, the data was exported through a data acquisition tool where it was processed and analysed. Results from all of the 40 heat cycles are given in Appendix E.

This chapter will present and discuss results from the heat cycle test. This includes selected results from transition resistance measurements and temperature monitoring.

4.1.1 Test object resistance results

Results from transition resistance measurements in heat cycle 5, 15, 25 and 40 are presented in Figure 4.1.

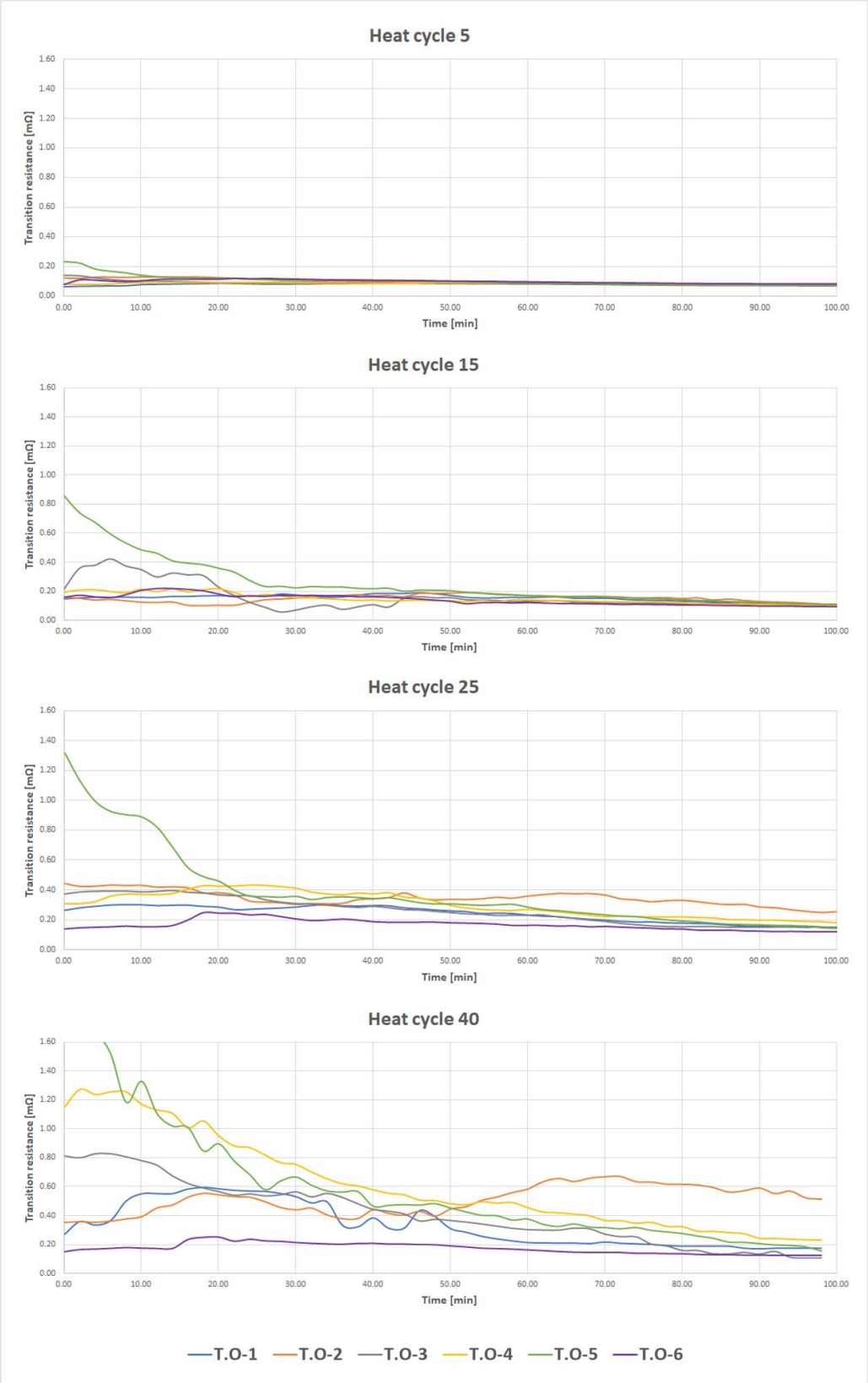

Figure 4.1. Transition resistance results from heat cycle 5, 15, 25 and 40.

It should be mentioned that since the resistance contribution from the cable screen and joint screen on each side of the force spring in each test object have been subtracted from the measured resistances (see chapter 3.2.2), the results mainly consist of the contact resistance in the force springs.

Increased contact resistances

The results show a visible increase in contact resistance for almost all of the test objects. Figure 4.1 shows how all test objects have low and stable resistance values in heat cycle 5. Throughout heat cycle 15 and 25 the resistance values start to increase especially at the beginning of the heat cycles. Going into heat cycle 40 the results show a noticeable increase in contact resistance as well as variating measurements compared to the initial heat cycles.

Table 4.1 gives a summarized resistance development for all test objects from the start of heat cycle 1 to the end of heat cycle 40.

Table 4.1. Summarized resistance development from start of heat cycle 1 to end of heat cycle 40.

Heat cycle test resistance results							
	TO-1	TO-2	TO-3	TO-4	TO-5	TO-6	**Average**
Start of 1st heat cycle [mΩ]	0.037	0.041	0.038	0.040	0.047	0.057	**0.043**
End of 40th heat cycle [mΩ]	0.173	0.516	0.107	0.232	0.158	0.124	**0.218**
Change from 1st to 40th [%]	468	1259	282	494	336	218	**507**
Minimum during cycling [mΩ]	0.037	0.041	0.038	0.040	0.047	0.057	**0.043**
Maximum curing cycling [mΩ]	0.621	0.563	0.970	1.221	1.955	0.163	**0.916**

The resistance development in Table 4.1 show that the contact resistance in all test objects have had a significant increase with an average increase of 507 % from start of heat cycle 1 to end of heat cycle 40. From the table it can also be noticed that the minimum resistance measurements throughout all heat cycles were measured at the beginning of heat cycle 1. The reason for the increase in contact resistance is due to temperature variations caused by the applied screen- and conductor currents. The currents that are applied to the cable system generates heat that causes the test object temperatures to increase from ambient temperatures to around 90 °C. This leads to an increased material resistivity. However, when a heat cycle is finished, and the temperature drops again, so will the material resistivity.

The main reason for the increased contact resistance is because of cyclic relative movements inside of the test objects. The increase in temperature causes thermal expansion of the different materials inside of the screen connections and this can lead to a decrease of mechanical load inside the force spring. The heat cycles introduce many sequences of these small movements inside the screen connection and this causes fretting corrosion between the electrodes. When the electrodes move relative to each other this will initiate growth of oxide layers on the load bearing area, effectively increasing the contact resistance over time.

Resistances at a stabilized temperature of 90 °C

Test object resistances at a stabilized test object temperature of 90 °C for each heat cycle is given in Figure 4.2.

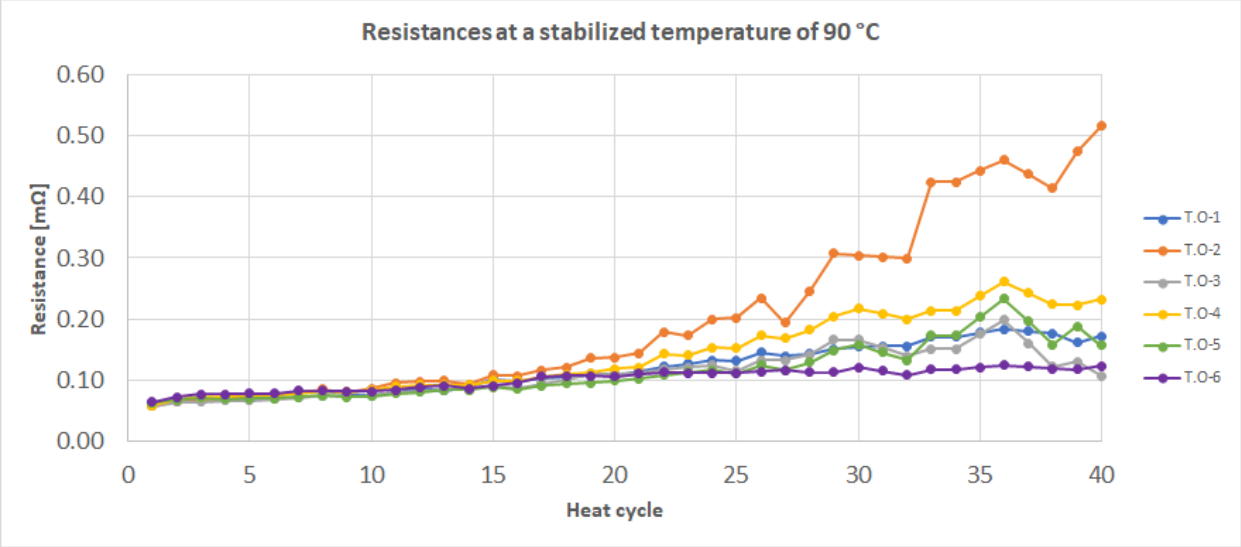

Figure 4.2. Test object resistances at a stabilized temperature of 90 °C for each heat cycle.

Figure 4.2 show how the resistances gradually increased throughout the heat cycles. These results support the theory that the cyclic relative movements cause the increase in contact resistance over time. This implies that the heat cycles were gradually deteriorating and weakening the ampacity of the screen connections throughout the heat cycles. The figure also show that the resistances were still increasing and developing after 40 heat cycles, suggesting that more heat cycles should have been performed to see the full development of the test object resistances.

It can also be noticed from Figure 4.2 that the test object resistances at 90 °C experience the biggest increase after approximately 20 heat cycles. It seems like the heat cycles needed a "conditioning period" before the test procedure could have a noticeable effect on the screen connections. Performing more than 40 heat cycles would most likely continue the same development and lead to even higher and more variating contact resistances. These results does however not explain why the contact resistances are so high and variate at the beginning of the heat cycles as shown in Figure 4.1.

Figure 4.2 also show a substantial spread in contact resistance between the test objects after 40 heat cycles. At the initial heat cycles there was almost no spread, but after 20 heat cycles the test objects started to experience different contact resistances. T.O-2 had the highest contact resistance after 40 heat cycles with 0.52 mΩ compared to T.O-3 which only measured a contact resistance of 0.11 mΩ after 40 heat cycles.

Variating pressure inside the test objects at low temperatures

Figure 4.3 show the average test object resistances at ambient temperature (beginning of the heat cycles) and at a stabilized temperature of 90 °C for all heat cycles.

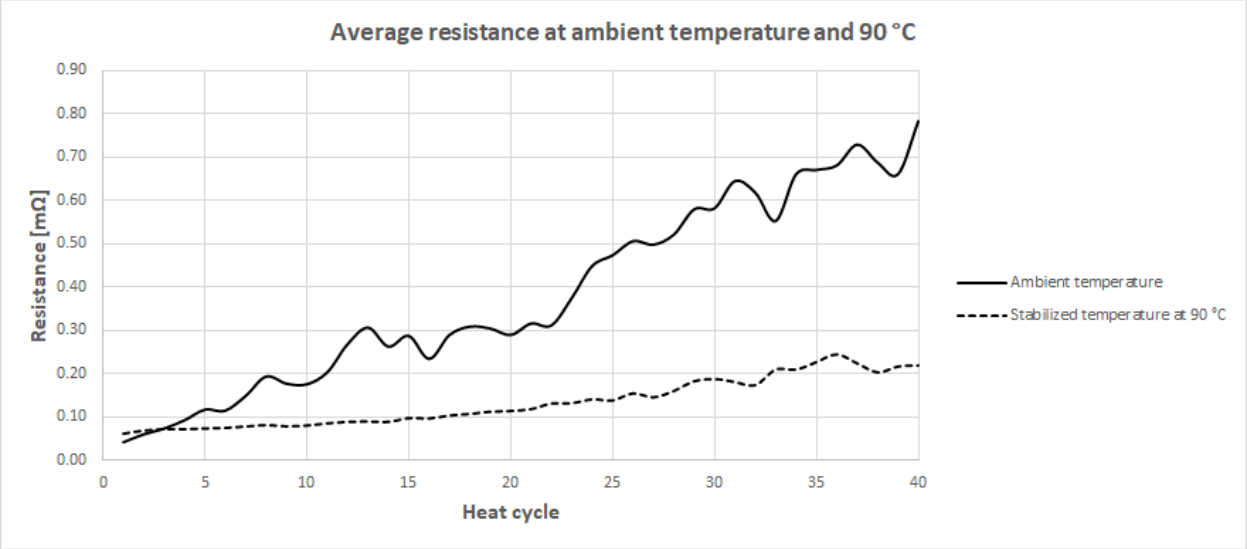

Figure 4.3. Average test object resistances at ambient temperature and 90 °C.

Figure 4.3 show how the test objects had equal resistances at ambient temperature and 90 °C in the initial heat cycles. However, after approximately 5-10 heat cycles a clear difference in contact resistance can be noticed from ambient temperature to a stabilized temperature of 90 °C. The difference seemed to be enhanced as more heat cycles were conducted. The reason for the differences in contact resistance also has to do with thermal expansion of the materials inside the force spring.

The variation of temperature and volume expansion will have a resulting mechanical force on the cable system and the installed accessories. Because of this the pressure inside the test objects will variate. As contact resistance between two electrodes is directly affected by mechanical load and pressure, this phenomenon will have an evident impact on the measured test object resistances.

When the temperature inside the test objects rises, the volume of the different materials increases. This leads to an increased mechanical load and higher contact pressure inside the force springs. As a result, the contact resistance decreases. This explains why the contact resistance is lower at 90 °C compared to ambient temperature in Figure 4.3. When the applied currents are turned off again the temperatures will start to decrease and so will the volume expansion of the materials inside the force springs.

Film resistance and instability

As the volume decreases, the contact pressure inside the force springs also decrease. Looking at Figure 2.8 in chapter 2.2.3, the force spring connection will reach instability if the contact pressure is reduced to a certain point. This will reduce the number of contact spots in the screen connections and introduce a high film resistance between the electrodes. This can explain why the measured resistances is variating at the start of the heat cycles as seen in Figure 4.1.

At the start of the heat cycles, when the test objects are at ambient temperature, the volume expansion is at its lowest and the contact resistance is at its highest. When the currents are turned on, the thermal expansion of the test objects are initiated, and the contact pressure starts to increase. As the contact pressure increases,

oxide layers will be pierced, and film resistance decreased. This causes the contact resistance to go from variating to stable and low values at high temperatures as seen in Figure 4.1.

The overall resistance at a stabilized temperature of 90 °C did however gradually increase throughout the heat cycles. This implies that the force springs were not able to entirely remove the produced oxide layers at each heat cycle.

4.1.2 Temperature results

Results from temperature monitoring in heat cycle 5, 15, 25 and 40 are presented in Figure 4.4.

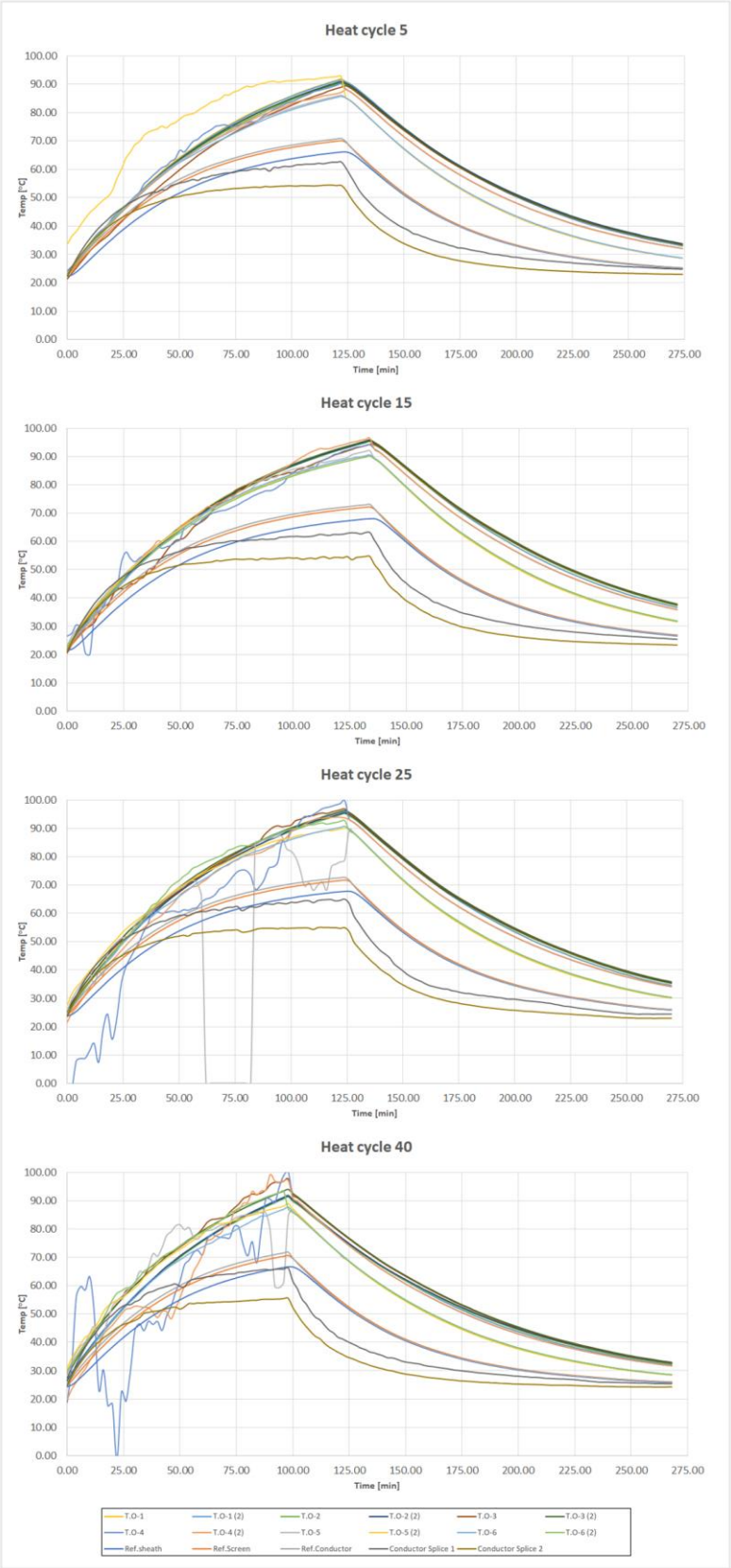

Figure 4.4. Temperature results from heat cycle 5, 15 ,25 and 40.

Difference from reference cable and instability

Temperature results from the heat cycle test show a noticeable difference in temperatures between the test objects and the reference cable for all heat cycles. As seen in Figure 4.4, the reference cable temperatures stabilized at approximately 15-20 °C lower than the test objects and never reached temperatures over 80 °C. This indicates that the test objects represent a bottleneck in the cable system which constrains the ampacity of the system compared to unsullied cable.

The test objects seem to generate approximately the same temperatures and follow the same patterns throughout the heat cycles. Looking at Figure 4.4 it can however be noticed that some of the test object temperatures turned unstable and started to variate while the temperatures were increasing. The variating temperatures were most likely influenced by the variating contact resistances as shown in Figure 4.1, but only to a certain extent.

The generated temperatures were directly dependent on the test object contact resistance as dissipated power depends on resistance, but it does not explain the large temperature variations in some of the test objects. There were installed two thermocouples per test object (e.g. Thermocouple T.O-1 and T.O-1(2)) and some of the thermocouples measured temperatures that had high deviations from the corresponding thermocouple in the same test objects. This indicated that the most extreme variations were caused by a fault in either the thermocouple or the in the input of the data acquisition tool.

Fault in thermocouples

The first large variations occurred already in the 1^{st} -5^{th} heat cycle in thermocouple T.O-2 and T.O-5(2). Before conducting any further heat cycles, it was decided to troubleshoot the thermocouples and a fault was detected on the termination of the thermocouples. Similar variations were detected in thermocouple T.O-4 and T.O-5 after the 15^{th} heat cycle, as seen in Figure 4.4. The thermocouples seemed to have been affected by the thermal expansion and the movement that occurred in the test objects which caused a fault in the mentioned thermocouples. It was therefore decided to disregard the measurements that were collected from the defective thermocouples.

The variations that were caused by the defective thermocouples triggered the safety circuit of the test setup since the measurements exceeded the high limit of 100 °C in some of the heat cycles. This caused the current sources to deenergize before the test objects could reach the desired temperature of 90 °C in heat cycle 31, 35 and 37. Results from all heat cycles are given in Appendix D.

Time to reach 90 °C

It can also be noticed from Figure 4.4 that the time to reach test object temperatures of 90 °C was reduced as more heat cycles were conducted. Figure 4.5 compares the time to reach test object temperatures of 90 °C for heat cycle 2 and heat cycle 40.

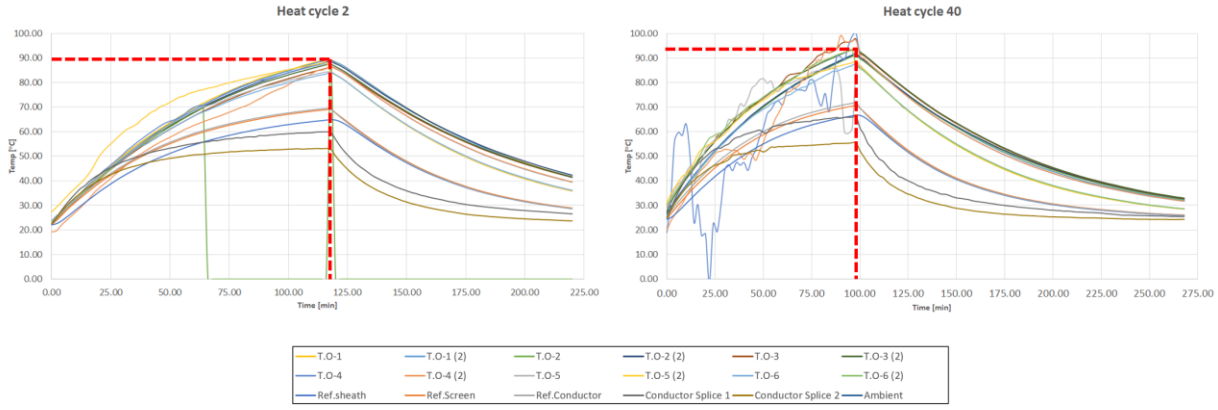

Figure 4.5. Reduced time to reach test object temperatures of 90 °C from heat cycle 2 to heat cycle 40.

As seen in Figure 4.5, it takes approximately 120 minutes to reach 90 °C in heat cycle 2 while it takes 100 minutes in heat cycle 40. This is a direct consequence of the increased contact resistances that developed throughout the heat cycles and proves that the heat cycles had a noticeable negative effect on the ampacity of the cable system.

4.2 Constant current test

The constant current test lasted for 55 days where contact resistance and temperature were measured every 5 minutes throughout the test period. After finalizing the test procedure, the data was exported trough a data acquisition tool where it was processed and analysed. To smooth out short-term fluctuations and highlight longer-term trends the time series are presented with a moving average in this chapter. Results with raw data (no moving average) are presented in Appendix E.

This chapter will present and discuss results from the constant current test. This includes results from transition resistance measurements and temperature monitoring.

4.2.1 Test object resistance results

Results from transition resistance measurements are given in Figure 4.6. The time series data is presented with a moving average that is calculated with a 300-measurement interval.

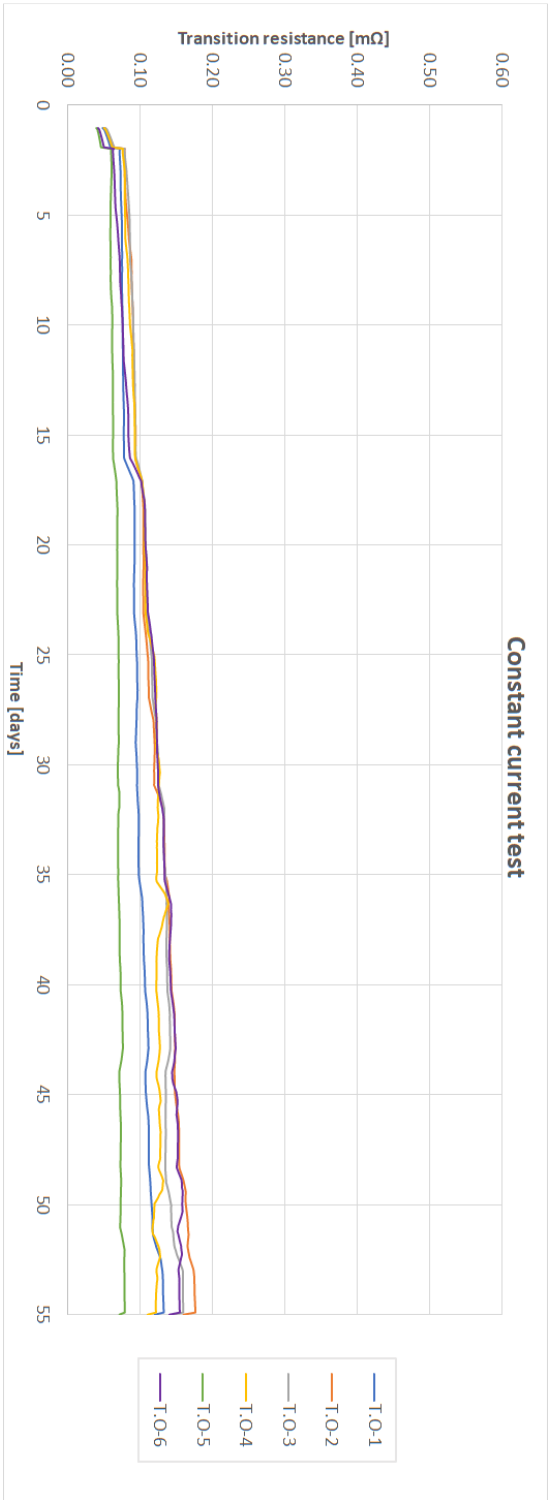

Figure 4.6. Transition resistance measurements from the constant current test. The time series is presented with a moving average.

Increased contact resistances

Results from the resistance measurements show a gradually increasing contact resistance in all test objects throughout the test period. The test setup experienced a power outage after one day which can be observed at the start of the test period, as seen in Figure 4.6. After the power outage, the test objects show a stable development throughout the rest of the test period.

Table 4.2 gives a summarized resistance development for all test objects in the constant current test.

Table 4.2. Summarized resistance development from the constant current test.

Constant current test resistance results							
	TO-1	TO-2	TO-3	TO-4	TO-5	TO-6	**Average**
Start of cycle [mΩ] (after power outage)	0.076	0.081	0.078	0.079	0.059	0.062	**0.072**
End of cycle[mΩ]	0.132	0.176	0.159	0.121	0.077	0.155	**0.137**
Change from start to end [%]	388	476	418	303	257	596	**190**
Minimum during cycle [mΩ]	0.076	0.081	0.078	0.079	0.059	0.062	**0.072**
Maximum curing cycle [mΩ]	0.134	0.178	0.162	0.148	0.080	0.166	**0.145**

The resistance development in Table 4.2 show a noticeable increase in contact resistance for all test objects, with an average increase of 190 % from start to end of the test period. Like the heat cycle test, the test objects experienced the minimum resistance measurements at the beginning of the test period. In this case the resistance is not affected by change of material resistivity since the test object temperatures were stable at 85-90 °C most of the test period. The increase in contact resistance is most likely due to a loss of contact area at the electrode interface inside the test object. This loss may be due to, among various other mechanisms, oxide formation or perhaps a loss of mechanical force throughout the test period.

Oxide formation

The oxide formation was however not caused by cyclic movements in this case since the test object temperatures were stable throughout most of the test period. Thus, the contact resistances were not affected by cyclic thermal expansion and movement inside the test objects. The corrosion processes that took place could be caused by chemical reactions or because of the different materials that were used in the test objects.

The copper in the joint screen may have different properties compared to the cable screen which could have caused electrochemical potentials between the interfaces of the screen connection. Further, this could cause alloys to form at the interfaces which would contribute to increase the contact resistance. Different thermal expansion in the metals may also have caused sideways displacements in the contacts and the loss of mechanical force and pressure inside of the test objects.

Offset in corrections values

From Figure 4.6 it can be noticed some collective leaps in the resistance values for all of the test objects. The reason for this is unclear, but it seems like there was some disturbances in the correction values of the data acquisition tools. The resistance measurements might have experienced an offset from the correction values that was adjusted at the beginning of the test procedure which caused these collective leaps. This is considered an error in the resistance measurements and should be ignored. The offset was not considered substantial and the contact resistance development from the resistance measurements were still used to compare the test procedures.

4.2.2 Temperature results

Results from temperature monitoring in the constant current test are presented in Figure 4.7. The time series data is given with a moving average that is calculated with a 100-measurement interval.

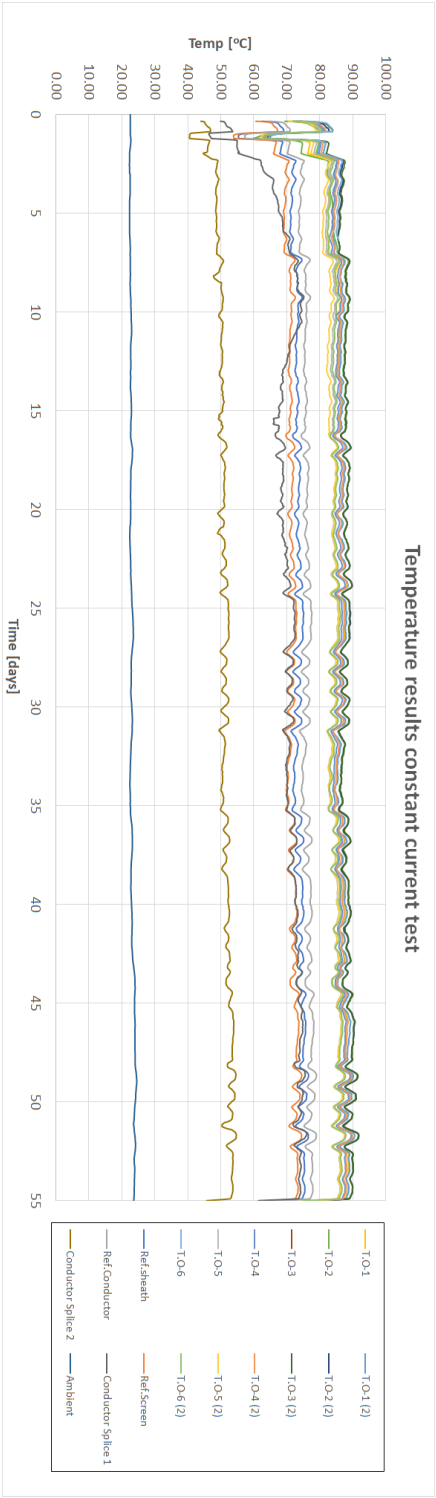

Figure 4.7. Temperature results from the constant current test. The time series data is presented with a moving average.

Difference from reference cable

As in the heat cycle test, temperature results from the constant current test also show a noticeable difference in test object temperatures compared to reference cable temperatures. As seen in Figure 4.7, test object temperatures stabilized around 85-90 °C, while the reference cable never reached temperatures over 80 °C. This is another indication that force springs introduces a bottleneck in the cable system which contributes to reduce the ampacity of the system.

As mentioned earlier, the test setup experienced a power outage after one day which can be observed at the start of the test period in Figure 4.7. The figure also shows a rapid change in temperature just after the power outage. This is caused by the increase in screen current which was adjusted to reach test object temperatures around 85-90 °C, see Chapter 3.3.2.

Induced currents and temperature variations

Looking at Figure 4.7, clear variations in temperatures can be noticed throughout the test period. These variations were caused by induced currents in the test setup. The heat cycle test and the constant current test were run in the same test laboratory cell with only small distances between the test setups as seen in Appendix C. This caused the cable systems to interact with each other.

When a heat cycle was initiated, the AC current which was applied to the conductor in the heat cycle test generated an induced current in the constant current test cable system. This current combined with the currents that already were applied to the constant current test setup caused undesired variations in the test object temperatures. The temperature variations could have had a small effect on the contact resistance of the test objects since this could also cause small cyclic movements inside the force springs, similar to the heat cycle test. These small movements could have had a small contribution to the increased contact resistances.

Increase in test object temperatures

To determine the average increase in test object temperature throughout the constant current test the average of the first five days (after the screen current was increased to the desired level) and the average of the last five days were calculated as illustrated in Figure 4.8. The time series data is presented with a moving average that is calculated with a 300-measurement interval.

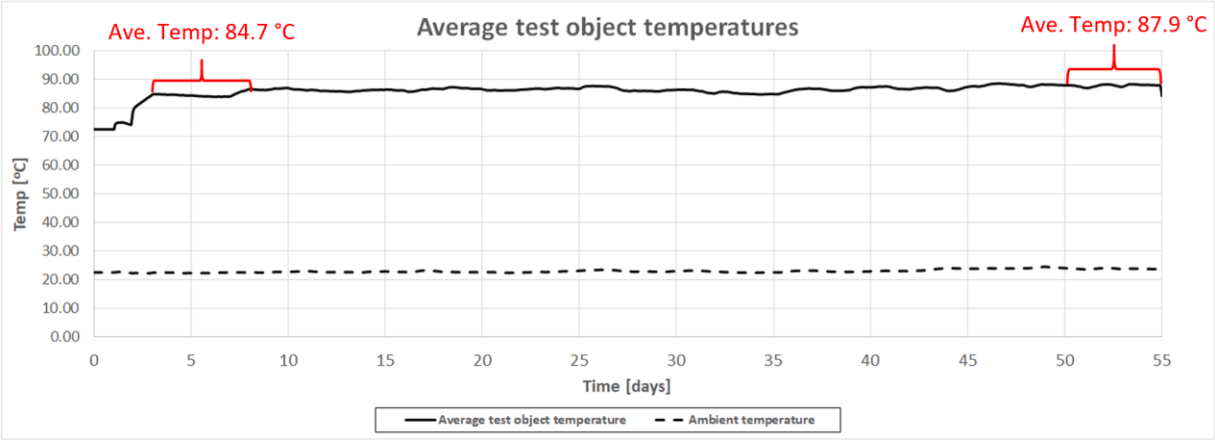

Figure 4.8. Average test object temperatures in the constant current test. The time series data is presented with a moving average.

Figure 4.8 show how the average test object temperatures experienced a small increase in temperature throughout the test period from 84.7 °C to 87.9 °C. This is a direct consequence of the increased contact resistances that developed throughout the constant current test and show that the ampacity of the cable system is slightly reduced.

4.3 Comparison of test procedures

4.3.1 Resistance and temperature results

This chapter will use data and results from both test procedures with emphasis on comparing the test procedures. Table 4.3 gives an overview of the average resistance development for all test objects in both test procedures.

Table 4.3. Average resistance development for both test procedures.

Average resistance development for both test procedures		
	Heat cycle test	**Constant current test**
Start of test [mΩ]	0.043	0.072
End of test [mΩ]	0.218	0.137
Change from start to end [%]	507	190
Minimum during test [mΩ]	0.043	0.072
Maximum during test [mΩ]	0.916	0.145
Spread in contact resistance [mΩ]	Heat cycle 1 at 90 °C: 0.008	Start: 0.021
	Heat cycle 40 at 90 °C: 0.401	End: 0.098

From the numbers presented in Table 4.3, the test objects in the heat cycle test had a higher increase in average contact resistance from start to end of the test procedure compared to the constant current test. The heat cycle test had an average increase of 507 % from start to end of the test procedure while the constant current test had an average increase of 190 %. The heat cycle test ending up with an average test object contact resistance of 0.218 mΩ compared to the average test object contact resistance of 0.137 that the constant current test experienced.

There is also a substantial larger development for spread in contact resistance between the test objects in the heat cycle test compared to the constant current test. At the end of the heat cycle test the spread was 0.401 mΩ, while the spread was only 0.098 at the end of the constant current test.

Maximum test object contact resistance

Looking at the average maximum contact resistance that the test procedures experienced, another clear difference can be noticed. The heat cycle test reached an average maximum contact resistance of 0.916 mΩ which is noticeable larger than the maximum contact resistance of 0.145 mΩ that the constant current test experienced.

The reason why the heat cycle test experienced such high peaks in contact resistances compared to the constant current test is because the heat cycles introduce variating thermal expansions and pressure inside of the test objects. As mentioned in Chapter 4.1.1 this caused high film resistances and instability at the start of the heat cycles, when the test objects were at ambient temperatures. The constant current test is not exposed to this phenomenon since the temperatures are constant at 85-90 °C throughout most of the test period.

Variating resistances in the heat cycle test

Results from the heat cycle test showed that the test object resistances at 90 °C also seemed to experience a noticeable increase in contact resistances after approximately 20 heat cycles. Figure 4.9 compares the average test objects resistances for the heat cycle test and the constant current test. The heat cycle contact resistances are given at a stabilized test object temperature of 90 °C.

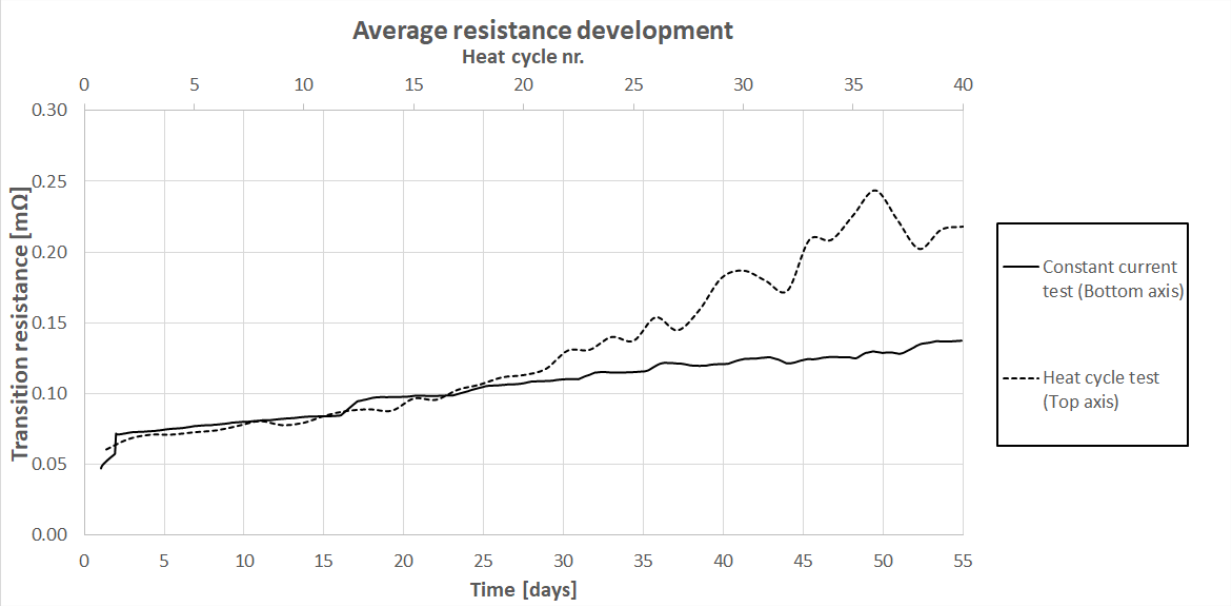

Figure 4.9. Average test object resistance development. The heat cycle contact resistances are given for a stabilized test object temperature of 85-90 °C.

Since the test object resistances in Figure 4.9 were measured at a stabilized test object temperature of 85-90 °C for both test procedures, they were measured at a point where the test objects in both test procedures experienced approximately the same thermal expansion.

Figure 4.9 show that the test object resistances in the heat cycle test and the constant current test seem to have followed the same trend and development for the first 20 heat cycles. However, after 20 heat cycles the test objects from the heat cycle test gradually worsened and gained variating contact resistances compared to the test objects in the constant current test. Both test procedures experienced an increase in contact resistance, but the heat cycle test seemed to have had a bigger impact on the ampacity of the screen connections over time.

Time at high temperatures

Figure 4.10 illustrates the average time that the test objects spent over 80 °C for both test procedures.

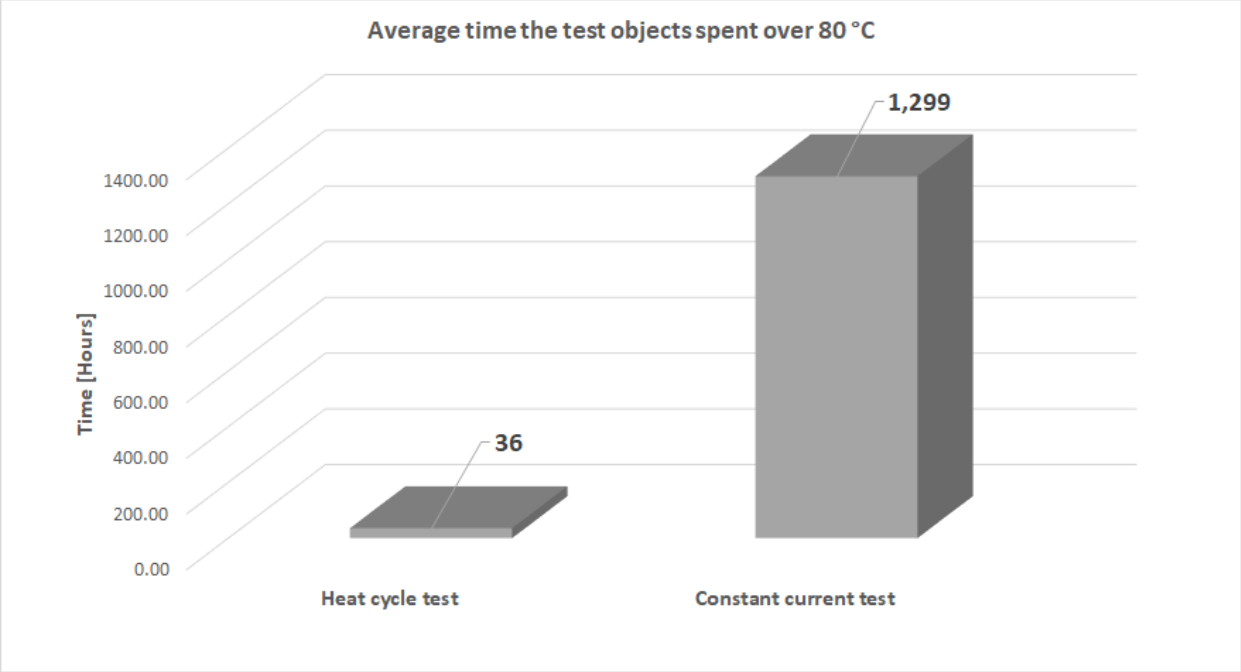

Figure 4.10. Total time the test objects spent over 80 °C for both test procedures.

From Figure 4.10 it can be noticed that the test objects in the constant current test obviously spent a lot more time over 80 °C than the test objects from the heat cycle test, with an average time of 1299 hours compared to only 36 hours in the heat cycle test. Even though the test objects in the constant current test spent so much more time at high temperatures it was still the test objects from the heat cycle test that experienced the highest variations and peaks in contact resistance throughout the test procedures.

Test object resistances from the constant current test had no noticeable development after 36 hours compared to the heat cycle test. This also show that the cyclic strains and impacts that the test objects were subjected to under the heat cycle test, had a bigger influence on the ampacity of the screen connections than the continuously high temperatures that the constant current test introduced.

Standardized resistance values

The results this far are purely based on the development of contact resistance and comparison of the two test procedures. The resistance values are not evaluated against standardized resistance values for screen connections. In further testing of screen connections, it would be essential to determine resistance specifications for screen connections to be able to determine whether the screen connections are acceptable or not.

4.3.2 Dissection of test objects

This chapter provides observations made during the visual inspection of the test objects after finishing the heat cycle test and the constant current test. Selected pictures from the dissection are discussed and used to compare the different test procedures.

Upon visual inspection of the test setups there were no signs of excessive overheating on the thermal insulation or on any of the test objects. The test objects generally seemed to have maintained a functionally good screen connection and had not changed noticeably from when they were installed.

Dissection of Test object 2 in both test procedures

From the resistance results in Figure 4.2 and Figure 4.6 it can be noticed that Test object 2 experienced the highest contact resistances at a stabilized temperature of 85-90 °C in both test procedures. Figure 4.11 show a picture of Test object 2 from both test procedures after the thermal insulation was removed. Test object 2 from the heat cycle test is marked TO1-2 and Test object 2 from the constant current test is marked TO2-2.

Pictures from the dissection of the other test objects are not presented, as the same general observations were made on most of the test objects.

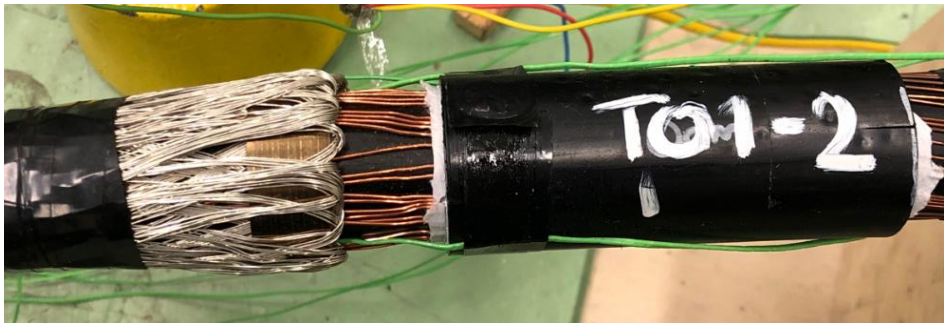

a) Test object 2 from the heat cycle test

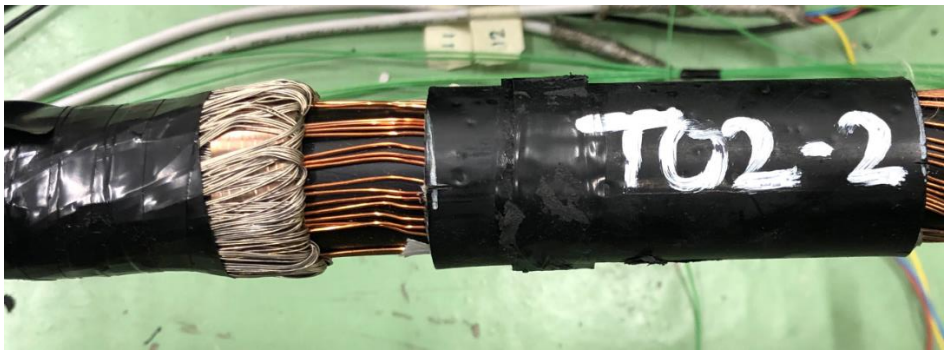

b) Test object 2 from the constant current test

Figure 4.11. Pictures of test object 2 in both heat cycles after the thermal insulation was removed.

As seen in the figure there were no signs of superficial overheating or damage to the cable or on either of the test objects. There were no comprehensive discoloring of the force springs and the radial force exerted from the force springs seemed to have been preserved.

After opening and removing the force springs there was however signs of small deformations in the outer-semiconductor and the XLPE-insulation. Selected pictures from the visual inspection of Test object 2 in both test procedures are given in Figure 4.12. Pictures of Test object 2 from the heat cycle test are given in the left column. Pictures of Test object 2 from the constant current test are given in the right column.

Heat cycle Test – Test object 2

a)

Comment: No signs of overheating or discoloring

b)

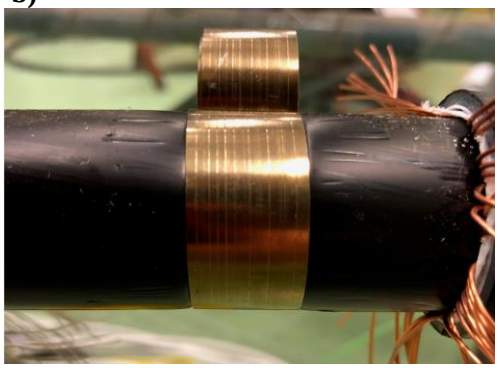

Comment: The force spring had embedded into the cable

c)

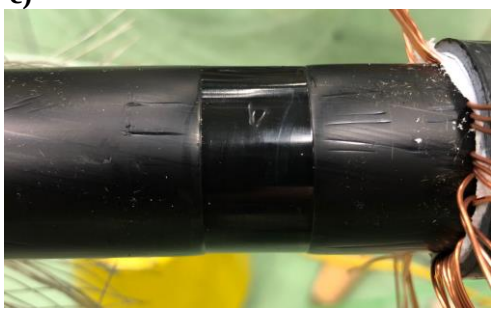

Comment: The force spring had caused engravements in the outer semiconductor.

Constant current test – Test object 2

d)

Comment: Joint screen had signs of minor discoloring

e)

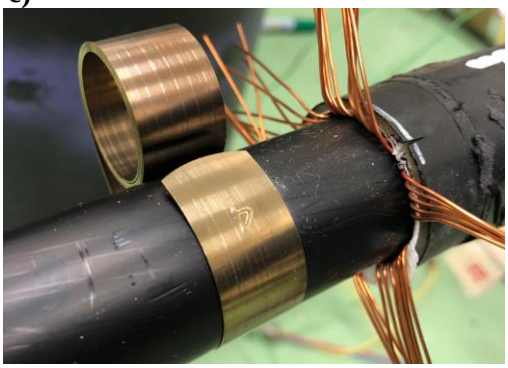

Comment: No signs of overheating or discoloring

f)

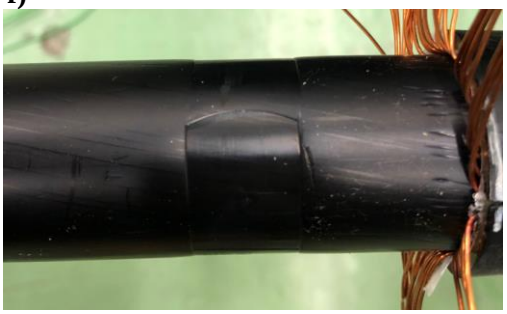

Comment: The force spring had caused insignificant deformation of the outer semiconductor.

Figure 4.12. Selected pictures from the dissection of Test object 2 in both the heat cycle test and the constant current test. Pictures of Test object 2 from the heat cycle test are given in the left column. Pictures of Test object 2 from the constant current test are given in the right column.

Upon opening the thermal insulation of the test setups there were a slight color difference between the joint screens of the different test procedures. The joint screen from the heat cycle test appeared to be totally unaffected by the heat cycles while the joint screen from the constant current test had minor discoloring and seemed to be more affected by the test procedure.

The reason for this is the time that the test objects spent at 85-90 °C. The test objects from the constant current test spent an average time of 1299 hours over 80 °C as opposed to the test objects from the heat cycle test who only spent an average time of 36 hours above 80 °C, see Figure 4.10. Obviously, time at high temperatures is a main factor in general thermal aging of the materials inside of the test objects and this caused the minor discoloring of the joint screen from the constant current test.

Minor deformation of the outer semiconductor

Nevertheless, it was the test objects from the heat cycle test that experienced the highest contact resistances. As seen in Figure 4.12 picture b) and c), the force spring from the heat cycle test had slightly embedded into the outer semiconductor. This caused a minor deformation of the outer semiconductor. This did not happen to the same extent for the force springs in the constant current test, even though it spent a lot more time over 80 °C.

It seems like the heat cycles had a bigger effect on the screen connection itself compared to the constant current test. The repeating thermal expansion and "de-expansion" that the heat cycles introduced, caused small movements inside of the force springs which again caused the mechanical pressure inside of the force springs to variate.

As the outer semiconductor and the XLPE-insulation have a higher coefficient of thermal expansion compared to the stainless steel in the force springs, the cable insulation experienced a bigger expansion than the force springs. This caused an increasing radial pressure between the outer semiconductor and the force springs that variated each cycle. These repeated forces that were caused by the heat cycles seems to have affected the screen connections to a bigger extent than the constant current test did.

The influence of the incorrect force spring installations

As mentioned in Chapter 3.2, the screen connections were not installed in a way that follows the correct installation method. The force springs should have been applied to the outer sheath of the power cable, not the outer semiconductor like the test objects in this project were. As mentioned in Chapter 4.1.1 and Chapter 4.2.1, the test objects generated higher temperatures than the reference cables and introduced bottlenecks in the cable system.

This could be a direct consequence of the modified force spring installation as the installation method could have generated more heat compared to a correct installation. Since the force springs were placed on the outer semiconductor, heat from the conductor would easier transport into the force spring and cause higher temperatures compared to the correct installation method.

The general perception after the dissection of all test objects was that the screen connections seemed to be in good shape and that the force springs seemed to have maintained a functionally acceptable screen connection. It was not observed any severe damage to the outer semiconductor and only minor deformations were noticed. Therefore, it cannot be concluded whether the modified installation of the force springs had a big influence on the cable insulation compared to a correct installation.

For a better understanding of the impacts that the modifications might have caused, they should have been compared to a correctly installed force spring. The modified screen connections and a correct installation should have been run through the same test procedure to be able to evaluate the difference between the two installation methods.

4.3.3 Short-circuit test

Results from resistance measurements in the short circuit test is given in Table 4.4 and Figure 4.13.

Table 4.4. Resistance measurements from the short circuit test.

			Heat cycle test		Constant current test	
Test Nr	Current level [A]	Time [Seconds]	T.O-5 [mΩ]	T.O-6 [mΩ]	T.O-5 [mΩ]	T.O-6 [mΩ]
Pretest	-	-	0.204	0.464	0.344	0.565
1	2500	1	0.281	0.232	0.243	0.522
2	2500	2	0.182	0.209	0.320	0.600
3	2500	3	0.217	0.263	0.451	0.321

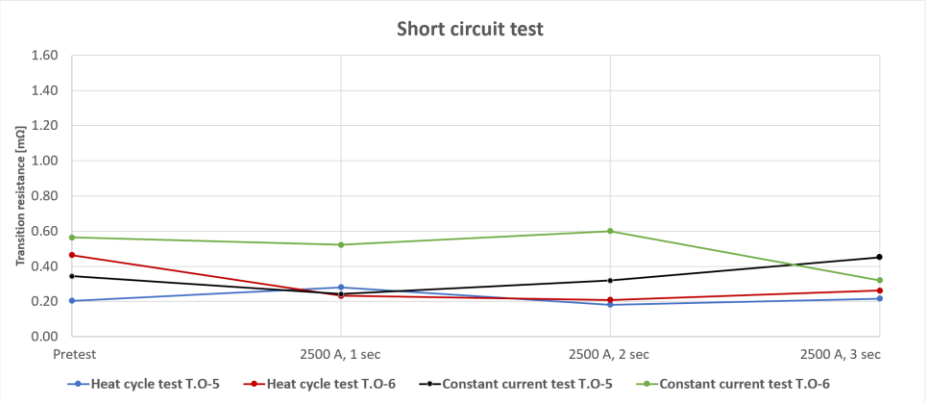

Figure 4.13. Resistance measurements from the short circuit test.

Inconclusive results

The resistance measurements given in Table 4.4 and Figure 4.13 does not show a clear difference between test objects from the heat cycle test as opposed to test objects from the constant current test. The short-term high currents caused small variations in all test object resistances, but the results cannot be used to point out a clear trend between the test objects. Therefore, these measurements cannot be used to separate the test objects from each other, giving inconclusive results.

The current used might actually have contributed to "weld" the screen connections together causing more equal contact resistances between the different test objects. Performing more short circuit tests with higher currents or longer time periods could have given a clearer development in contact resistance between test objects from the two test procedures.

The results do however show that the ampacity of the screen connections was still strong enough to withstand a short circuit current of 2500 A for 3 seconds. This indicates that the incorrect installation of the test objects did not have a crucial influence on the screen connections ability to withstand high short-term currents.

It can also be noticed that the resistance measurements that were conducted in the pretest does not fully correspond with values at the end of the heat cycle test and the constant current test given in Figure 4.1 and Figure 4.6. The reason for this is because the test objects had to be separated from their corresponding test setups and manually moved to the short circuit test setup. This most likely caused movements inside of the screen connections, affecting the contact resistances.

5. Conclusion

The work conducted in this master thesis has contributed to assemble a standardized test for power cable screen connections. A laboratory setup was made to evaluate two test procedures, a heat cycle test and a constant current test, that uses different load types and methodology for testing screen connections. The following conclusions were made:

Heat cycle test

Results from the heat cycle test show a significant increase in contact resistance for all of the test objects with an average increase of 507 % from start to end of the 40 heat cycles. The heat cycles introduce cyclic relative movement inside of the screen connections which leads to a decrease of mechanical load and fretting corrosion between the electrodes. This effectively increases the contact resistance over time and gradually weakens the ampacity of the screen connections as more heat cycles are conducted.

The heat cycles also introduce cyclic thermal expansion in the test objects which caused variating pressures inside of the force spring screen connections. As a result, the test objects experienced variating contact resistances with high peaks when going from ambient temperature to high temperature.

Constant current test

Results from the constant current test show a noticeable increase in contact resistance for all test objects with an average increase of 190 % from start to end of the test period. The constant load currents generate high temperatures which gradually causes a loss of contact area at the electrode interface inside the test object. This loss is due to, among various other mechanisms, oxide formation or perhaps a loss of mechanical force throughout the test period.

Comparison of test procedures

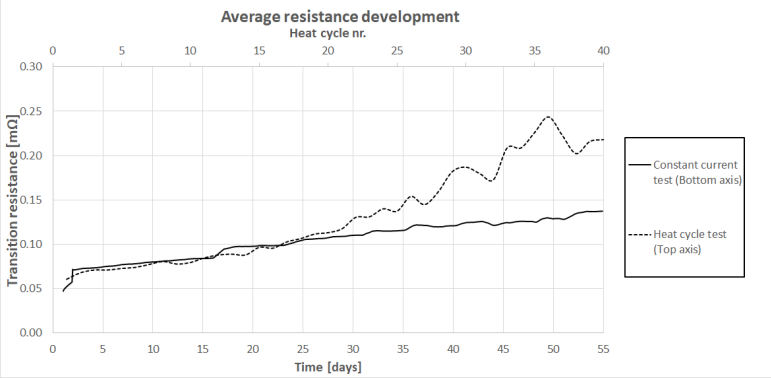

Figure 4.9. Average test object resistance development at 85-90 °C.

The figure compares the average test object resistances for the heat cycle test and the constant current test at stabilized test object temperatures of 85-90 °C. The results show that the test objects from the heat cycle test gradually worsened and gained variating contact resistances compared to the test objects from the constant current test. Both test procedures experienced an increase in contact resistance, but the heat cycle test seemed to have had a bigger impact on the ampacity of the screen connections over time.

The experiments performed in this master thesis proved that both test procedures give a certain value for testing screen connections, but the results showed that the cyclic strains from the heat cycle test is a necessary factor to fully evaluate the properties of power cable screen connections.

6. Further Work

This master thesis addressed only a few topics of laboratory challenges and there are several possibilities of topics than can be further investigated to introduce a standardized test for screen connections. Based on the work conducted in this project the following topics can be of interest:

- Automation of the experimental setup, to allow heat cycling to continue constantly.
- Removing the possibility of disruptive elements like induced current between the test setups.
- Perform more heat cycles to see the full range of the heat cycle test.
- Further testing of incorrectly installed force springs for a better understanding of the impacts that the modifications might cause.
- Investigate range of standardized contact resistances for screen connections. Determine maximum level of contact resistance to be used in the standardized test.
- Assemble a concrete diagnostic method for ground screen connections, both online and offline.
- Find a better solution for temperature monitoring around the whole circumference of the screen connections.
- Investigate what current level and time to use in a standardized short circuit test for screen connections.

References

1. Halvorson, H.L., Kulbotten, H., Lervik, J., Benjaminsen, J.T., *Feiltyper og feilmekanismer i skjermtilkoblinger - WP1*. 2017, SINTEF AS.
2. Søndenå, P., *Reliable Power Cable Ground Screen Connections - Specialization project*. 2018, NTNU.
3. Bakken, R., *Fault mechanisms of incorrectly installed force spring*. 2018, SINTEF AS.
4. Bakken, R., *Reliable voltage measuring points*. 2018, NTNU.
5. IEC, *Compression and mechanical connectors for power cables for rated voltages up to 30 kV. 61238-1* 2018.
6. Søndenå, P., *Reliable power cable ground screen connections - Master thesis*. 2018, NTNU.
7. DRAKA. *TSLF 145 kV CU*. 2018 [cited 2018 04.12]; Available from: http://draka.no/cables/tslf-145kv-cu/.
8. CENELEC, *Distribution cables with extruded insulation for rated voltages from 7,2 to 42 kV*. 2010. **HD620**.
9. Lervik, J., Solheim, K., et al., *XLPE Cables with aluminum laminated sheath*. 2015, SINTEF AS.
10. Chen, X., WU, K., et al, *Sheath circulating current calculations and measurements of underground power cables*. 2007.
11. Sobral, A., Moura, A., Carvalho, M., *Technical implementation of cross bonding on underground high voltage lines projects*. 2011: CIRED.
12. Reychem. *Reychem Heat Shrink joint for copper cables*. 2018 [cited 2018 04.12]; Available from: http://www.samm.com/en/product/1162/raychem-heat-shrink-joint-for-copper-cables-6-10-15-kv.html.
13. SINTEF Energi AS, *Metoder for sammenkobling av AL-laminat/kobberskjerm i vanntette PEX kabler*. 2015: infoblad.no.
14. Niayesh, K., Runde, M., *Power Switching Components*. 2016: Springer.
15. Ruppert, C., *Thermal fatigue in stationary aluminium contacts*. 2001, NTNU.
16. Gedeon, M., *The importance of contact force*. Brush Wellman, 2009.
17. Kongsjorden, H., *Electric contacts between aluminium conductors - A study of factors influencing their formation and degradation*. 1977, NTNU.
18. Runde, M., *Kontakter og Kontaktmaterialer*. 2019: SINTEF AS.
19. Elert, G. *Electric resistance*. 2018 [cited 2018 12.11]; Available from: https://physics.info/electric-resistance/.
20. Hennuy, B., Steennis, F., Aerns, B., et al., *Measurement of the forcees induced by thermal expansion of conductor of MV cables and impacts on MV joints*. 2013: IEEE.
21. Ensto. *Mechanical forces and movement in underground cables and cable accessories*. 2017; Available from: https://www.ensto.com/globalassets/brochures/underground-cable-networks/english/mechanical_forces_and_movement_in_cable_accessories_2017.pdf.
22. hyperphysics. *Volume expansion*. 2019; Available from: http://hyperphysics.phy-astr.gsu.edu/hbase/thermo/thexp2.html.
23. Kocatepe, C., Kumru, C.F., Taslak, E., *Analysis of magnetic field effects of underground power cables on human health*. 2014: Researchgate.
24. info, T. *Type K Thermocouple*. 2011; Available from: https://www.thermocoupleinfo.com/type-k-thermocouple.htm.
25. CIRED, *Test recommendations for ground screen power cable connections*, W. 2017-1, Editor. 2017.
26. Nexans, *Håndbok for e-verkskabler*. 2014.
27. Draka, *Teknisk Håndbok Kraftkabel*. 2010.
28. BV Twentsche Kabelfabriek, *Medium-voltage XLPE cables*. 2019.

Appendices

Appendix A – List of thermocouples and voltage sensors

Logging channels test setup 1 – Heat cycle test

Card 1 – Voltage sensors

Sensor number	Description	Marking	Channel
1	Test object 1	1.TO-1	101
2	Test object 2	1.TO-2	102
3	Test object 3	1.TO-3	103
4	Test object 4	1.TO-4	104
5	Test object 5	1.TO-5	105
6	Test object 6	1.TO-6	106
7	-	-	107
8	-	-	108
9	-	-	109
10	-	-	110
11	-	-	111
12	-	-	112
13	-	-	113
14	DC current meter	DC-1	114
15	AC current meter	AC-1	115

Card 2 – Temperature sensors

Sensor number	Description	Marking	Channel
1	Test object 1, sensor 1	1.TO-1 (1)	201
2	Test object 1, sensor 2	1.TO-1 (2)	202
3	Test object 2, sensor 1	1.TO-2 (1)	218
4	Test object 2, sensor 2	1.TO-2 (2)	204
5	Test object 3, sensor 1	1.TO-3 (1)	205
6	Test object 3, sensor 2	1.TO-3 (2)	206
7	Test object 4, sensor 1	1.TO-4 (1)	207
8	Test object 4, sensor 2	1.TO-4 (2)	208
9	Test object 5, sensor 1	1.TO-5 (1)	209
10	Test object 5, sensor 2	1.TO-5 (2)	210
11	Test object 6, sensor 1	1.TO-6 (1)	211
12	Test object 6, sensor 2	1.TO-6 (2)	212
13	Ref. cable: Outer sheath	1.Ref. sheath	219
14	Ref. cable: Screen	1.Ref. screen	214
15	Ref. cable: Conductor	1.Ref. conductor	215
16	Conductor splice 1	1.Splice 1	216
17	Conductor splice 2	1.Splice 2	217

Logging channels test setup 2 – Constant current test

Card 1 – Voltage sensors

Sensor number	Description	Marking	Channel
1	Test object 1	TO-1	101
2	Test object 2	TO-2	102
3	Test object 3	TO-3	103
4	Test object 4	TO-4	104
5	Test object 5	TO-5	105
6	Test object 6	TO-6	106
7	DC current meter	DC-2	107
8	AC current meter	AC-2	108

Card 2 – Temperature sensors

Sensor number	Description	Marking	Channel
1	Test object 1, sensor 1	2.TO-1 (1)	201
2	Test object 1, sensor 2	2.TO-1 (2)	202
3	Test object 2, sensor 1	2.TO-2 (1)	203
4	Test object 2, sensor 2	2.TO-2 (2)	204
5	Test object 3, sensor 1	2.TO-3 (1)	205
6	Test object 3, sensor 2	2.TO-3 (2)	206
7	Test object 4, sensor 1	2.TO-4 (1)	207
8	Test object 4, sensor 2	2.TO-4 (2)	208
9	Test object 5, sensor 1	2.TO-5 (1)	209
10	Test object 5, sensor 2	2.TO-5 (2)	210
11	Test object 6, sensor 1	2.TO-6 (1)	211
12	Test object 6, sensor 2	2.TO-6 (2)	212
13	Ref. cable: Outer sheath	2.Ref. sheath	213
14	Ref. cable: Screen	2.Ref. screen	214
15	Ref. cable: Conductor	2.Ref. conductor	215
16	Conductor splice 1	2.Splice 1	216
17	Conductor splice 2	2.Splice 2	217
18	Ambient temperature	Ambient	218

Appendix B – List of laboratory equipment

Item number	Equipment	Specifications	Quantity
1	Farnell DC power supply H30/100	30 – 100 A	2
2	AC current source		2
3	Ring transformer		2
4	Agilent Data logger module	Model: 34901A	2
5	Agilent Data logger card		4
6	Fluke Current meter AC/DC	Model: i1010 600VAC 600A 2KHz	2
7	Fluke Current meter AC	Model: i1000s 10/100/1000 A	1
8	Smoke detector	Model: D-1211 Optical & ionic	1
9	Thermocouple K-Type, Farnell		35
10	EMC cable		12
11	TSLF Cable	24 kV 240 mm^2 / 35 mm^2 Aluminum single-core	6 m
12	Force spring screen connections		12
13	Computer for data logger		2
14	Relay coupling box for safety circuit		1
15	Thermal insulation	Fiberglass pre-slit pipe insulation & Armaflex	
16	Four-point resistance measurement equipment		1

Appendix C – Pictures from laboratory setup

Picture 1 – Stripped cable sheath

Comment: A stripped cable following the dimensions given in Figure 3.2. With out the installed test objects.

Picture 2 – Installation of test object

Comment: Pictures from the installation of a test object following the installation method given in Chapter 3.1.2.

Picture 3 – Test object 3 and 4 from the heat cycle test

Comment: Installed test objects in test setup 1 (Heat cycle test) with thermocouples and transition resistance measurement.

Picture 4 – Layout of test setups

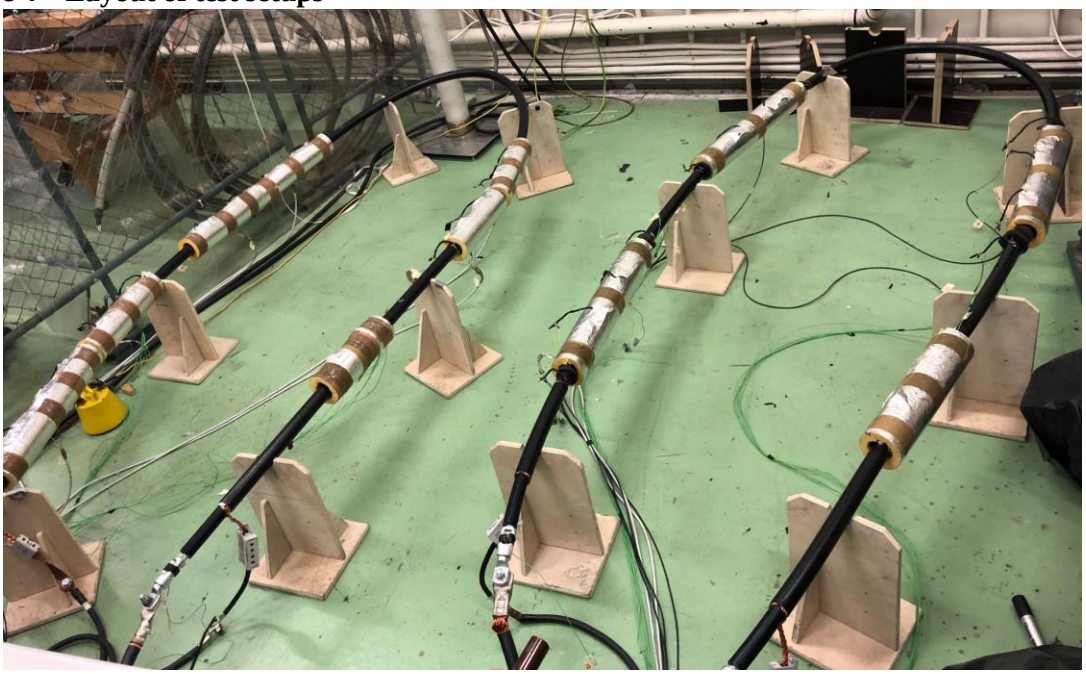

Comment: Test setup 1 (Heat cycle test) to the left and test setup 2 (Constant current test) to the right.

Picture 5 – Control units and data acquisition tools

Comment: Picture of the test cell, the AC control units and the data acquisition tools. The DC sources were placed inside the test cell with the test setups.

Picture 6 – Short circuit test setup

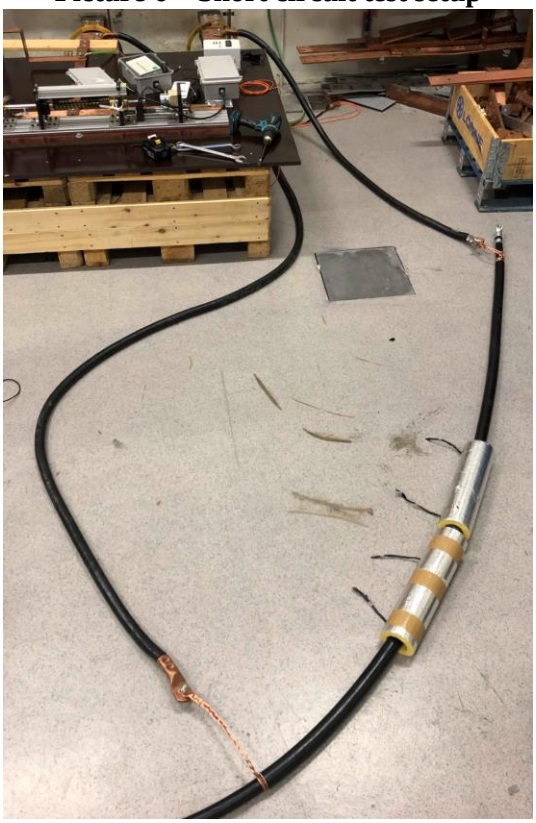

Comment: Picture of Test object 5 and Test object 6 from the heat cycle test, being connected to the short circuit test setup.

Picture 7 – Resistance measurement from the short circuit test

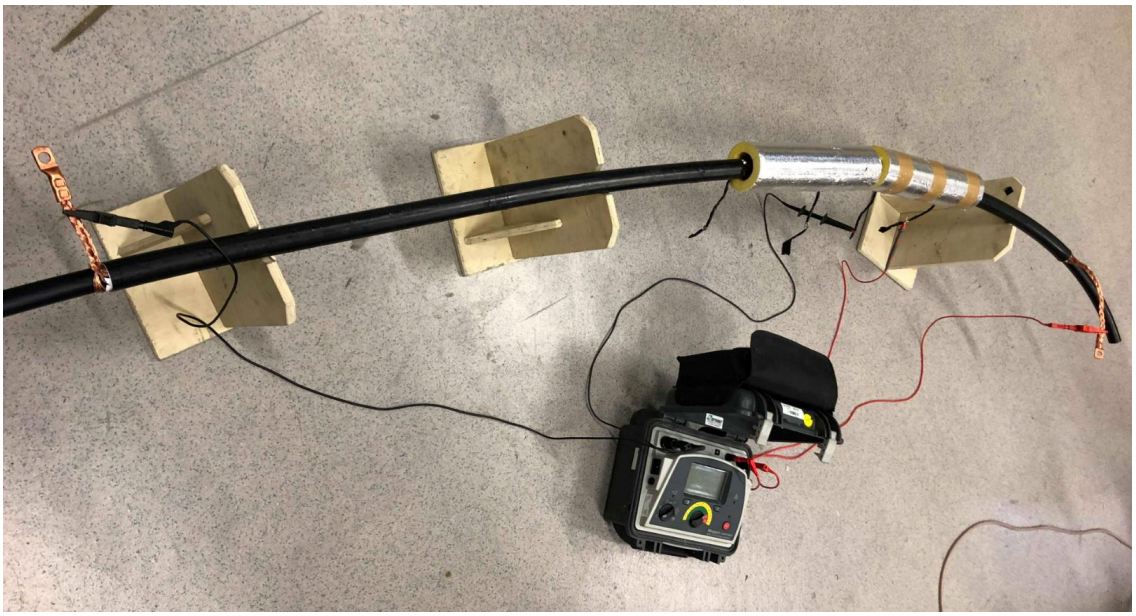

Comment: Low resistance ohm meter measuring test object resistances in the short circuit test.

Appendix D – Heat cycle test results

Heat cycle 1 – 450 A in the conductor, 70 A in the screen. (Initial test)

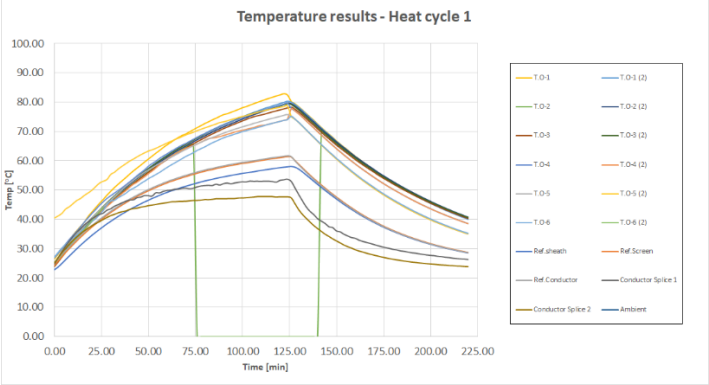

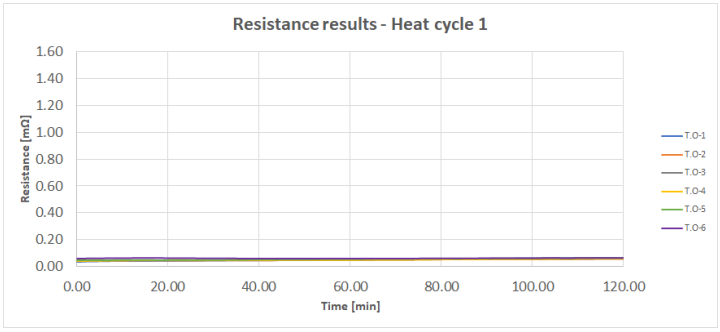

Heat cycle 2 – 500 A in the conductor, 70 A in the screen.

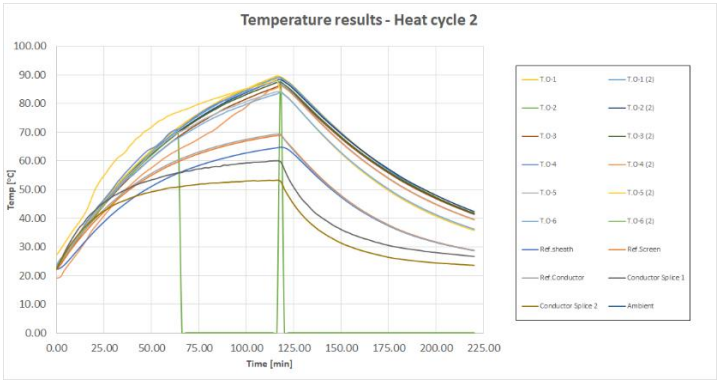

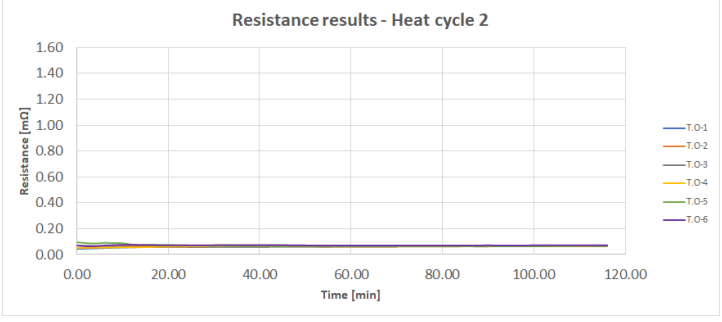

Heat cycle 3 – 500 A in the conductor, 70 A in the screen.

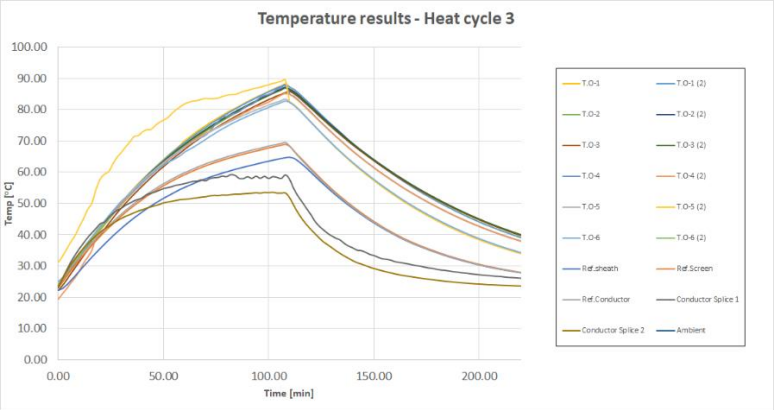

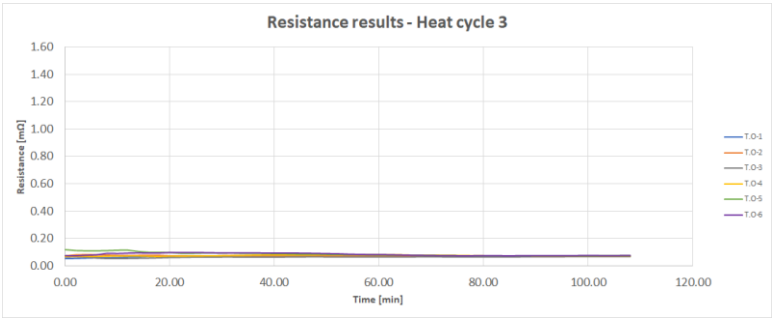

Heat cycle 4 – 500 A in the conductor, 70 A in the screen.

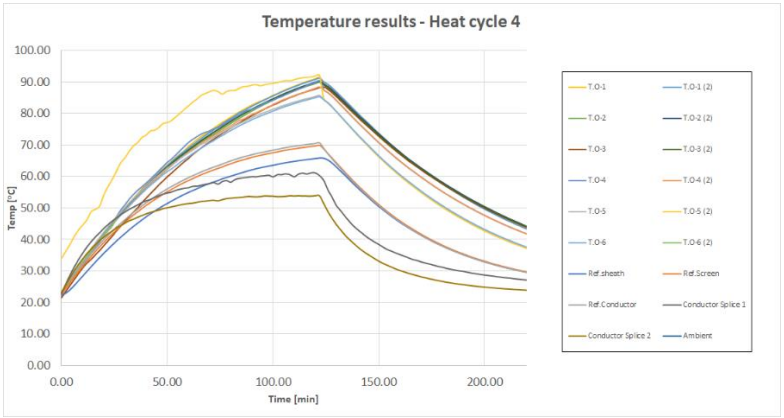

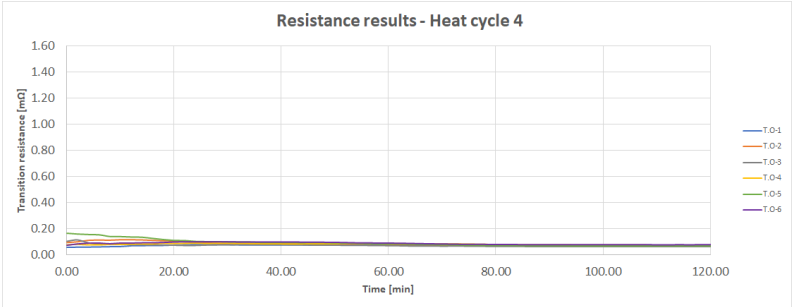

Heat cycle 5 – 500 A in the conductor, 70 A in the screen.

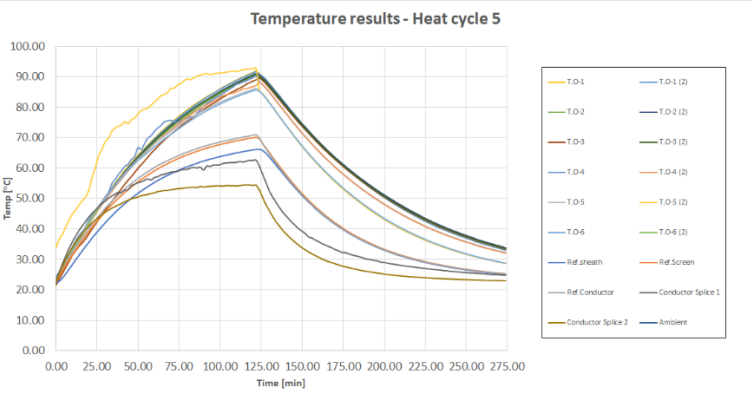

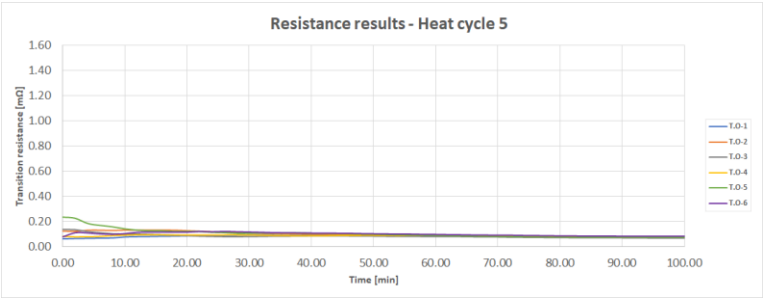

Heat cycle 6 – 500 A in the conductor, 70 A in the screen.

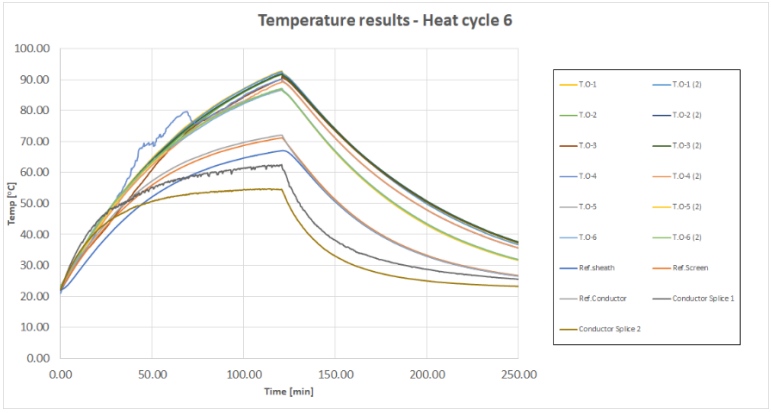

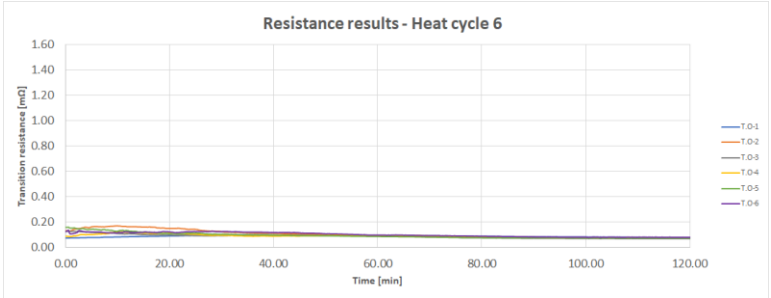

Heat cycle 7 – 500 A in the conductor, 70 A in the screen.

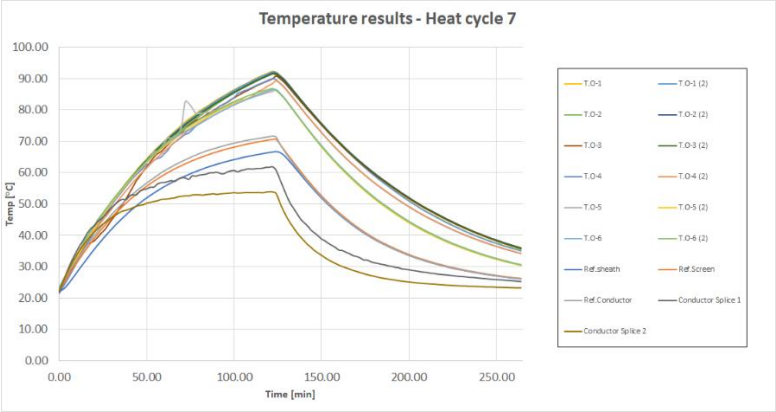

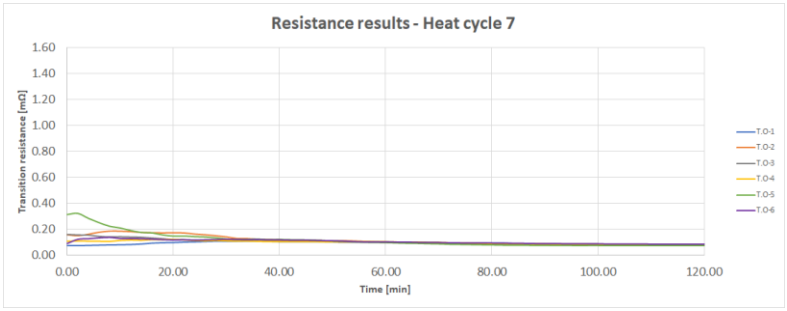

Heat cycle 8 – 500 A in the conductor, 70 A in the screen.

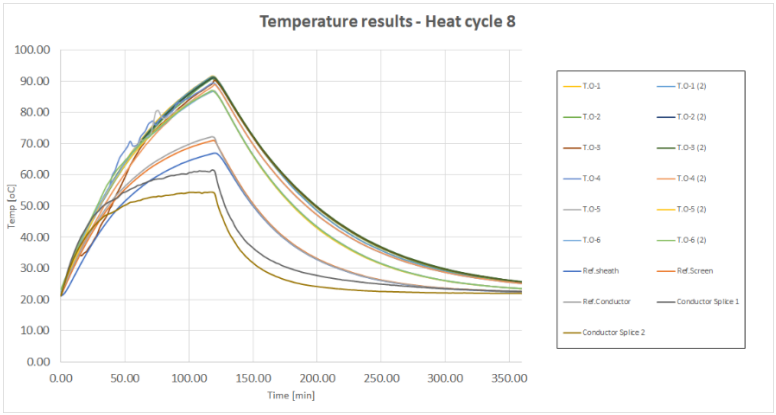

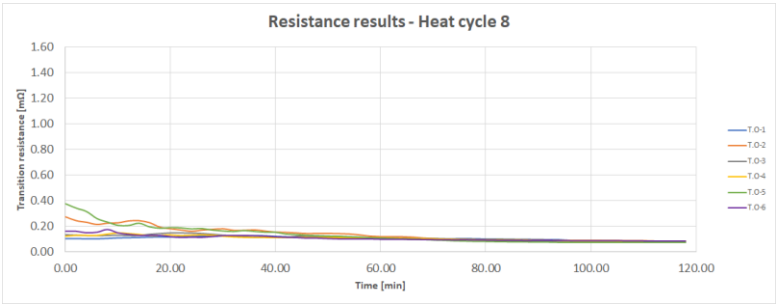

Heat cycle 9 – 500 A in the conductor, 70 A in the screen.

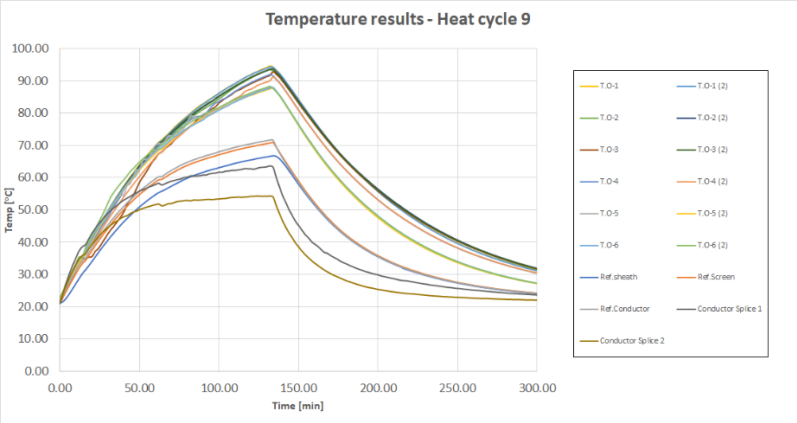

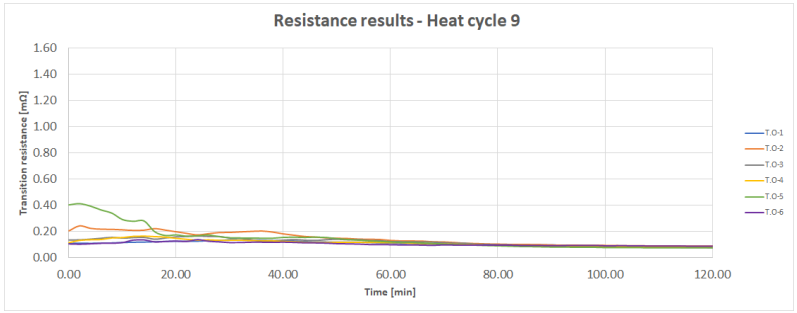

Heat cycle 10 – 500 A in the conductor, 70 A in the screen.

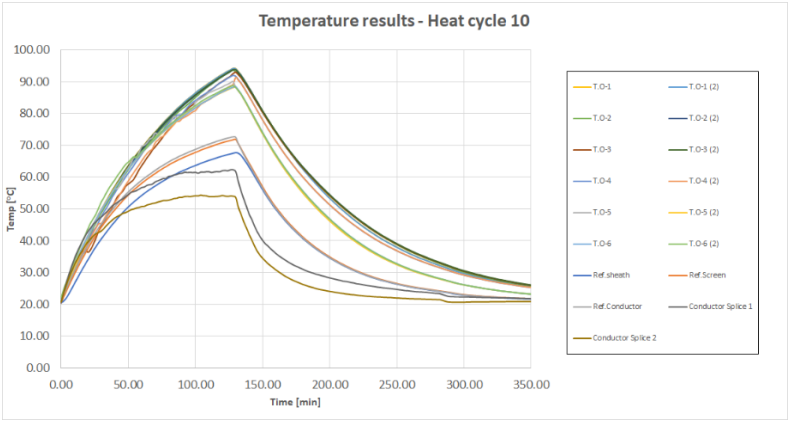

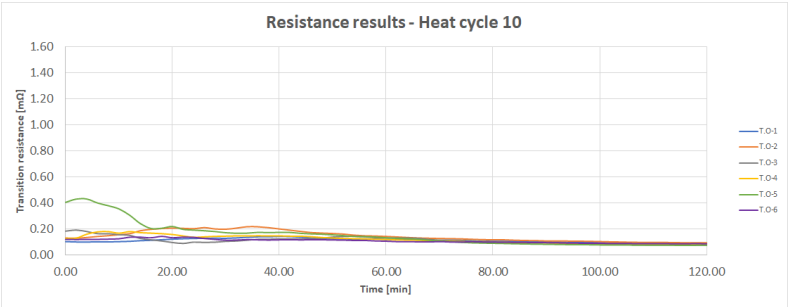

Heat cycle 11 – 500 A in the conductor, 70 A in the screen.

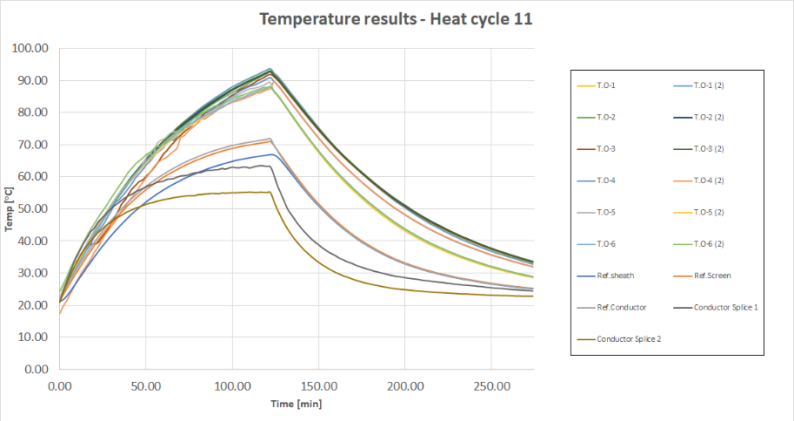

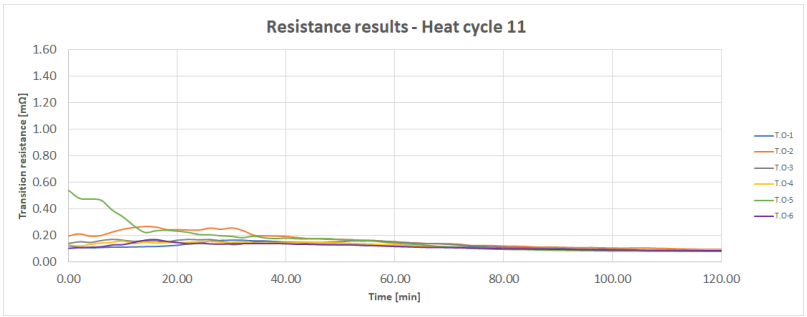

Heat cycle 12 – 500 A in the conductor, 70 A in the screen.

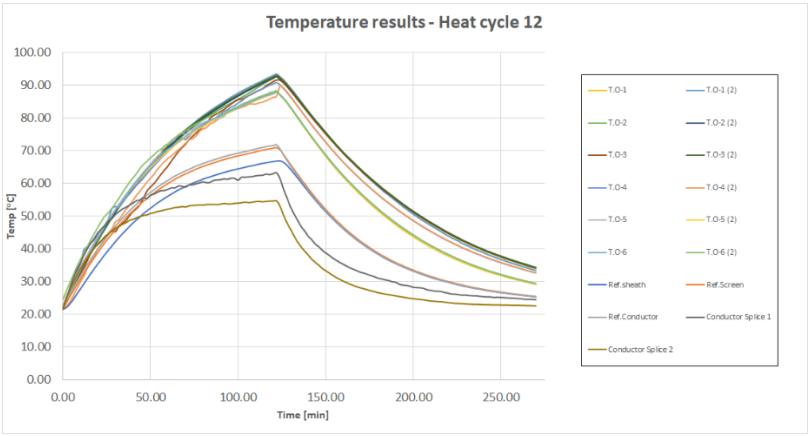

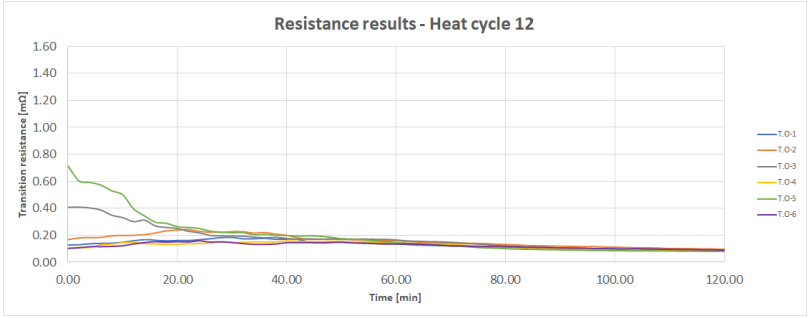

Heat cycle 13 – 500 A in the conductor, 70 A in the screen.

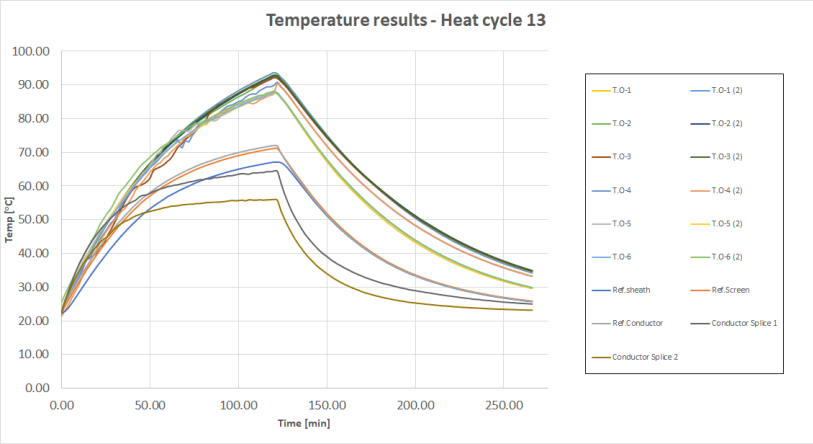

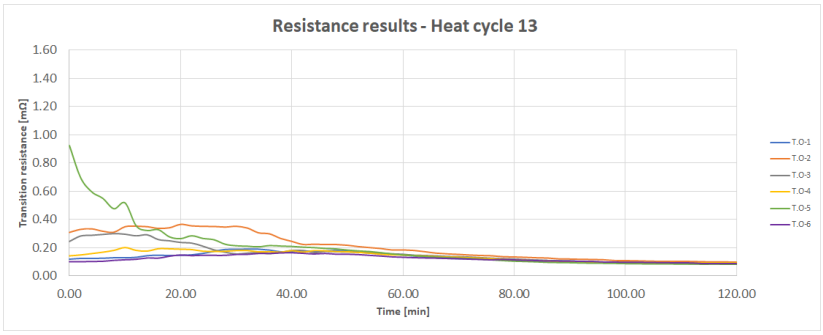

Heat cycle 14 – 500 A in the conductor, 70 A in the screen.

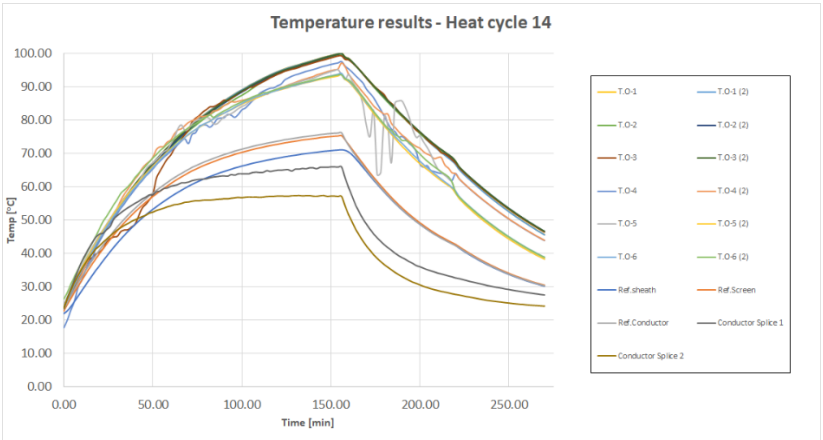

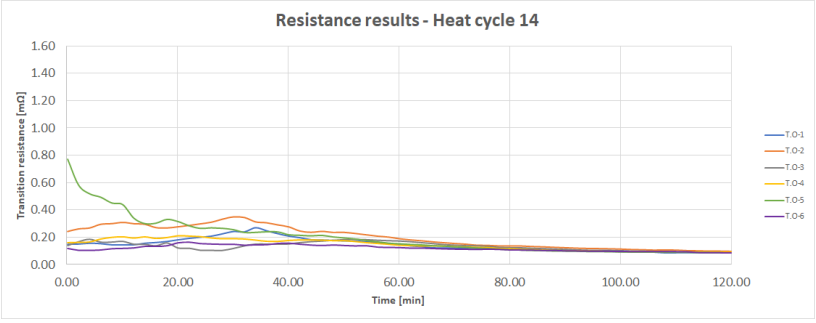

Heat cycle 15 – 500 A in the conductor, 70 A in the screen.

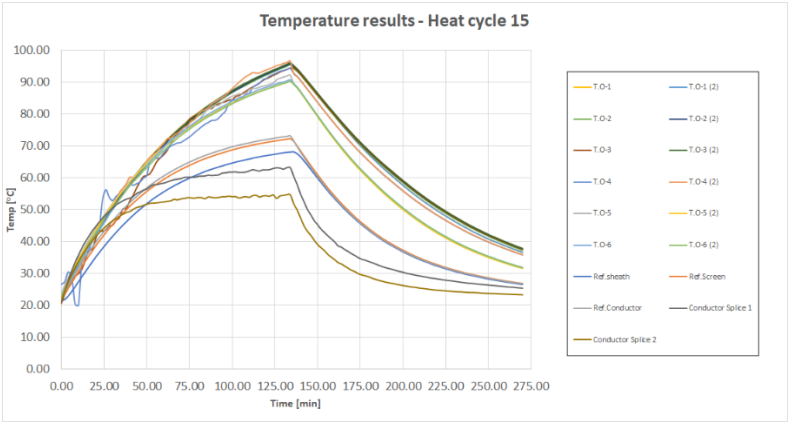

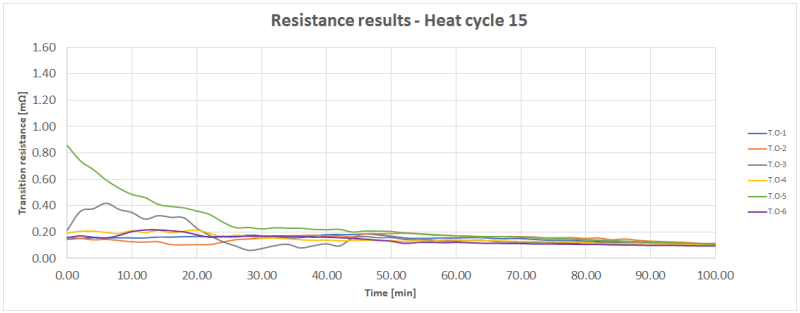

Heat cycle 16 – 500 A in the conductor, 70 A in the screen.

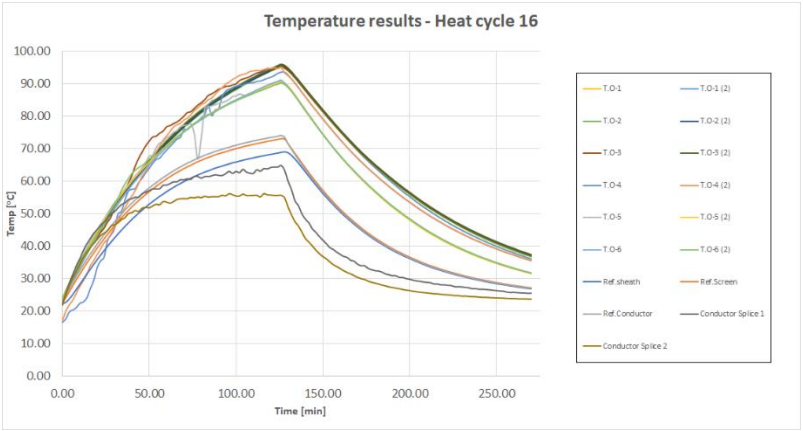

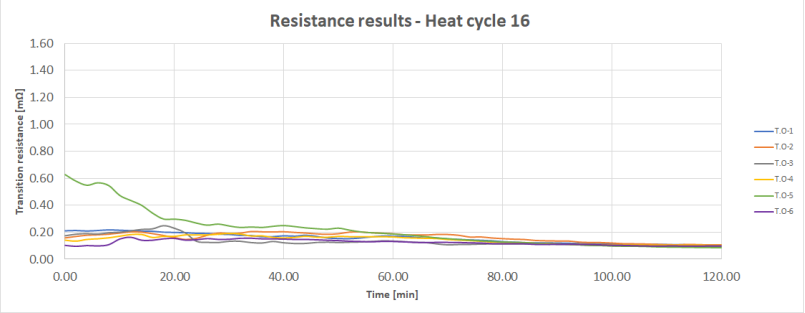

Heat cycle 17 – 500 A in the conductor, 70 A in the screen.

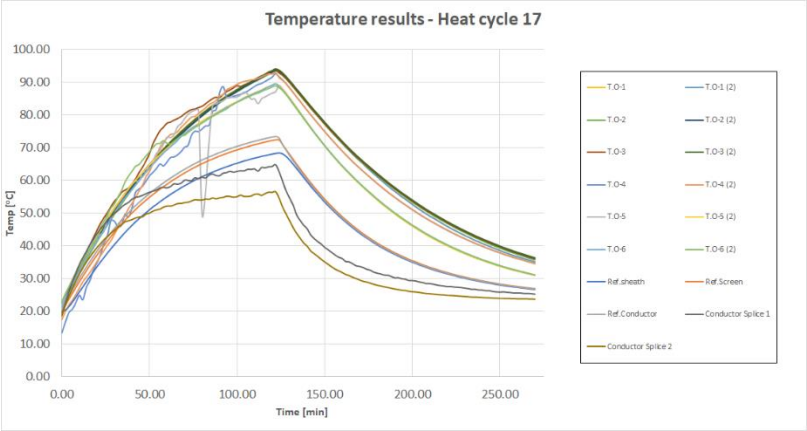

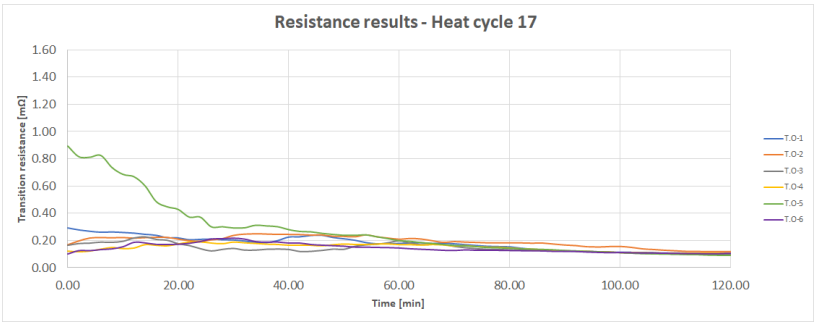

Heat cycle 18 – 500 A in the conductor, 70 A in the screen.

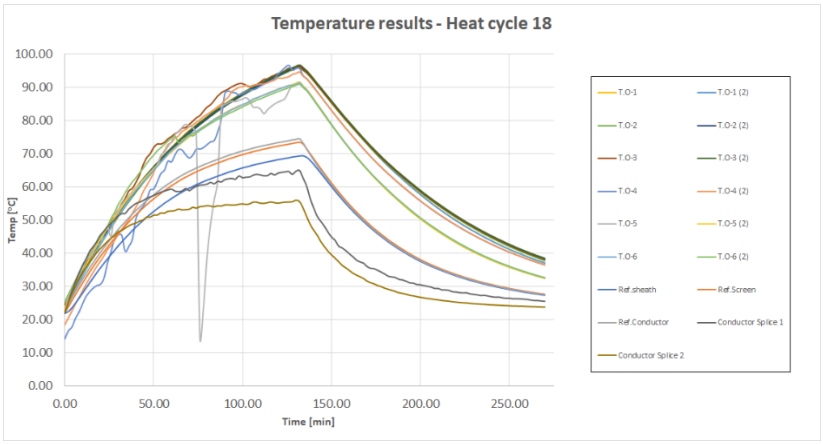

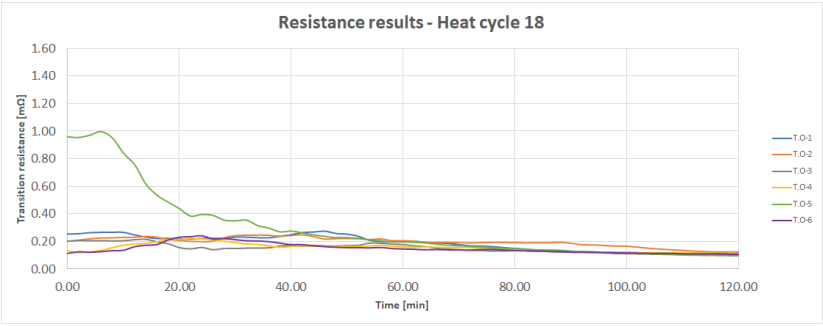

Heat cycle 19 – 500 A in the conductor, 70 A in the screen.

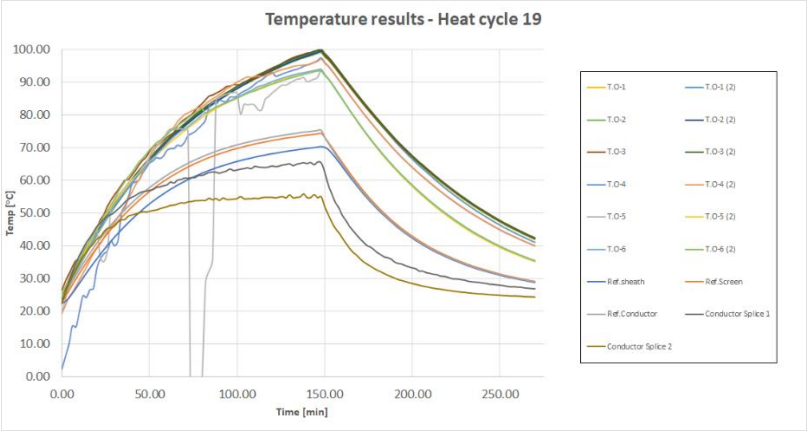

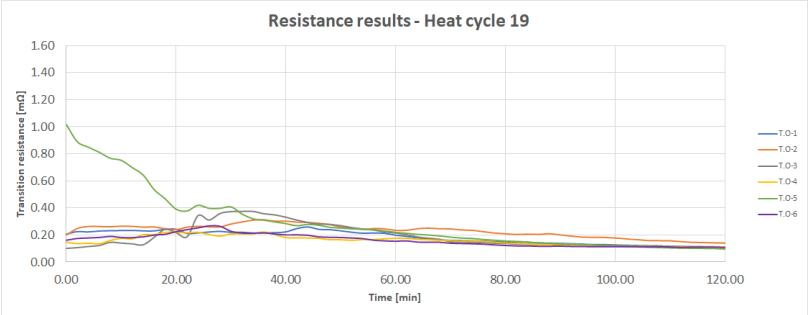

Heat cycle 20 – 500 A in the conductor, 70 A in the screen.

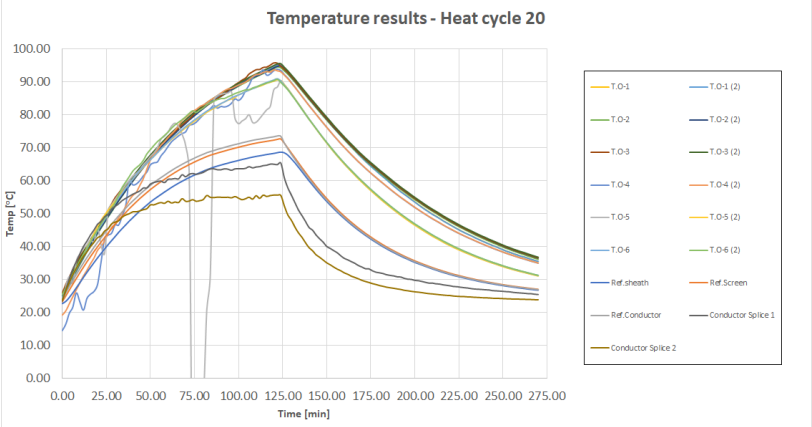

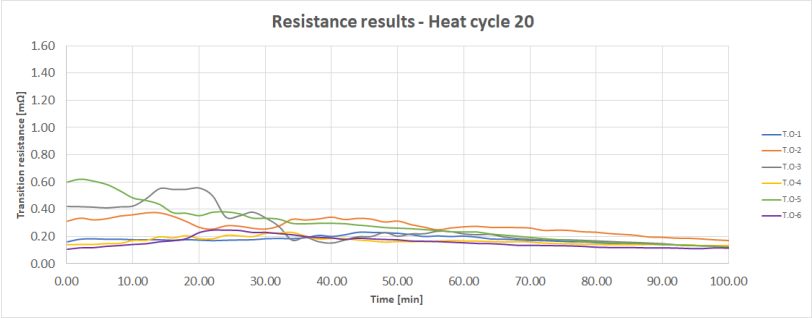

Heat cycle 21 – 500 A in the conductor, 70 A in the screen.

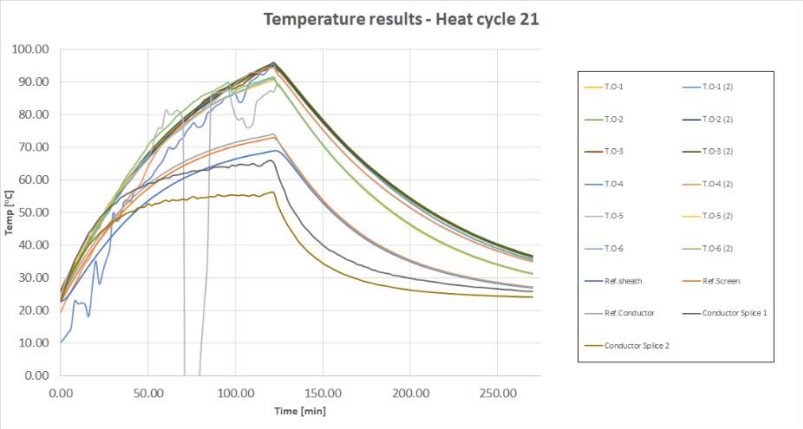

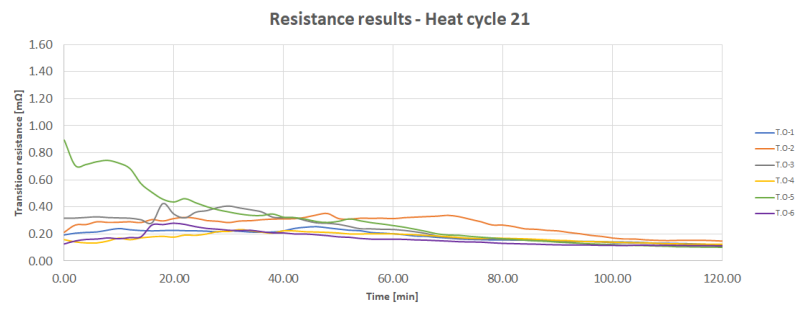

Heat cycle 22 – 500 A in the conductor, 70 A in the screen.

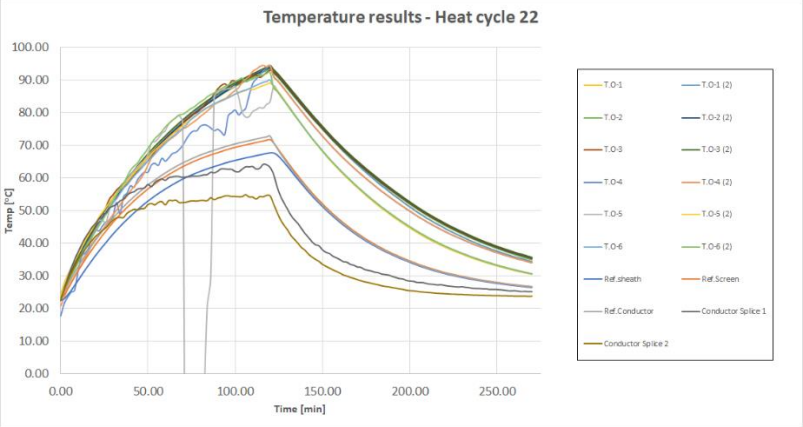

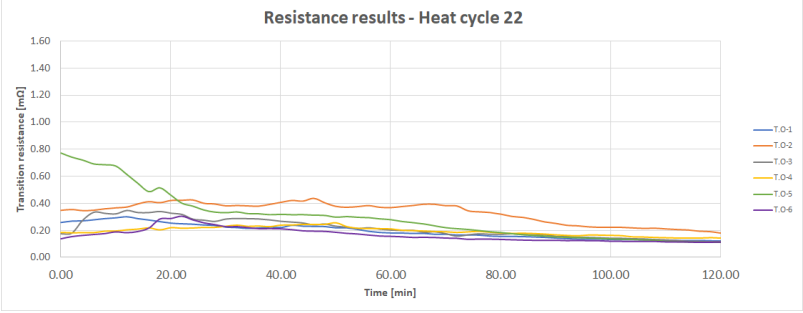

Heat cycle 23 – 500 A in the conductor, 70 A in the screen.

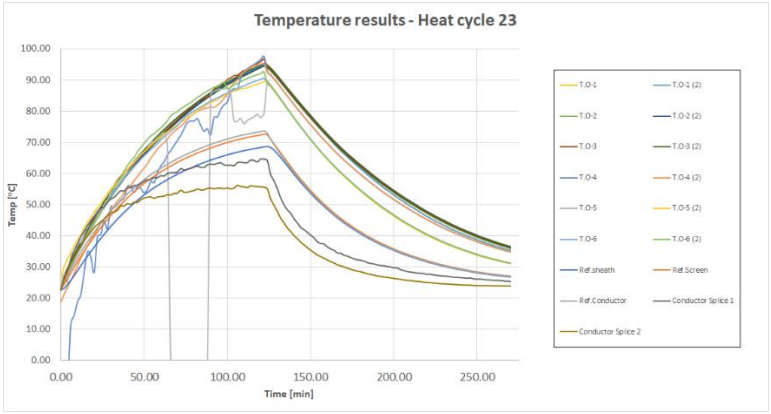

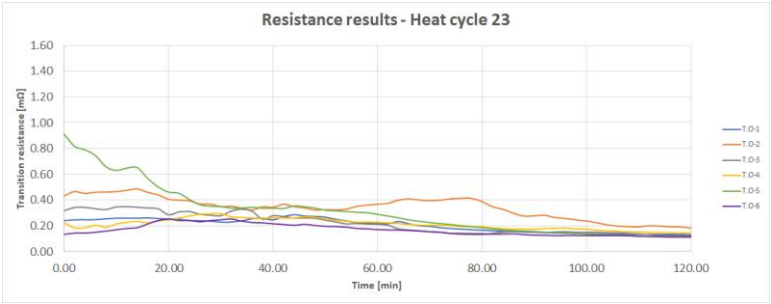

Heat cycle 24 – 500 A in the conductor, 70 A in the screen.

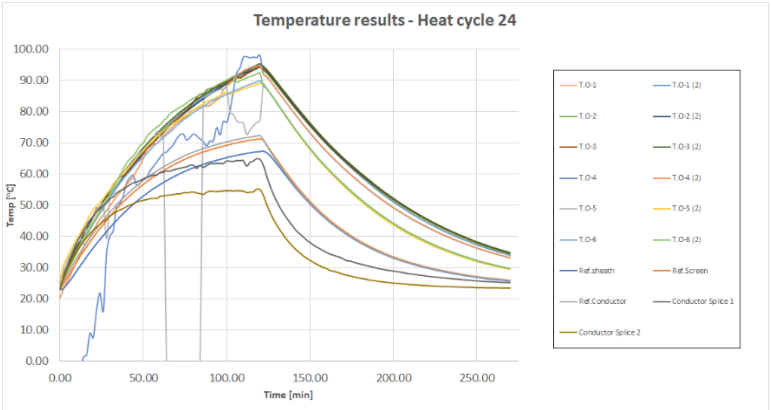

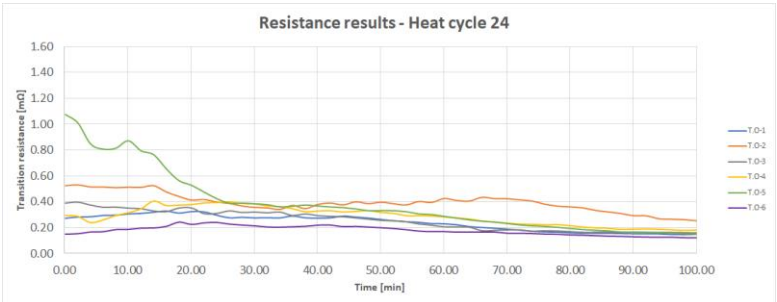

Heat cycle 25 – 500 A in the conductor, 70 A in the screen.

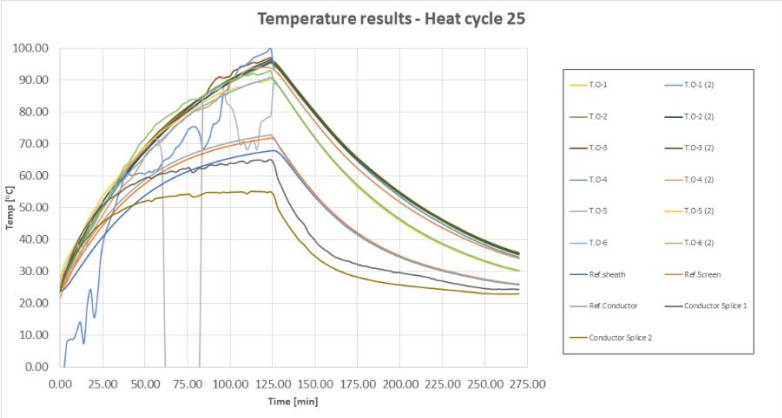

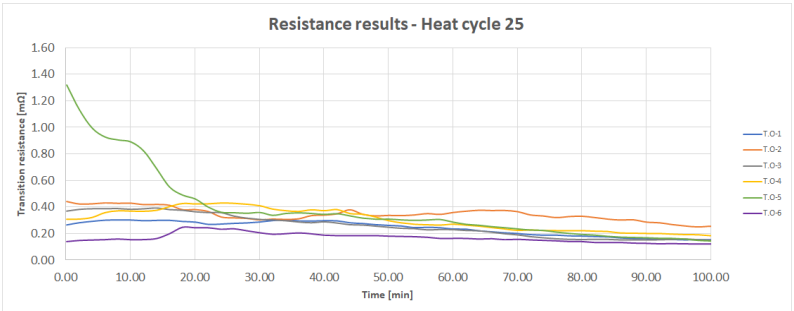

Heat cycle 26 – 500 A in the conductor, 70 A in the screen.

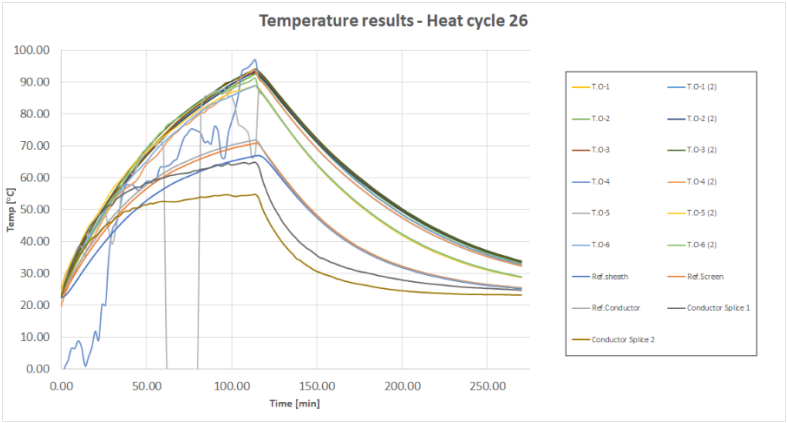

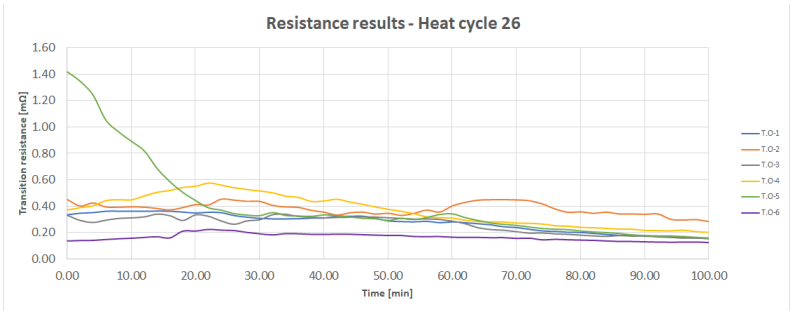

Heat cycle 27 – 500 A in the conductor, 70 A in the screen.

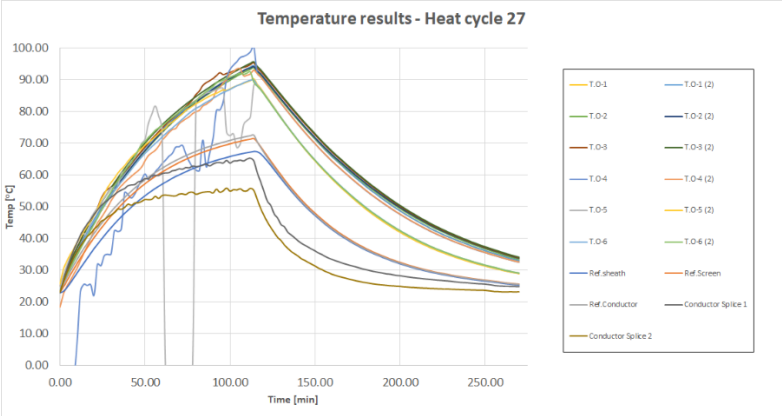

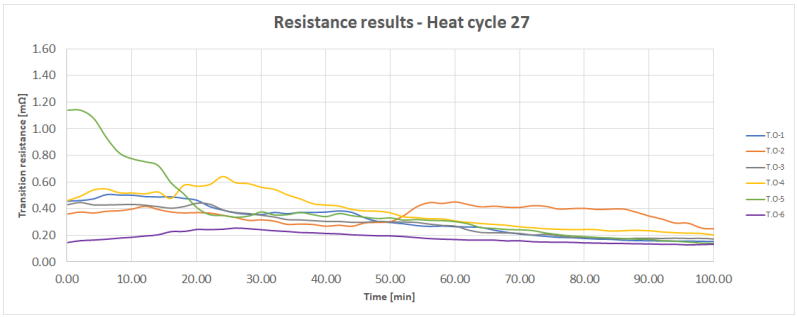

Heat cycle 28 – 500 A in the conductor, 70 A in the screen.

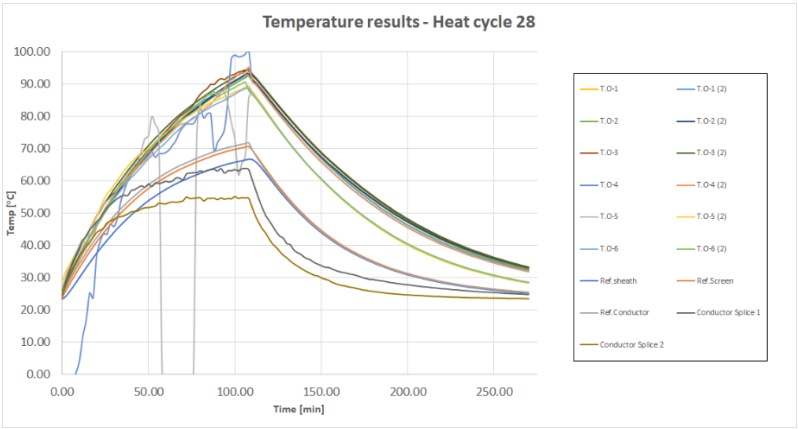

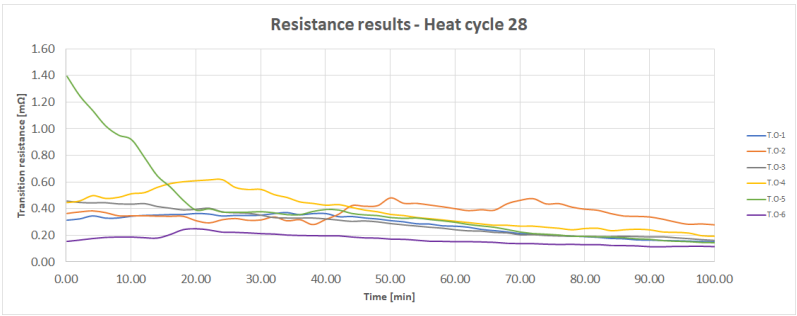

Heat cycle 29 – 500 A in the conductor, 70 A in the screen.

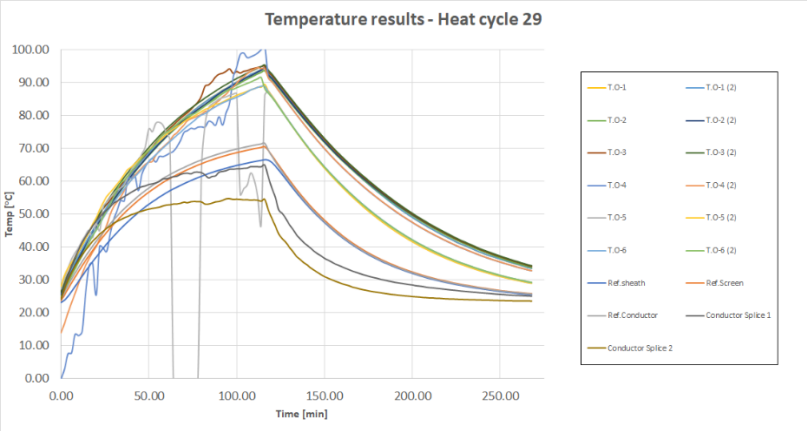

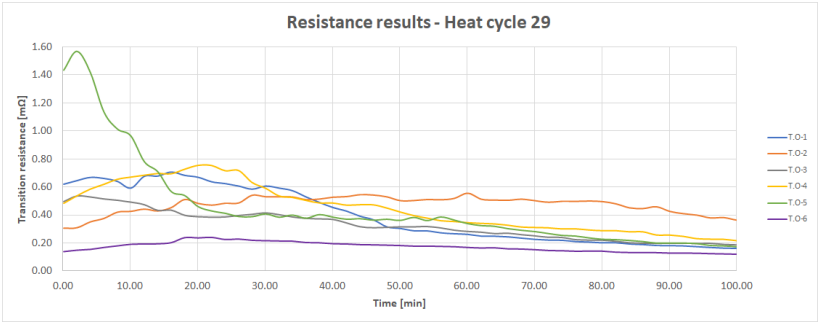

Heat cycle 30 – 500 A in the conductor, 70 A in the screen.

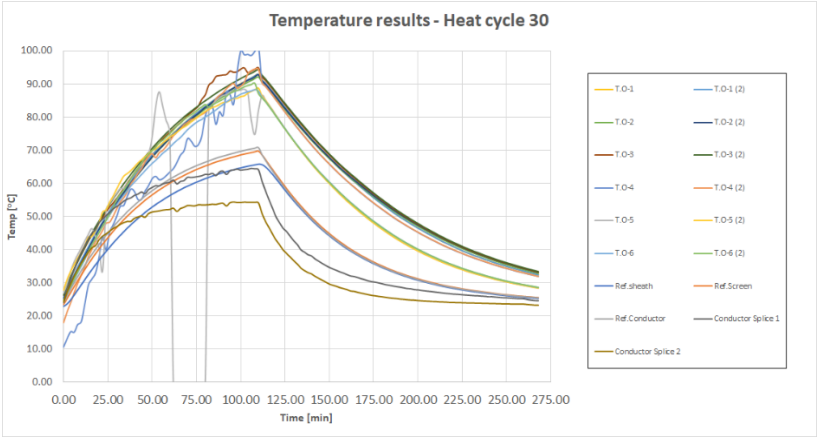

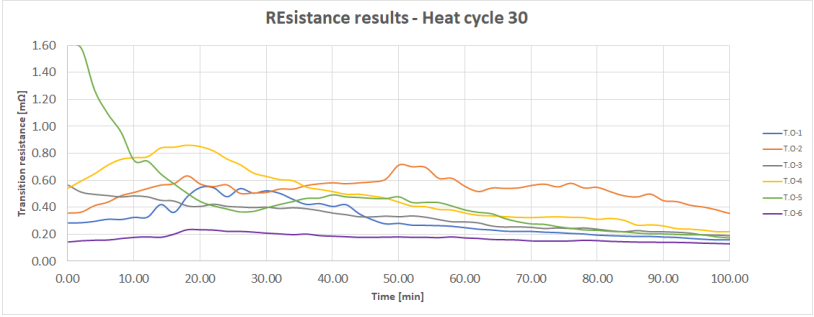

Heat cycle 31 – 500 A in the conductor, 70 A in the screen.

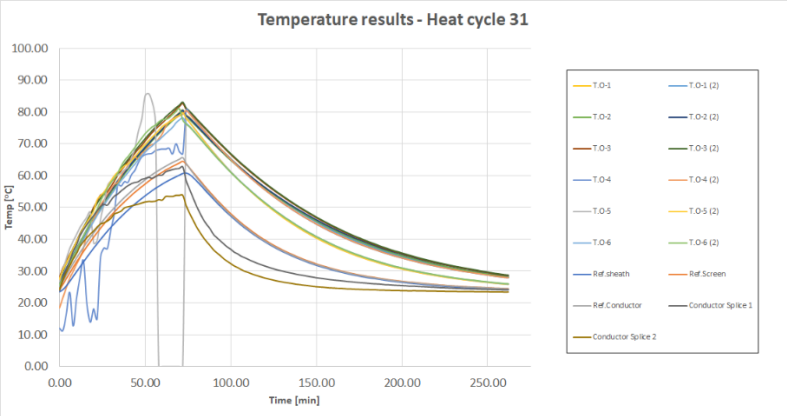

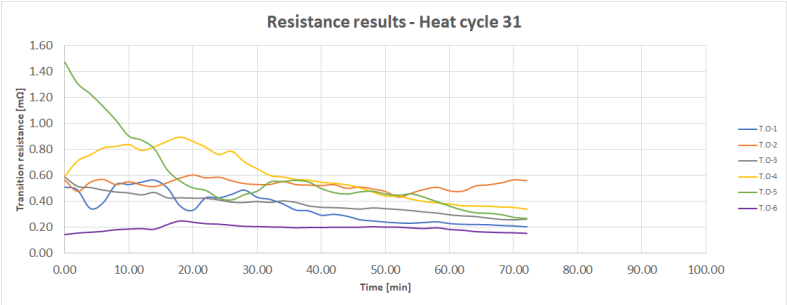

Heat cycle 32 – 500 A in the conductor, 70 A in the screen.

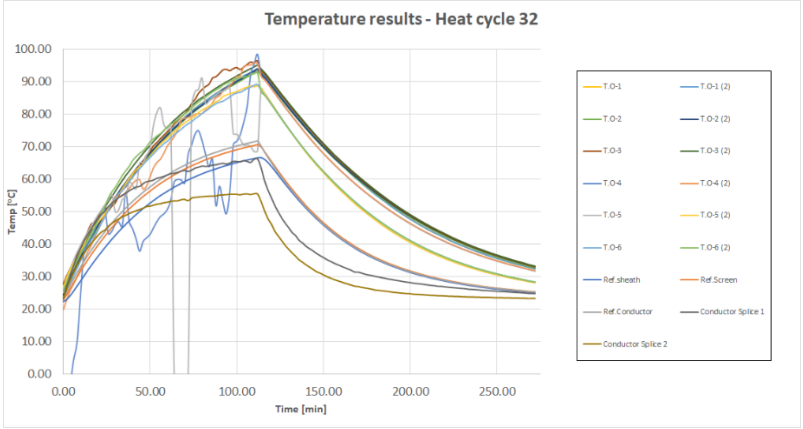

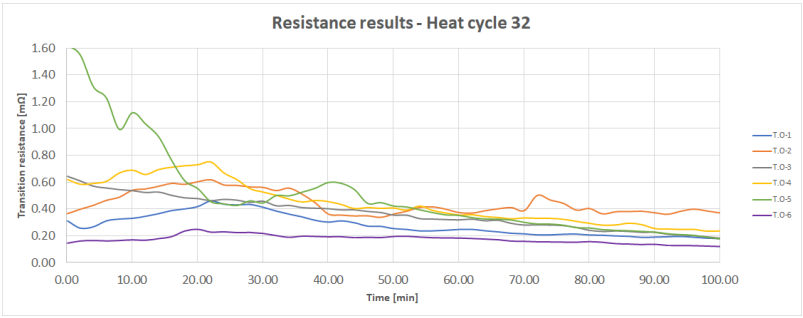

Heat cycle 33 – 500 A in the conductor, 70 A in the screen.

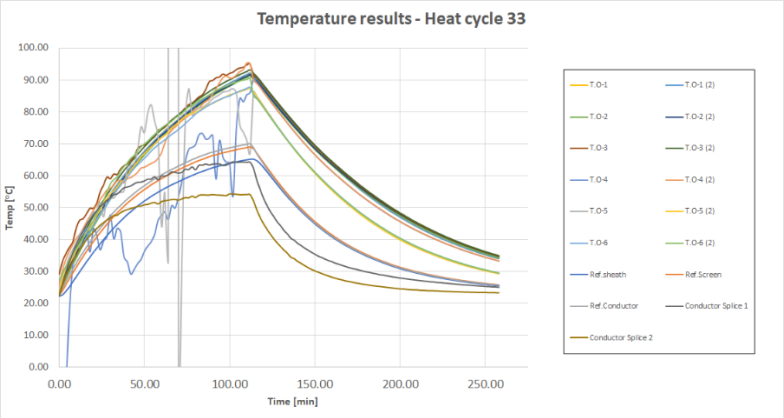

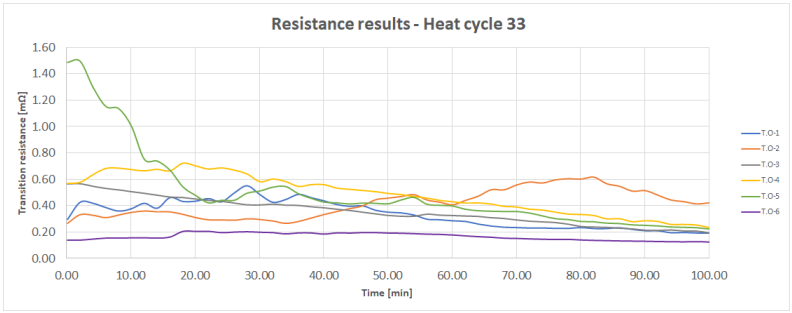

Heat cycle 34 – 500 A in the conductor, 70 A in the screen.

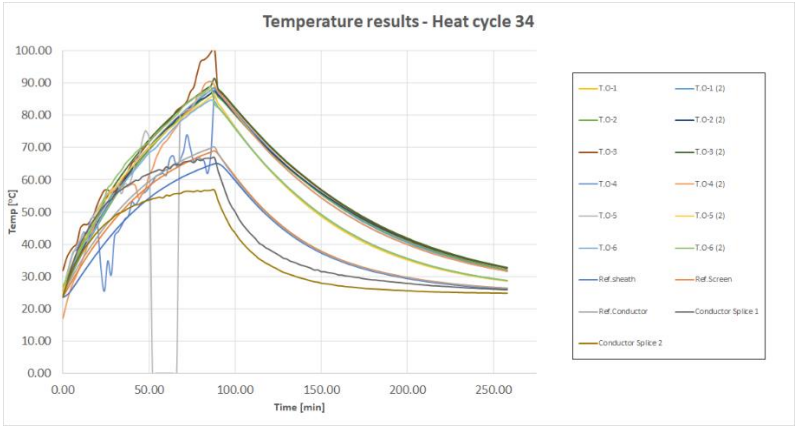

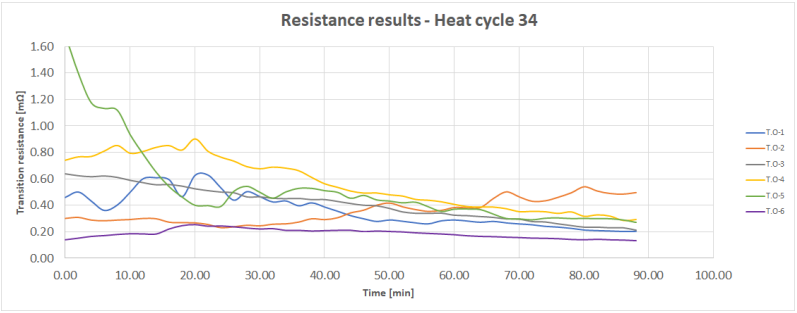

Heat cycle 35 – 500 A in the conductor, 70 A in the screen.

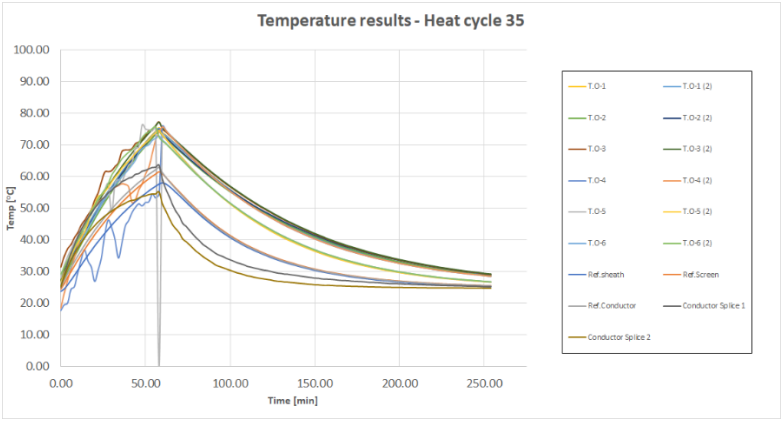

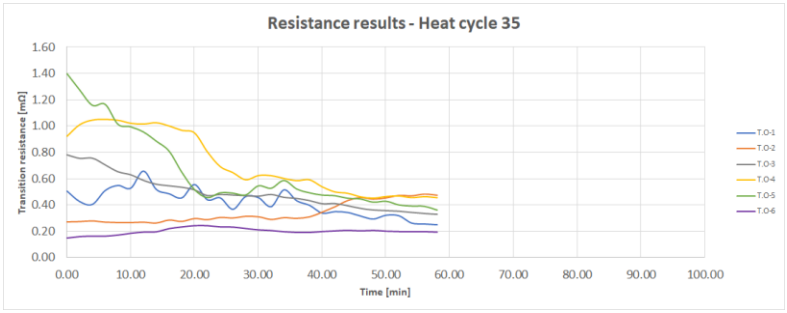

Heat cycle 36 – 500 A in the conductor, 70 A in the screen.

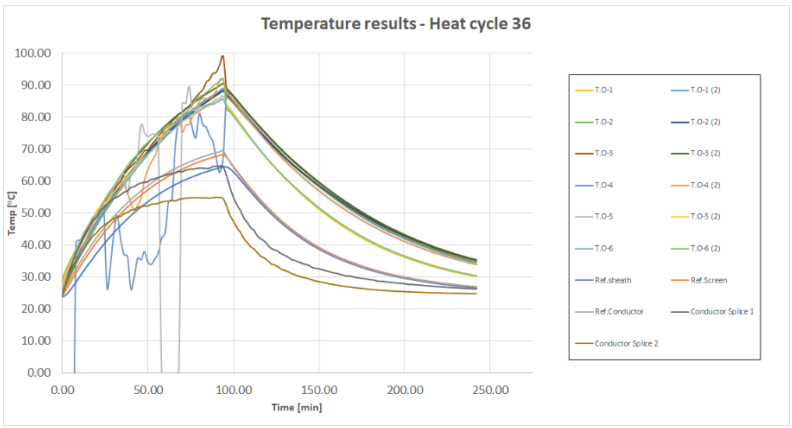

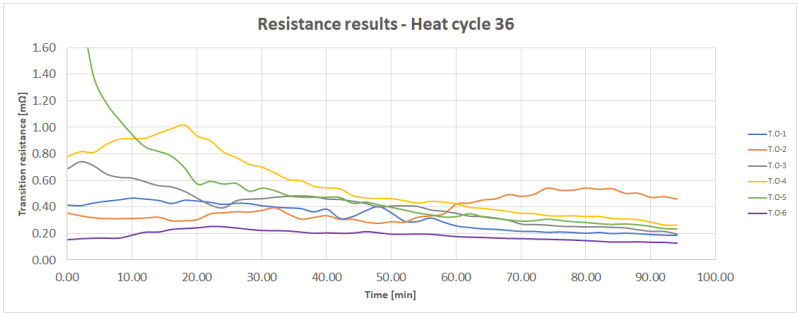

Heat cycle 37 – 500 A in the conductor, 70 A in the screen.

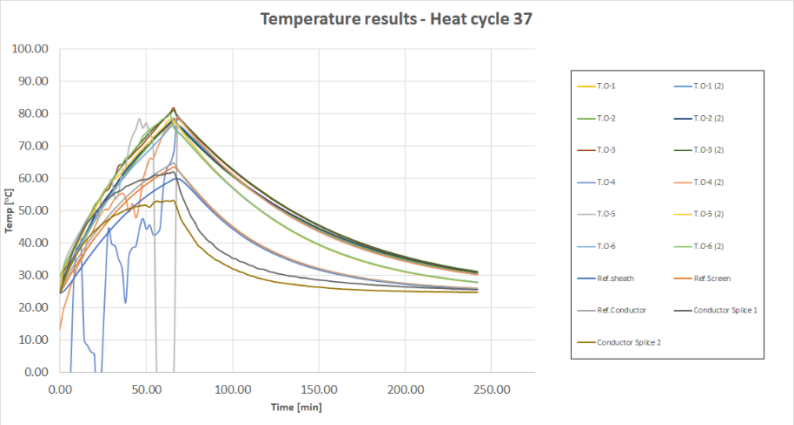

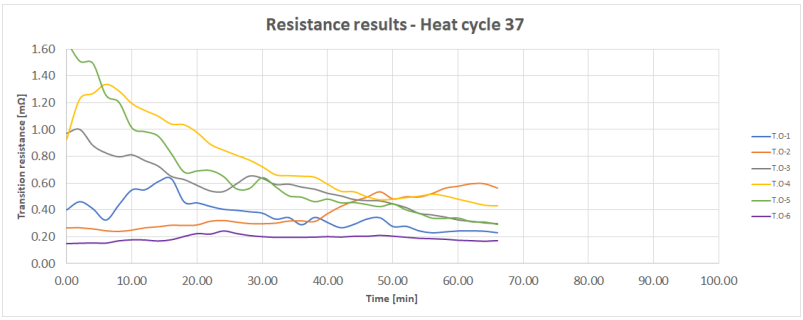

Heat cycle 38 – 500 A in the conductor, 70 A in the screen.

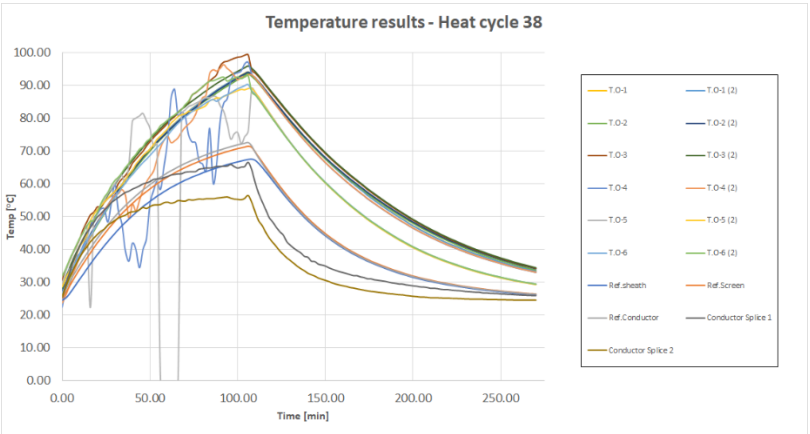

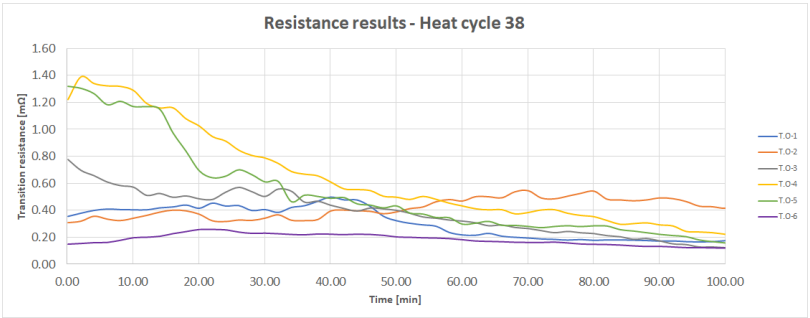

Heat cycle 39 – 500 A in the conductor, 70 A in the screen.

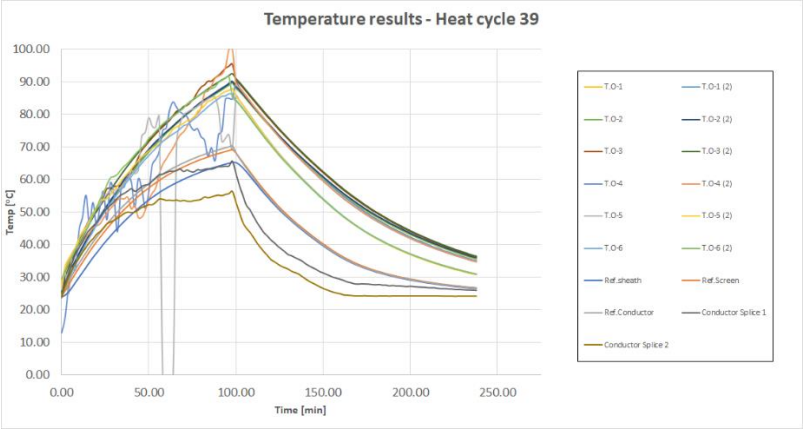

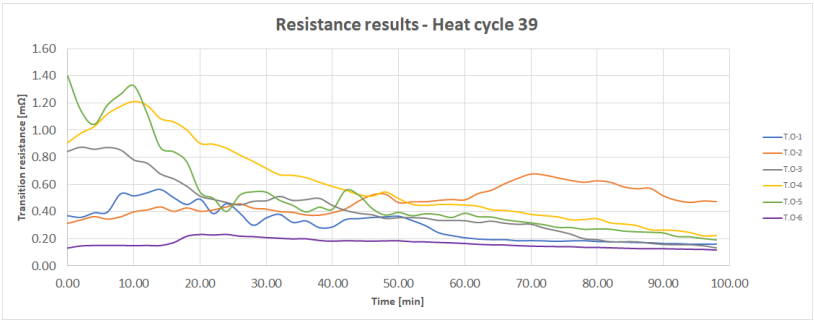

Heat cycle 40 – 500 A in the conductor, 70 A in the screen.

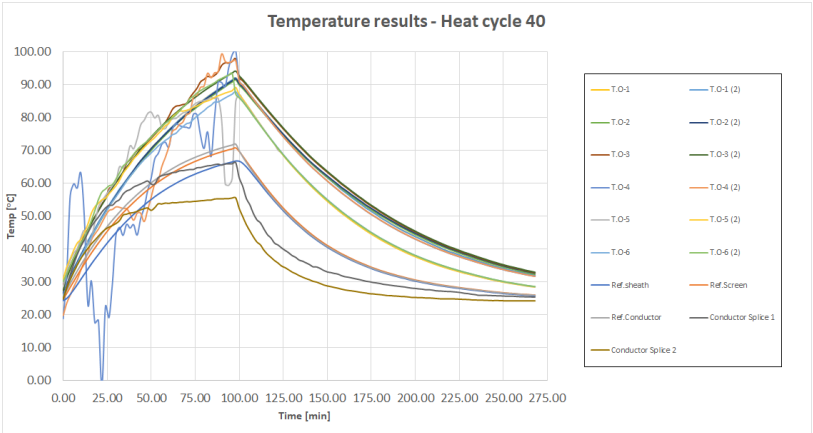

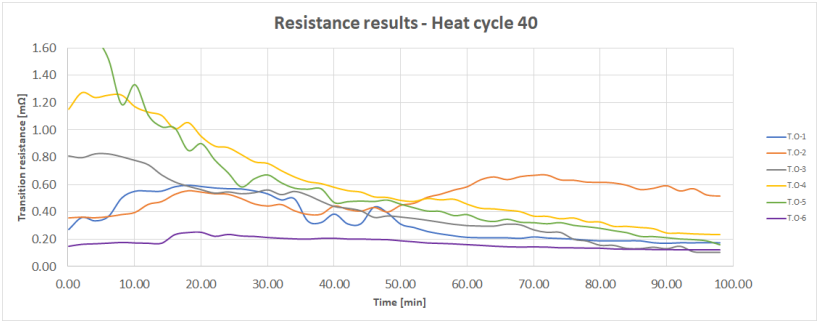

Appendix E – Constant current test results

450 A in the conductor, 55 A in the screen.

Temperature results

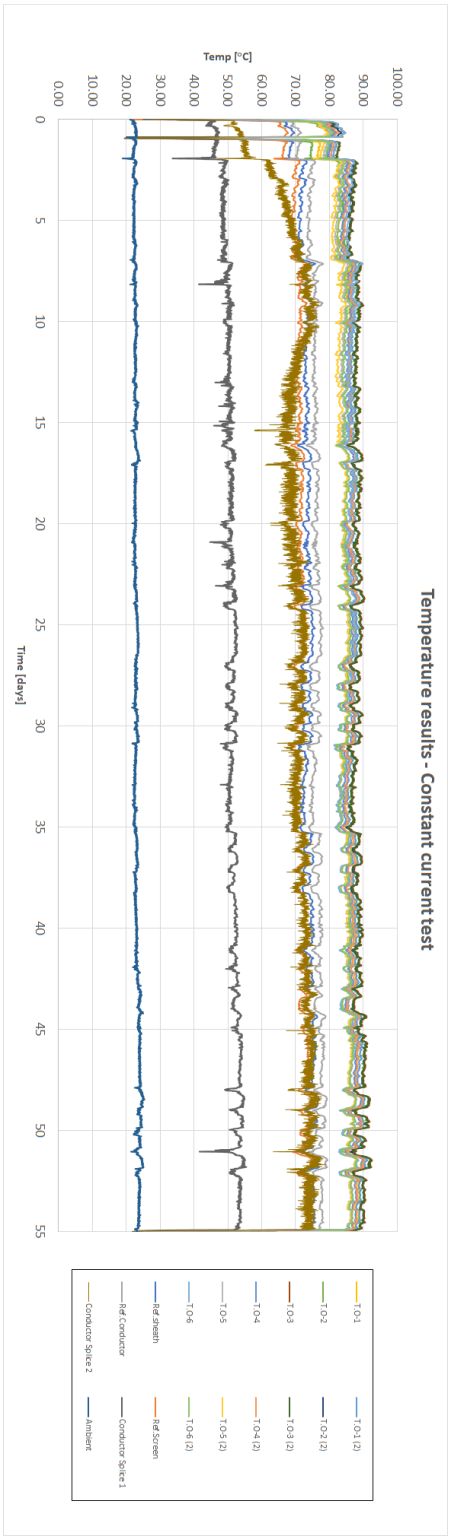

Resistance results

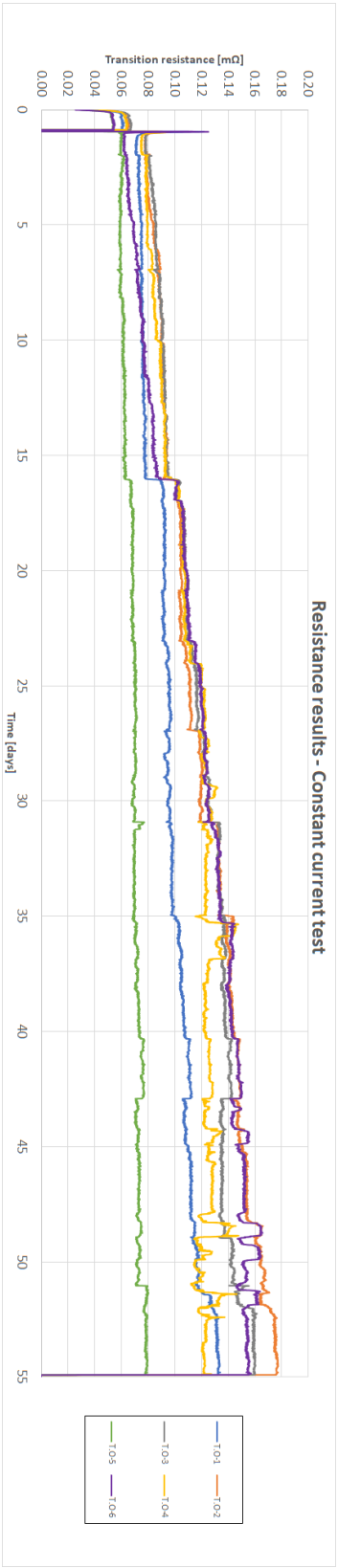

Robin Lyngseth Bakken

Reliable Power Cable Screen Connections

NTNU
Norwegian University of
Science and Technology